

**Aus dem Institut für Physiologie - Neurophysiologie
der Universität Würzburg**

Vorstand: Professor Dr. med. Manfred Heckmann



**Charakterisierung und Anwendung neuer optogenetischer Werkzeuge in
*Drosophila melanogaster***

**Characterisation and application of new optogenetic tools in *Drosophila
melanogaster***

Inaugural - Dissertation

zur Erlangung der Doktorwürde der

Medizinischen Fakultät

der

Julius-Maximilians-Universität Würzburg

vorgelegt von

Alexander Grotemeyer

geboren in Münster

Würzburg, 2018

Referent:	Prof. Dr. Robert J. Kittel
Korreferent:	Prof. Dr. Georg Nagel
Dekan:	Prof. Dr. Matthias Frosch
Tag der mündlichen Prüfung:	15.03.2019

Der Promovend ist Arzt.

Hiermit versichere ich an Eides statt, dass ich die Dissertation selbständig angefertigt habe. Übernommene Inhalte wurden von mir eindeutig gekennzeichnet. Die Gelegenheit zum Promotionsverfahren wurde mir nicht kommerziell vermittelt. Insbesondere wurde keine Person oder Organisation eingeschaltet, die gegen Entgelt Betreuer bzw. Betreuerinnen für die Anfertigung von Dissertationen sucht. Ich erkläre weiterhin, dass ich die Regeln der Universität Würzburg über gute wissenschaftliche Praxis eingehalten habe. Meine Dissertation wurde weder vollständig noch teilweise schon einmal einer anderen Fakultät mit dem Ziel, einen akademischen Grad zu erzielen, vorgelegt. Ich habe bis zum heutigen Tag keine akademischen Grade erworben, noch versucht solche zu erwerben. Es wurde mir kein akademischer Grad entzogen, noch wurde gegen mich diesbezüglich ein strafrechtliches Ermittlungsverfahren oder Disziplinarverfahren eingeleitet.

Contents

1 Introduction	1
1.1 The Synapse	1
1.2 Mechanosensation	8
1.3 Drosophila <i>melanogaster</i>	10
1.3.1 Background	10
1.3.2 Neuromuscular junction (NMJ).....	12
1.3.3 Chordotonal organ (ChO).....	14
1.4 Optogenetics and its usage	18
1.5 Motivation of the study	23
2 Materials and Methods	25
2.1 Fly stocks	25
2.2 Electrophysiology	27
2.2.1 The two-electrode voltage clamp (TEVC) technique.....	27
2.2.2 TEVC setup for recordings in general	31
2.3 Confocal microscopy	33
2.3.1 Basics of confocal microscopy	33
2.3.2 Immunohistochemistry of the ChO	34
2.3.3 Immunohistochemistry of the NMJ	35
2.3.4 Immunohistochemistry of the ventral nerve cord (VNC)	36
2.3.5 Data acquisition.....	37
2.4 Optogenetic tools	38
2.4.1 Channelrhodopsin2-XXM at the NMJ.....	38
2.4.2 GtACR at the larval NMJ and muscle tissue	39
2.4.3 Channelrhodopsin2-XXM in the ChO.....	39
2.5 Data analysis	42

3 Results	43
3.1 Characterization of Channelrhodopsin2-XXM at the <i>Drosophila</i> NMJ .43	
3.1.1 Expression of ChR2 ^{XXM} ::tdtomato at the larval NMJ	43
3.1.2 Electrophysiological recordings at the larval NMJ.....	45
3.1.3 Larval behaviour.....	46
3.1.4 Adult behaviour	47
3.2 Analysis of the chordotonal organ using Channelrhodopsin2-XXM	50
3.2.1 Expression in the chordotonal organ.....	50
3.2.2 Electrophysiological recordings.....	52
3.2.3 Light-induced head-swing behaviour	53
3.3 Application of <i>Guillardia theta</i> Anion Channelrhodopsin at the <i>Drosophila</i> NMJ	56
3.3.1 Expression at the larval NMJ	57
3.3.2 Electrophysical recordings at the larval NMJ	58
3.3.3 Larval behaviour.....	61
4 Discussion	62
4.1 Channelrhodopsin2-XXM	62
4.1.1 Channelrhodopsin2-XXM – a new optogenetic tool	62
4.1.2 Mechanosensation by light – ChR2-XXM in the <i>lch5</i>	65
4.2 GtACR	66
4.2.1 Use of GtACR as an optogenetic inhibitor tool.....	66
4.2.2 ‘Baseline-shift’ as a mentionable side effect of GtACR.....	66
4.3 Chordotonal organ and <i>dCIRL</i>	69
4.4 Clinical relevance of this thesis and Outlook	72
4.4.1 Application of optogenetic tools for therapeutic purposes	72
4.4.2 Latrophilin.....	74
5 Summary	76
6 References	77
7 Abbreviations	97

8 Register of illustrations	100
9 Appendix.....	101
9.1 Acknowledgments	101
9.2 Curriculum vitae	102

1 Introduction

1.1 The Synapse

In the late 19th century Santiago Ramón y Cajal was the first person who described the contact zone between two neurons histologically (Ramon y Cajal, 1894). Three years later, Sir Charles Scott Sherrington termed this very specialised contact zone as 'synapse', a composition from the greek word 'syn' for 'together' and 'haptain' for 'catch, grab, grope' (Sherrington, 1897; Bennett, 1999). At this point, most investigators thought that synapses could only form direct electrical connections even though it remained uncertain. However, by a series of remarkable experiments, Otto Loewi could show that a chemical compound (Acetylcholine) transmitted signals from the Vagus nerve to the heart (Loewi, 1921) and could reinforce observations of chemical transmission T. R. Elliot had made two decades earlier in the context of adrenaline (Elliot, 1905).

Nevertheless, it still remained opaque, if a chemical way of signalling existed, how chemicals could trigger action potentials in neurons. It took around 30 years and a lot of improvement in technology to verify that both ways of neuronal communication, electrical and chemical, co-exist (Fatt, 1954) albeit to different extents. Though, Ramon y Cajal already assumed in 1894 that learning might cause alterations in synaptic connections, which in turn was defined in more detail by Donald Hebb (Hebb, 1949), who described a basic concept of learning. Later it could be demonstrated that the chemical synapse plays a key role in learning and memory formation, due to its ability to modify signals in an activity-dependent manner, a process known as 'synaptic plasticity' (Abbott and Nelson, 2000; Kandel, 2009; Glanzman, 2010; Feldman, 2012). Especially investigations on the determinants of learning at a cellular level became an intensively studied issue in both the invertebrate (Kandel, 1976; 2001) and the vertebrate system (Bliss and Lømo, 1973; Bliss and Collingridge, 1993)

Recently, it has been shown that synaptic plasticity can occur on both synaptic sites, as presynaptic changes in transmitter release or as alterations of the postsynaptic receptors properties (Choquet and Triller, 2013). Even though main parts of this study are performed at chemical synapses, I will distinguish electrical synapses from chemical synapses in the following.

Communication between chemical synapses is based on vesicle fusion with the presynaptic membrane due to depolarization-induced opening of calcium (Ca^{2+}) channels. Subsequently, these vesicles are released into the synaptic cleft where they diffuse and bind to the receptors of the postsynaptic (or presynaptic) membrane. Basically, a synapse consists of two parts. First, the presynapse with its specialised compartment the active zones (AZ) where vesicles, filled with transmitter substances, are bound and released (Südhof, 2012). Second, the corresponding postsynaptic receptors that are sensitive to the distinct neurotransmitters released from vesicles at the presynaptic terminal (Harris and Littleton, 2015). Even though this principle is highly conserved, there are morphological differences of the AZ between mammals and invertebrates as well as some neurotransmitters, which are employed in different contexts.

Main functional parts of the chemical synapse, as in *Drosophila*, are the presynaptic active zones where clusters of synaptic vesicles (SV) and voltage-gated Ca^{2+} -channels can be found. Within the glutamateric synapses of the *Drosophila* NMJ, the activation of the corresponding postsynaptic glutamate receptors (GluR), localised in the postsynaptic density (PSD), leads to changes of polarisation at the postsynaptic membrane due to facilitated ion flux (cf. Fig. 1.A,B).

In *Drosophila melanogaster* a prominent dense structure visible in electron microscopy (EM) defines the AZ (Kittel et al., 2006). One component that makes up this structure is called “Bruchpilot” (Brp; crash pilot) which is a homolog of ELKS/CAST in mammals (Ohtsuka et al., 2002; Wang et al., 2002) and was first described in 2006 (Wagh et al., 2006). Brp acts as an essential

part of the cytomatrix of the active zone (CAZ) and its absence leads to extinction of T-bar structures (T-bar is shown in Fig.1.C), loss of Ca^{2+} -channel clustering, a significant decrease in neurotransmitter release and defects in short-term plasticity (Kittel et al., 2006). These are far-reaching consequences, as it is known that the anatomical association of SVs (that are associated to the T-bar) and voltage-gated Ca^{2+} -channels (VGCCs) are mandatory for effective excitation-secretion coupling.

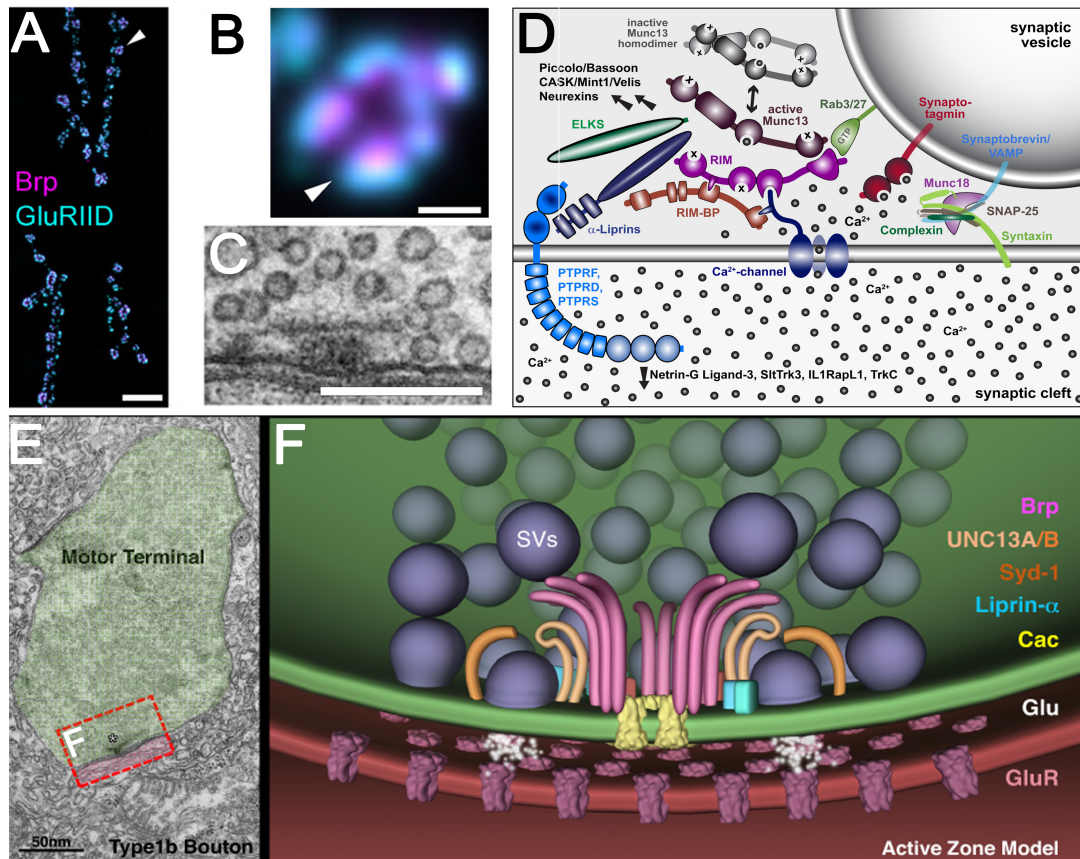


Figure 1 | Histological and functional parts of the active zone

(A) Confocal image of neuromuscular junction with specific staining for Brp (magenta) and postsynaptic GluRIID subunit staining (cyan). Arrowhead indicates enlarged region shown in B. Scale bar = 10 μ m. (B) Confocal image of single bouton with staining like in A. Arrowhead indicating GluRIID. Scale bar = 1 μ m (C) Electron microscopy images of T-bar structure of an AZ. Scale bar = 200 nm. (D) Scheme of vertebrate active zone proteins demonstrating their variety and their multiple interaction patterns. (E) Electron microscopy image of a type 1b bouton (green) displays a site of synaptic neurotransmitter release, or active zone (red box inset F corresponds to cartoon in panel F). Asterisk marks T-bar structure. Scale bar = 50 nm. (F) Active zone model as found on mature NMJ. Proteins are in coloured in accordance to their names. (A,B,C) Taken and modified from Ehmann et al. (2015) (D) Taken and modified from Südhof (2012). (E,F) Taken and modified from Van Vactor & Sigrist (2017)

Besides fathoming Brp function, structure of Brp has been intensively studied and elucidated in the last decade. Brp weighs around 200 kDa and consists mainly of an elongated filament where the N-term is fixed at the presynaptic membrane (Fouquet et al., 2009; Ehmann et al., 2014). The C-term reaches into the cytosol of the bouton and is the main structure where synaptic vesicles are tethered (Fouquet et al., 2009) (cf. Fig 1.F). These structures appear as a T-bar in electron microscopy imaging (cf. Fig. 1.C,E). The described histological features of the active zone have been found by employing several different microscope techniques over the recent years. Initially, the T-bar structure was discovered by employing classical electron microscopy (Atwood et al., 1993). Then, it could be demonstrated that Brp forms a torus or donut shaped structure (Kittel et al. 2006) by using subdiffraction resolution STED (stimulated emission depletion) fluorescence microscopy. Subsequently, by employing electron microscopy of high-pressure freezed (HPF) preparations, it could be shown that Brp molecules are most likely to be clustered in 10-nm filaments (Jiao et al., 2010) (cf. Fig. 1.C). Recently, by using dSTORM (direct stochastic optical reconstruction microscopy), it was found that each T-bar is composed of ~137 Brp molecules (Ehmann et al., 2014). The dSTORM imaging disclosed a increasing size of the CAZ from proximal to distal that also appeared to be functionally relevant (Ehmann et al., 2014).

Even though Brp acts as an essential protein at the AZ, there are also many other important components moulding the CAZ. For instance, lack of RIM-binding protein (RBP; forms the ring of the Brp core) leads to irregular T-bars, reduced density of SVs and Ca^{2+} -channel clustering (Liu et al., 2011). Moreover, defects in Syd-1 and Liprin-alpha lead to misfolded or ectopic T-bars and malpositioning of the transsynaptic adhesion protein Neurexin (Nrx). Hence, appropriate positioning of pre- and postsynapse is impaired because Nrx is needed for PSD organisation and apposition of postsynaptic receptors (Kaufmann et al., 2002; Fouquet et al., 2009; Oswald et al., 2010, 2012). But this is only an excerpt of the proteinaceous variety of the CAZ. (Südhof, 2012; Van Vactor & Sigrist, 2017) (cf. Fig. 1.B,F).

At the postsynaptic side highly specified morphologies can be observed as well. As an important morphological part the postsynaptic membrane forms the subsynaptic reticulum (SSR) that is characterised by multiple invaginations to extend its surface (Johansen et al., 1989). Just as clusters of specialised proteins in the presynaptic membrane, there are important protein clusters at the postsynaptic side. Here, disc large (Dlg) is one essential component, which is part of the membrane associated guanylat kinase (MAGUK) family (Elias and Nicoll, 2007; Zheng et al., 2011). At the SSR it participates in recruitment of other SSR-proteins and the formation of the SSR itself (Zito et al., 1997; Gorczyca et al., 2007; Thomas et al., 2012).

At the *Drosophila* NMJ, further crucial postsynaptic components are the excitatory ionotropic glutamate receptors, each consisting of four out of five possible subunits (GluRIIA-E) (Schuster et al., 1991; Petersen et al., 1997; DiAntonio et al., 1999; Featherstone et al., 2005; Qin et al., 2005). Whereby a single receptor consists of either GluRIIA (A-type) or GluRIIB (B-type) combined with GluRIIC-E that are indispensable for receptor function. The specific combination is crucial to determine functional parameters, since subunit composition affects desensitisation (DiAntonio et al., 1999). Moreover, incorporation of IIA/IIB is activity dependent and influences synapse maturity (Schmid et al., 2006 and 2008). However, IIA and IIB can partially substitute each other since only complete depletion of IIA and IIB simultaneously lead to embryonic lethality (Petersen et al., 1997; DiAntonio et al., 1999; Marrus et al., 2004; Featherstone et al., 2005; Qin et al., 2005).

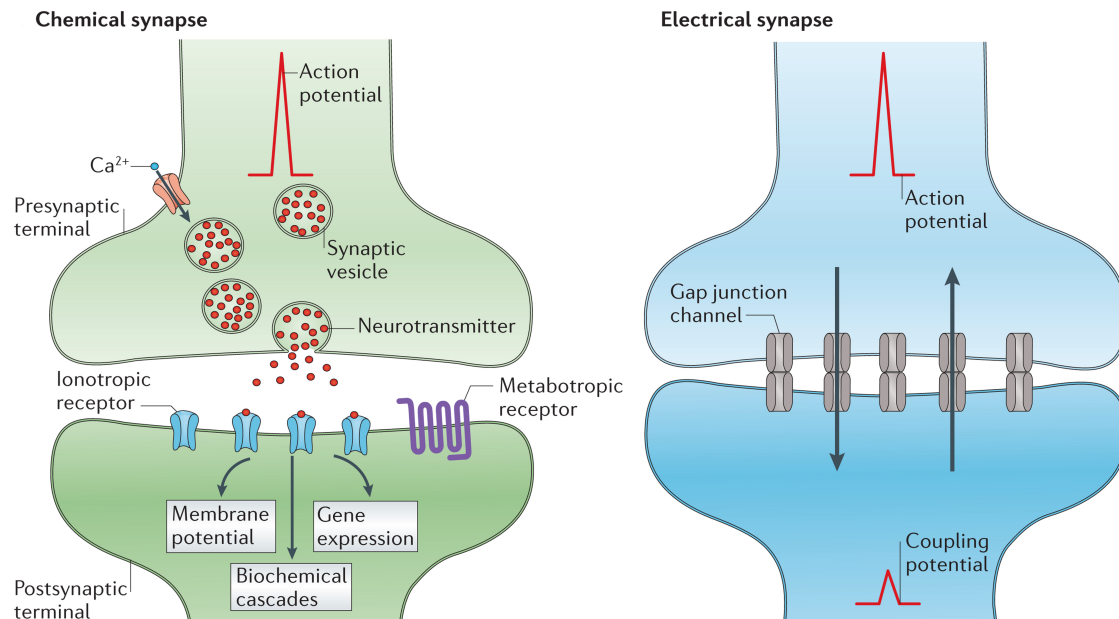


Figure 2 | Chemical synapse compared to electrical synapse

This figure illustrates differences of a chemical synapse and an electrical synapse. Most obvious differences of anatomy are sketched. The chemical synapse works mainly unidirectional, uses neurotransmitter that are emitted at the presynaptic side and bind to receptors on the postsynaptic side, whereas the electrical synapse works bidirectional via direct cell connections (gap junctions) and does not amplify the incoming electrical signal (action potential). Electrical synapses only transmit signals in contrast to chemical synapses that can induce various modulation processes at the presynapse and the postsynaptic terminal depending on expressed receptors. Modified from (Pereda, 2014).

Electrical synapses, in contrast, transmit current per continuitatem whereby two or more neurons are connected by gap junctions, which reduce resistance and facilitate current transmission (Pereda, 2014). Therefore, the synaptic cleft of electrical synapses is around ten times narrower than the cleft of chemical synapses (~3,5 nm vs. ~30nm) (Kandel et al., 2012). At electrical synapses current is transmitted instantaneously, unamplified and bidirectional due to their interim stage free transmission (Bennett and Zukin, 2004). Furthermore, no 'real' action potential is needed to trigger the following cell (Bennett and Zukin, 2004; Pereda, 2014). Due to these profound functional differences, electrical synapses can fulfil disparate tasks, chemical synapses are not suitable for. Electrical synapses can be found in great extent in neuronal networks where non-delayed signalling is highly functionally relevant. Therefore, electrical synapses are well designed to detect coincidence of simultaneous

depolarisation within coupled neuronal populations that increases neuronal excitability and enhances synchronous neuronal activation (Getting, 1974; Getting and Willows, 1974; Galarreta and Hestrin, 2001; Veruki and Hartveit, 2002; Curti and Pereda, 2004; Curti et al., 2012). A well-known example where electrical synapses are employed and indispensable, apart from the central nervous system, is the heart. Here, the neuronal network of electrical synapses is designed for a coordinated and directed excitation of the different parts of the heart tissue (Pape et al., 2010). Moreover, electrical synapses are employed to increase sensitivity of sensory systems by lateral excitation, e.g. in the mammalian retina (DeVries et al., 2002; Veruki and Hartveit, 2002). Furthermore, they are known to occur in conserved escape networks (Pereda et al., 1995; Herberholz et al., 2002; Curti and Pereda, 2004) and even in *Drosophila* absence of electrical synapses has far-reaching consequences on effective escape behaviour (Phelan et al., 1996).

This manifold and different application range of electrical and chemical synapses makes further studies of both types indispensable. Even though electrical synapses are expressed to lower extent in the nervous system, they are equally important to chemical synapses due to their highly specialised functions (Pereda, 2014). Interestingly, electrical synapses are most likely required for physiological synaptogenesis of chemical synapses (Todd et al., 2010).

1.2 Mechanosensation

Perception of our daily environment needs different sensory qualities. Defects in our sensory system may lead to massive difficulties in social participation (e.g. Usher syndrome; Domanico et al., 2015) and even to life-threatening proportions if pain sensation is impaired (e.g. SCNA9 channelopathy; Cox et al., 2006). Therefore, a profound understanding of how different sensory systems work and how they can be manipulated is strongly required to reduce effects of sensory disabilities.

Basically, recognizing a stimulus includes three main parts in the peripheral nervous system. When an adequate stimulus arrives at a sensory cell it will cause changes of the membrane potential (transduction) followed by a transformation of the incoming signals and transmission to the downstream neuron. Transduction, local depolarisation (or hyperpolarisation) of the receptor cell membrane by an occurring stimulus, is the first step of translating this input into an utilisable language for the organism. The change of the membrane potential is, due to its extent, transformed into a specific sequence of action potentials. This second step, called neuronal encoding or transformation, was primarily observed in the first half of the 20th century and matches frequency and amount of action potentials to an incoming stimulus (Adrian, 1926; Adrian et al., 1931; Loewenstein, 1959). In primary sensory neurons both steps are proceeded in one cell in contrast to secondary sensory neurons where changes in membrane potential lead to proportional transmitter release and action potentials in the downstream neuron (Kandel et al., 2012). Once the stimulus is encrypted, it is transmitted downstream to projection neurons where basic integrative processes take place. Whereby the most important mechanism is lateral inhibition to pinpoint the stimulus (Kandel et al., 2012). Afterwards the signal from several sensory neurons is transmitted to the central nervous system for further integration.

As a part of the sensory system, experiments in this thesis mainly addressed mechanosensation whereby sensation of pressure, tension, touch, vibration,

pain and proprioception are the main qualities. In mammals, there are different designed sensory endings tuned perfectly to one specific purpose (Pape et al., 2010; Kandel et al., 2012). Traditionally, they are subdivided in slowly adapting (SA) and rapidly adapting (RA) mechanoreceptors (Pape et al., 2010). SA-receptors show mainly proportional action and act as a sensor for stimulus intensity. In contrast, RA-receptors mainly react on intensity shifts as a differential receptor. However, both kinds of receptors are needed to determine a stimulus completely and to generate a better contrast. Therefore, most sensory cells perform as both SA- and RA-receptor and they are matched to each subdivision according to which type of receptor class they fit best (Pape et al., 2010). In fact, most receptors work as so-called proportional-differential-receptors (PD). When a stimulus occurs they show phasic discharges at the beginning which converts to long lasting but smaller tonic discharges (Pape et al., 2010)

An interesting example of an important PD-receptor in *Drosophila melanogaster* is the chordotonal organ that is crucial for mechanosensation, which will be explained in detail later.

1.3 *Drosophila melanogaster*

1.3.1 Background

Drosophila melanogaster, commonly known as the fruit fly, is one of the most used and modified organisms in biological research. Especially in the field of neuroscience, *Drosophila* is well established and widely capitalised to study development and physiology of synaptic systems (Kazama, 2015; Ugur et al., 2016) e.g. circadian rhythm (Konopka and Benzer, 1971; Koh et al., 2008; Ibanez, 2017) or learning and memory (Quinn et al., 1974). Moreover, these insights are not limited to *Drosophila* itself but have also huge impact on vertebrate neuroscience (Bellen et al., 2010).

There are a lot of good reasons why *Drosophila* can be found in a non-negligible amount of laboratories (and kitchens) around the world. The most obvious reason is that *Drosophila* is easy to keep and store, normally in plastic vials with egg lying medium. Due to their short life cycle *Drosophila* need to be transferred to new vials regularly to separate them from their offspring. On the other hand, the short life cycle guarantees a constant supply of enough experimental animals at the right developmental stage for investigational purposes.

The short life cycle and also an entirely sequenced genome (Adams et al., 2000) lead to a quite comfortable and easy accessible organism to work with. Moreover, a major advantage of *Drosophila* is a large number of very well described genetic tools (Bellen et al., 2010). There are well-characterised expression systems that allow targeted genetic modification in nearly any cell population. Especially the dyadic UAS-GAL4-system, derived from yeast, is broadly employed and allows targeted modification of gene expression in distinct cellular populations (Brand and Perrimon, 1993; Duffy, 2002). Over the years other two-parted expression systems have been described and are also commonly used in daily work with *Drosophila melanogaster*, e.g. LexA/LexAop and the Q/QF system (Lai and Lee, 2006; Potter et al., 2010).

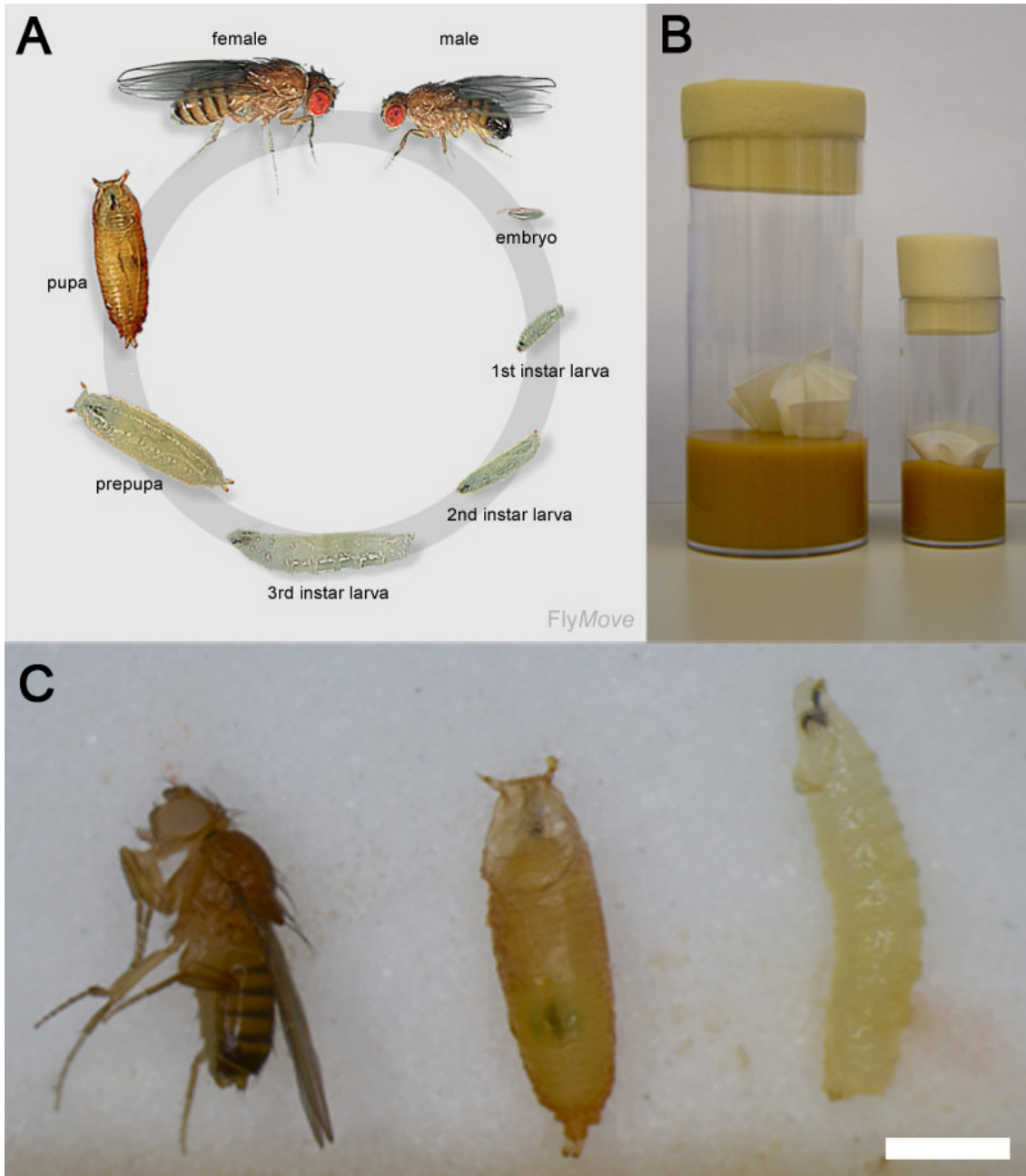


Figure 3 | Life cycle of *Drosophila melanogaster*

(A) Life cycle of *Drosophila melanogaster* modified from (Weigmann et al., 2003) at 25°C. (B) Big and small vial normally used for breeding and keeping of *Drosophila* flies and larvae. (C) Arrangement of adult *Drosophila* fly (female), pupa and late 3rd instar larva. Genotype w^{1118} . Scale bar = 1 mm.

Additionally, the enormous amount of studies discussing behaviour, anatomy and development facilitate the detection of deviations from the common wild type fly and help to investigate genetic variations precisely. Consequently, there are many different models with determined defects, even mimicking human

neurological deficits, e.g. nociception deficits, amyotrophic lateral sclerosis, attention deficit hyperactivity disorder or even Parkinson's disease. (Tracey et al., 2003; Ratnaparkhi et al., 2008; van der Voet et al., 2015; West et al., 2015).

Figure 3.A shows the life cycle of *Drosophila melanogaster* at 25°C. Here, egg embryogenesis is the first developmental leap that lasts for about 24 hours until the first instar larva hatches. From now on the main task of the larva is gathering food and growth. This period lasts about four days and includes big developmental steps, from first instar to second instar and, finally, to third instar larvae. The two days old third instar larvae start wandering in search of a dry place where they can pupate. After a four-day long metamorphosis as a pupa the adult fly ecloses. Female flies are slightly bigger than males and nearly twice as heavy (1,4 mg vs 0,8 mg). Already 12h after eclosing the female flies are fertile and the life cycle can start anew. (Stocker and Gallant, 2008)

1.3.2 Neuromuscular junction (NMJ)

Watching *Drosophila melanogaster* larvae crawl can be quite delightful. Even if you think of how many single steps have been taken until only one single muscle contracts (initiation of the signal in the VNC, transmission to and along the motoneuron axon and finally signal transmission at the neuromuscular junction). Furthermore, how perfectly aligned and timed contractions of the muscle system lead to coordinated movements in a certain direction. An essential part of this process is the neuromuscular junction (NMJ), the junction between neuronal system and muscle tissue. Following its first detailed physiological description in 1976 (Jan & Jan 1976a) its anatomy and function are meanwhile well described and fundamentally understood (Menon et al., 2013).

The formation of the larval NMJ is an important part of embryogenesis. It begins with the outgrowth and morphological transition of the axons from the VNC as a flat growth cone and a directed formation of axonal varicosities to the

predetermined muscle (Yoshihara et al., 1997). This initial process is followed by a more defined formation of synaptic branches (Schuster et al., 1996; Zito et al., 1999). Distinct formation of the *Drosophila* NMJ begins 13 hours after egg laying when the innervating nerve has established first contact to the muscle surface and ends after 22 hours when full functionality is achieved (time intervals for 25°C ambient temperature) (Broadie and Bate, 1993; Saitoe et al., 1997). During larval development the arborisation of synaptic varicosity increases 5- to 10-fold (Keshishian et al., 1993; Harris and Littleton, 2015) and an elevated amount of synapses as well as an increased quantity of vesicles per bouton can be found due to an 100-fold increase of the muscle surface (Schuster et al., 1996; Prokop, 1999).

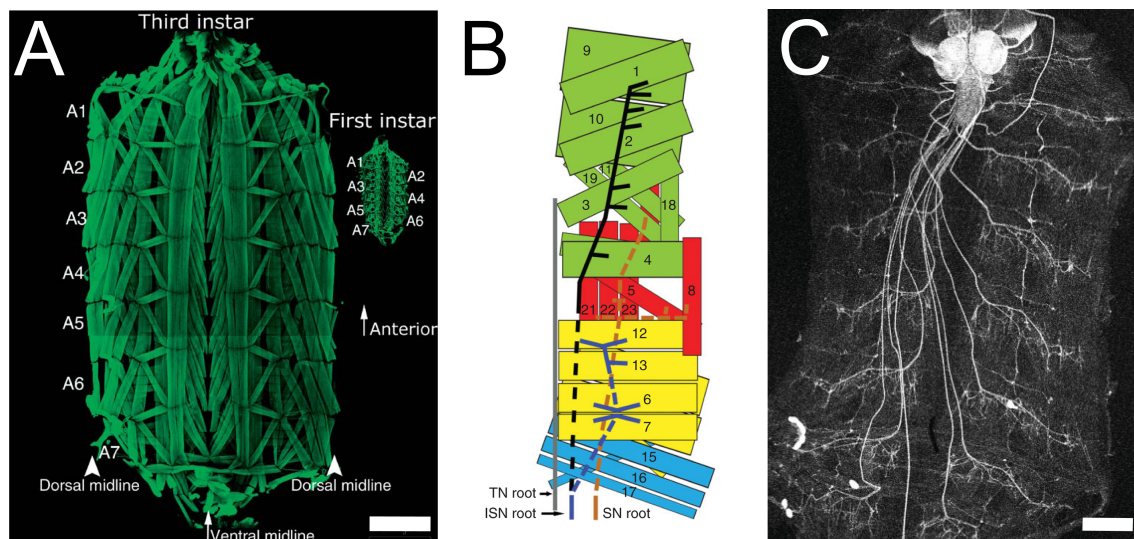


Figure 4 | Anatomy of *Drosophila* body wall and neuronal arrangement

(A) FITC-conjugated Phalloidin staining of larval body wall preparations. Showing third instar larva compared to first instar larva. Scale bar 500 μ m. Modified from (Gorczyca and Budnik, 2006). (B) Schematic representation of the three nerve roots: the intersegmental nerve (ISN), the segmental nerve (SN), and the transverse nerve (TN), and their respective innervation patterns. (C) Third instar larval body preparation expressing green fluorescent protein (GFP) in all motoneurons. Scale bar 250 μ m. (B,C) Modified from (Menon et al., 2013).

For investigational purposes different time points and muscles can be chosen. Depending on the scientific issue, analysis of a late embryonic or a mature NMJ of a third instar larvae is commonly performed (Kittel et al., 2006; Ehmann et al., 2014). Moreover, the investigator can choose between several well-described

NMJ to address a certain scientific question specifically. Often, synaptic function of muscle 6/7 is studied in different experimental setups due to their exposed localisation in ventral longitudinal body wall musculature making this pair of muscles easily accessible (Jan & Jan, 1976a ; Harris & Littleton, 2015). The stereotypic nerve muscle arrangement allows to distinguish each muscle based on its positioning in the common larval preparation and, thus, to perform electrophysiological measurements at the NMJ (Fig. 4.A-C). The ventral longitudinal body wall muscles (VLM) 6/7 are innervated by two mainly glutamateric motoneurons (Jan & Jan 1976b), MN6/7-Ib and MNSN b/d-Is, whereby MN 6/7 forms Ib (big, 3-6 μ m) boutons similar to tonic motor neurons (Atwood et al., 1993) and MNSN b/d forms Is (small, 2-4 μ m) that are assumed to be more phasic nerve endings (Atwood et al., 1993; Hoang and Chiba, 2001; Harris and Littleton, 2015).

Aside from widespread type I motoneurons, *Drosophila* muscles are also innervated by type II or type III motoneurons (Hoang and Chiba, 2001). Type I motoneurons employ glutamate as their common neurotransmitter, even though peptidergic co-transmission can be assumed (Anderson et al., 1988; Zhong and Peña, 1995). Type II motoneurons form smaller boutons (~1 μ m) but spread over a larger area of muscle surface and possess more branches. In contrast to type I motoneurons type II motoneurons use octopamine as an additional neurotransmitter to glutamate (Monastirioti et al., 1995). Lastly, there are type III motoneurons that are known to form a synaptic connection only with muscle 12 and are receptive for insulin-specific antibodies (Gorczyca et al., 1993). These motoneurons are glutamateric and peptidergic and form as a morphological mimic of Is and II MNs even though they only match to one specific muscle (Hoang and Chiba, 2001).

1.3.3 Chordotonal organ (ChO)

The previously described neuromuscular system is the basic prerequisite for directional movement of adult *Drosophila* and larvae. But the ability to move is quite useless if you don't know where to go. Therefore *Drosophila melanogaster*

has a sophisticated mechanosensory system that includes the chordotonal organ (ChO), a proprioceptor, which has been studied very intensively lately (Lee et al., 2010; Zhou et al., 2012; Scholz et al., 2015, 2017; Langenhan et al., 2016; Prahlad et al., 2017). The ChO is also involved in perceiving temperature changes or sound (Liu et al., 2003; Kwon et al., 2010; Zhang et al., 2013; Scholz et al., 2017). Additionally, the larval ChO is the physiological counterpart to the Johnston organ of adult flies that is located in the antenna and works as a multimodal mechanoreceptor to sense mechanical stimuli, like wind and gravity, but also sound (Zhang et al., 2013).

Anyhow, chordotonal organs are not exclusive to *Drosophila melanogaster*. Due to their multiple functionality they are common mechanoreceptors and important parts of the auditory system in other insects and arthropods (Yack, 2004). Even though, the anatomical arrangement of chordotonal neurons can vary. For example, in *Drosophila melanogaster* there are 'single' chordotonal neurons and 'clustered' chordotonal neurons whereby only the 'clustered' neurons form the chordotonal organ or lch5 (it consists of five chordotonal neurons)(cf. Fig. 5.C,D). The anatomy of each chordotonal neuron does not vary noticeably whether they are 'clustered' or not. The configuration of the lch5 is as follows: Bipolar neuronal cells are located at the bottom of the ChO projecting directly uncrossed into the larval VNC (Langenhan et al., 2016; Tsubouchi et al., 2017). The dendrite directly runs into a specialised structure that surrounds all incoming dendrites – the scolopale cell. Upon the dendritic tip a cilium is placed and mechanically fixed to the cap cell (dendritic cap), which itself is anchored to the inside of the larval cuticle. Moreover, an important protein is located in the membrane of the cilium, Latrophilin (LPHN/*CIRL*)(Langenhan et al., 2016). In *Drosophila melanogaster* the homologue to the *CIRL* protein (expressed in vertebrates) is called *dCIRL* (Südhof, 2001; Yack, 2004; Scholz et al., 2015; Langenhan et al., 2016).

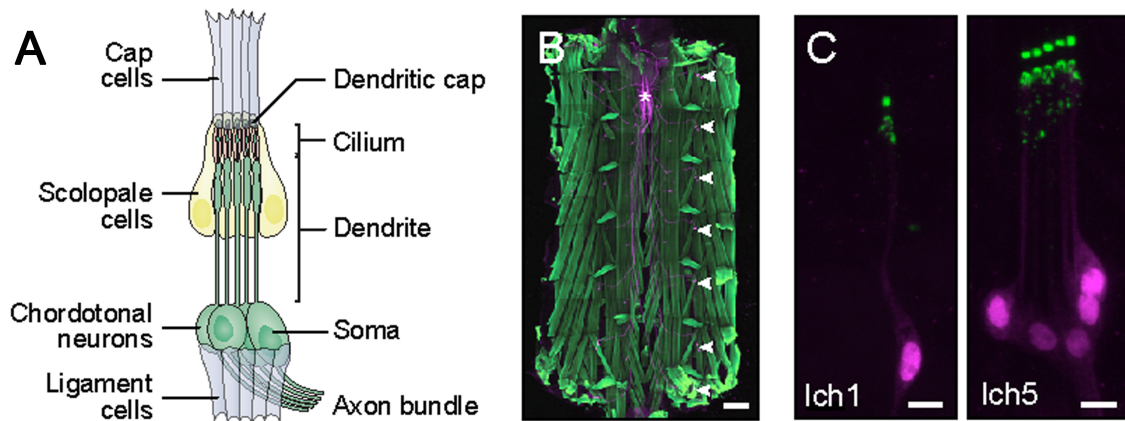


Figure 5 | Anatomy of the chordotonal organ

(A) Anatomical sketch of the pentascolopodial organ (lch5) with designation of the main structures. (B) Location of larval chordotonal organs visualised by an *iav-GAL4* (inactive-GAL4) promoter element (anti-GFP, magenta). Counterstaining of the body wall muscles with phalloidin (green). Arrowheads indicate seven of eight lch5 on one side of the larva. As denoted by the asterisk Cho have traceable projections into the larval VNC. Genotype: *iav-Gal4* > UAS-EGFP. Scale bar 200 μ m. (C) The *dCirlp^{GAL4}* driver demonstrates neuronal expression of *dCirl* within a solitary chordotonal neuron (lch1) and an lch5 (anti-GFP, magenta) with a counterstaining of anti-HRP (horse radish peroxidase; green). Genotype: *dCirlp^{GAL4}* > UAS-GFP::nls. Scale bar = 5 μ m. (A) Adapted from (Scholz et al., 2017). (B) Same recording as shown in (Langenhan et al., 2016). (C) lch5 adapted from (Scholz et al., 2017); lch1 recorded by M. Nieberler and shown here with permission.

This protein is called latrophilin due to its sensitivity to α -LTX (α -latrotoxin; the toxin of the black widow spider, that is known to lead to exocytosis (Südhof, 2001)). It has been found to be important for effective proprioception and sound perception mediated by the larval chordotonal organ, but dispensable for perception of temperature (Krasnoperov et al. 1997; Südhof 2001; Scholz et al. 2015 & 2017). Latrophilin itself is part of a subclass family of G-Protein coupled receptors (GPCR), the adhesion-GPCRs (aGPCR) that are distinguished by a long amino-terminal extracellular domain (ECD) also employed for 'cell-cell-interaction' and a unique GPCR-Autoproteolysis-INDucing (GAIN) domain inside of the ECD (Krasnoperov et al., 1997; Araç et al., 2012). Like other GPCRs, aGPCRs have a seven-transmembrane domain (7TM) and an intracellular domain (ICD) to couple and interact with G-proteins (Hamann et al., 2015).

Besides *dCIRL*, there are also other proteins, transient receptor potential (TRP) channels, like NOMPC (no membrane potential C; TRPN channel; mediates

touch-sensation and partly sound response), NANCHUNG and INACTIVE (TRPV channel; absence of each leads to larval deafness) that are crucial for full functionality of the ChO (Walker et al., 2000; Gong et al., 2004; Liu et al., 2007; Zhang et al., 2013). These channels are important to sense intrinsic and extrinsic signals and stimuli, for example touch and hygrosensation (Clapham et al., 2001; Minke and Cook, 2002; Liu et al., 2007).

Furthermore, the chordotonal organ of *Drosophila melanogaster* offers numerous possibilities to address a variety of scientific issues. Particularly, ChOs work as an appropriate model to investigate different components of the sensory system in great detail.

1.4 Optogenetics and its usage

Francis Crick, one of the discoverers of the molecular DNA structure (Watson and Crick, 1953), stated just pre-millennial: ‘What is really needed is something with *regional specificity*, which acts on only *special types of neurons* and also has *temporal precision*.’ In this context, he thought of ‘some method’ with which one ‘can turn a gene on and off in a mature animal, by *some signal* or another.’ He also mentioned the possibility to employ light to obtain control over distinct neuronal populations, but called this idea ‘far-fetched’ at the same time (Crick, 1999). Interestingly, from our current point of view employing light is not ‘far-fetched’ at all and nowadays known as optogenetics.

The outset of optogenetics goes back in history approximately 150 years when Andrei Sergeyevich Faminzin found that *Chlamydomonas* locomotion was determined by light and its intensity (Faminzin, 1866). Subsequently, it took around 100 years until the first potential “optogenetic tools” were described, but not in the context of optogenetic issues. These “tools” were bacteriorhodopsin, an H⁺-pump microbial rhodopsin (Oesterhelt and Stoeckenius, 1971) and the light-sensitive chloride-pump Halorhodopsin (Hegemann et al., 1985). Around that time, it could be shown that “a rhodopsin” works as a photoreceptor in *Chlamydomonas reinhardtii* (Foster et al., 1984; Harz and Hegemann, 1991). Finally, three years after the statement of Francis Crick, Georg Nagel and colleagues could demonstrate that the photoreceptor-like sequence they found in the Kazusa cDNA database has channel-like behaviour. These light-inducible cation channels were termed Channelrhodopsin-1 and 2 (ChR1, ChR2) (Nagel et al., 2002 and 2003).

Interestingly, around 2002 a first approach was already successful in sensitising cultured neurons to light. In this attempt co-expression of the *Drosophila* photoreceptor genes encoding arrestin-2, rhodopsin and the alpha-subunit of the cognate heterotrimeric G protein, termed “chARGe” was employed (Zemelman et al., 2002) however, this construct was quite slow compared to a light-sensitive channel protein. Another approach to sensitise neurons to light

was chosen by Lima & Miesenböck in 2005. They designed a 'key-and-lock mechanism' consisting of the ionotropic purinoceptor P2X₂ ('the lock') and ATP stored in the cell ('the key') that was released if green light was applied and, thus, triggered light evoked eEPSCs (Lima and Miesenböck, 2005) in *Drosophila* motoneurons. Subsequently, the "breakthrough" came with expression of ChR2 in mammalian (and invertebrate) neurons where an excellent temporal precision, light sensitivity and a comparatively easy opportunity to precise expression could be shown (Boyden et al., 2005; Nagel et al., 2005). Just one year later ChR2 was successfully used in brain slices of mammals and the term "optogenetics" was defined (Deisseroth et al., 2006; Zhang et al., 2006). In the same year, ChR2 was already used to control complex behaviour in *Drosophila melanogaster* (Schroll et al., 2006). Moreover, after ChR2 was shown to work sufficient in an intact mammalian brain, *in vivo* (Arenkiel et al., 2007), many open questions in neurophysiology could be addressed more comfortably. For example, even complex networks like a amygdala–midbrain–medullary circuit (responsible for freezing behaviour and evolutionarily conserved response to threat) could be described and investigated in detail by using an optogenetic approach (Tovote et al., 2016). Interestingly, since 2007, publications related to the term 'optogenetics' increased tremendously (Fig. 6.C). By the way, in 2008 it could be shown that ChR1 is required for photophobic response in *Chlamydomonas* (Fig. 6.D,E) (Berthold et al. 2008), a behaviour observed by Faminzin 150 years ago (Faminzin, 1866).

Nowadays, ChR2 is the best-studied and most used Channelrhodopsin and thus its kinetics are quite well understood (Schneider et al., 2015). But even though, Georg Nagel et al. were initially able to show that Channelrhodopsin has determined non-specific cation selectivity $H^+ \gg Na^+ > K^+ \gg Ca^{2+}$ with a significant conduction preference for protons (Nagel et al., 2002 and 2003) it was unclear where the *pore* was localised. Therefore, research on novel ion-selective ChR2s was hampered until the description of the crystalline structure

of the chimera C1C2 could facilitate investigations on this crucial topic (Kato et al., 2012).

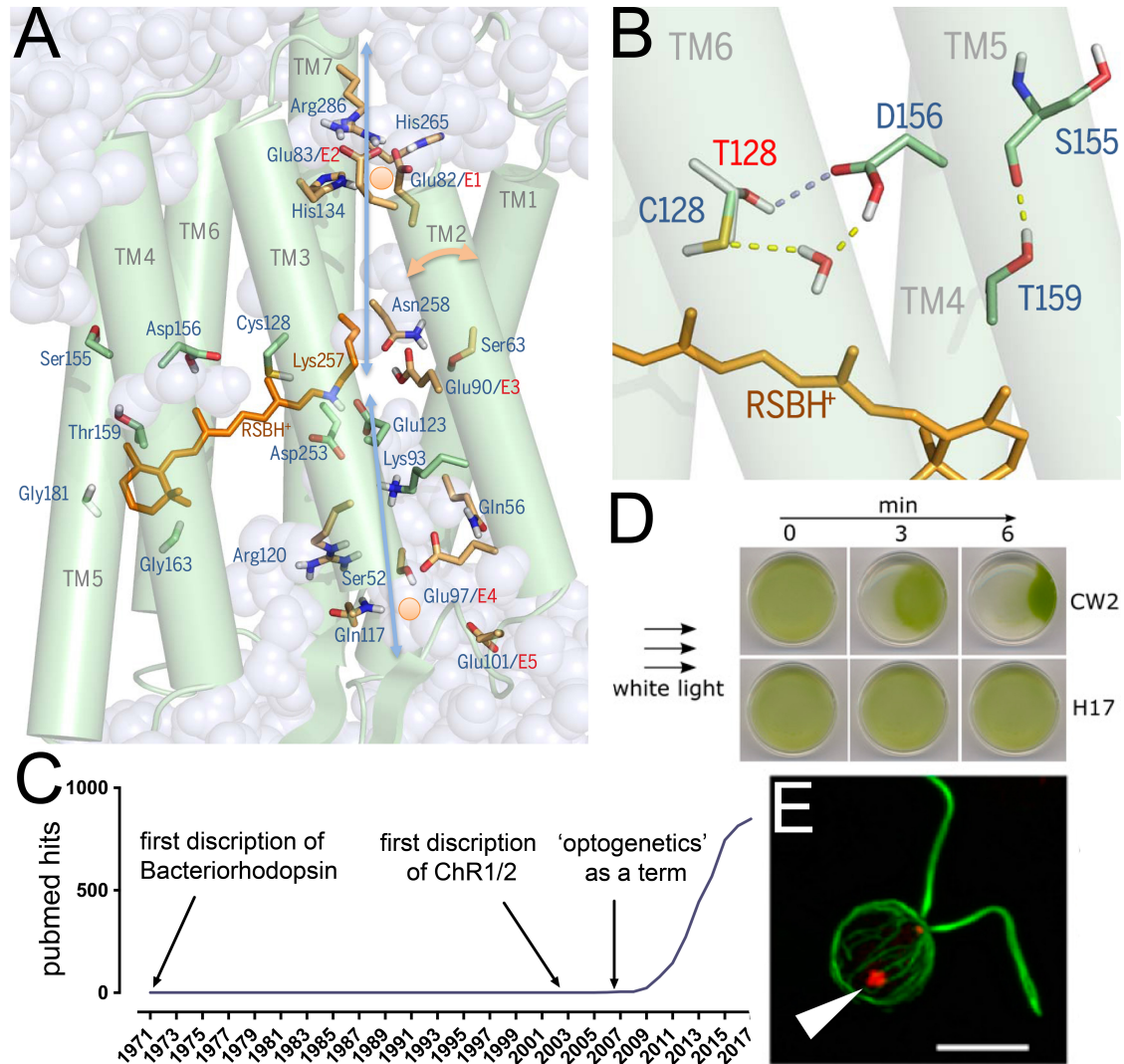


Figure 6 | Channelrhodopsin, optogenetics and *Chlamydomonas*

(**A,B**) Visualisation of C1C2 (functional chimera of ChR1 and ChR2) crystal structure. Enlarged view of the hydrogen bond where D156 has been replaced by a histidine in Channelrhodopsin2-XXM. (**C**) Graph indicating increasing number of hits for the term 'optogenetics' on pubmed (cf. Deisseroth 2011). Requested from pubmed on 11/2017. (**D**) Experiments to test phototaxis and photophobic response of *Chlamydomonas reinhardtii* at 7 W/mm² in presence (CW2, cell wall deficient strain) and reduced expression of ChR1 (H17). Indicating that ChR1 is necessary for photophobic behaviour in *Chlamydomonas*. (**E**) Single *Chlamydomonas* wildtype stained against ChR1 (red) that is expressed at the eyespot (arrowhead) and alpha tubulin (green). Scale bar 10 μ m. (**A,B**) adapted from (Deisseroth and Hegemann, 2017). (**D,E**) adapted and partly modified from (Berthold et al., 2008).

Now, the distinct structure of ChR2 is well known. The complete Channelrhodopsin-2 protein contains 737 amino acids whereby the complete photocurrent functionality is localised within the amino-terminal of approximately 300 amino acids that also form the seven trans-membrane domains at the N-terminal end (Nagel et al. 2003; Kato et al. 2012). The important chromophore, *all-trans-retinal* (ATR), is localised in the *retinal binding pocket* (RBP) and bound covalently to the protein back-bone via Lysine 257 (Fig. 6.A; Kato et al., 2012). It is crucial to protect Channelrhodopsin from fast (light-induced) degradation and opens the channel by a conformational change. Additionally, ATR has to be present while Channelopsin is about to bind to the cellular membrane (Channelopsin + chromophore = Channelrhodopsin). The reason is that a later presence of ATR leads to the same level of Channelopsin degradation as if ATR would not be present at all, except for certain ChR-mutants (Ullrich et al., 2013). Furthermore, an important structure of Channelrhodopsin-2 is the possible hydrogen bond between C128 and D156 in Helix 3 and 4 as it has been shown to be highly relevant for the lifetime of ChR2's conducting state (Fig. 6.A,B). Modifications at this determined structure result in ChR2 variants with multiple changes in physiological functionality (Berndt et al., 2009; Bamann et al., 2010; Dawydow et al., 2014; Scholz et al., 2017).

Apart from that, there are many different ChR descendants with altered open-state lifetimes, shifted absorption spectra, altered desensitization, better expression with increased photocurrent magnitude, amended photochemistry and even change of conductivity from cations to anions (Berndt et al., 2009, 2011, 2014; Wen et al., 2010; Gunaydin et al., 2010; Kleinlogel et al., 2011; Lin et al., 2013; Wietek et al., 2014; Dawydow et al., 2014; N C Klapoetke et al., 2014; Schneider et al., 2015; Scholz et al., 2017; Krause et al., 2017). Surprisingly, shortly after two working groups could attain changing the cation selectivity of Channelrhodopsin to anion selectivity (Berndt et al., 2014; Wietek et al., 2014), very effective naturally occurring anion selective light-sensitive channels were found in the alga *Guillardia theta* (Sineshchekov et al., 2015;

Govorunova et al., 2016). These mainly Cl⁻ conducting GtACRs (*Guillardia theta* anion-conducting Channelrhodopsin) turned out to be very effective as inhibition tools.

Moreover, there are metabotropic optogenetic tools that allow interfering with second messenger pathways by modifying the amount of cAMP (cyclic adenosine monophosphate, Stierl et al. 2011) or cGMP (cyclic guanosine monophosphate, Gao et al. 2015), which facilitates studies on main second messenger pathways. Especially, investigation of effects caused by changes in second messenger concentrations in a distinct cellular population is hardly possible *in vivo* without using optogenetic tools. As an example, it could be shown that the intracellular level of cAMP regulates the sensitivity of the chordotonal organ in *Drosophila melanogaster* (Scholz et al., 2017) by using bPAC (*Beggiatoa* photo-activated adenylate cyclase; increases intracellular cAMP level) (Stierl et al., 2011).

To sum up, optogenetics itself and especially the associated tools have seen tremendous improvements over the last decade – making optogenetic approaches simpler to realise and delivering a remarkable variety of tools to address different (neuro-)physiological questions.

1.5 Motivation of the study

Despite intensive studies on the chordotonal organ of *Drosophila melanogaster*, a recently described protein involved in signal perception, *dCIRL* (Scholz et al., 2015), remains understudied. It could be shown that loss of *dCIRL* leads to impaired perception of tactile, proprioceptive and auditory stimuli in *Drosophila* larvae (Scholz et al., 2015). However, little is known about how *dCIRL* is involved in signal transmission or perception of stimulus modalities. In contrast, many other proteins that mediate sensitive perception have been studied comparatively well (Gong et al., 2004; Lee et al., 2010; Yan et al., 2013; Zhang et al., 2013). To close this research gap, a combined approach of optogenetics and classical electrophysiology techniques was chosen to investigate distinct functions of *dCIRL* on signal transmission.

Since it is known that the ChO is sensitive, inter alia, to thermal changes (Liu et al., 2003) we searched for a very light sensitive Channelrhodopsin that also offers high resolution in time. Even though there is a great variety of different microbial opsins, most of these excitatory optogenetic tools need high light intensities to work efficiently (Nagel et al. 2003; Zhang et al. 2008; Gunaydin et al. 2010; Kleinlogel et al. 2011; Lin et al. 2013; Klapoetke et al. 2014) or, if they work at low light intensities, lack temporal precision (Dawydow et al., 2014). For this reason, research has been conducted to find next-generation microbial opsins that offer improved light-sensitivity to minimise possible thermal cell damage and heat side effects due to high light irradiation (e.g. direct stimulation of thermosensitive structures like the Cho). Moreover, temporal precision is an important requirement to interfere physiologically with neuronal cells, like the chordotonal organ.

In this study, a new Channelrhodopsin2 descendant, Channelrhodopsin2-XXM (ChR2^{XXM}), with improved light sensitivity and high temporal resolution is characterised and described. ChR2^{XXM} was employed to interrogate the ChO of *Drosophila* regarding the physiological functions of *dCIRL* and its effect on signal transmission.

Furthermore, a recently discovered light sensitive optogenetic inhibitory tool, called GtACR (Sineshchekov et al., 2015), was tested for its effectiveness at the *Drosophila* NMJ. Specifically, GtACR was checked for functionality at the *Drosophila* NMJ and possible side effects.

2 Materials and Methods

2.1 Fly stocks

For this study the following genotypes were employed and created (*).

RJK013, w^- ; *ok6-GAL4 w⁺* (2nd)

RJK021, w^+ ; *G7-GAL4 w⁺* / *CyO*

RJK382, w^{1118} ; *PBac{y⁺-attP-9A}VK00018 UAS -GtACR::YE [w⁺]/CyO*

RJK384, w^{1118} ; *PBac{y⁺-attP-9A}VK00018 UAS -GtACR::Flag [w⁺]/CyO*

Ch4, w^{1118} ;; *UAS-chop2³¹⁵/CyOGFPw⁻*

RJK200, w^{1118} ; *PBac{yellow⁺-attP-9AChop2_D156C(XXL)=pRK010w⁺}*
/CyOGFP(w⁻);;

RJK255, w^{1118} ; *PBac{yellow⁺-attP-*
9AChop2_D156C(XXL)::tdtomato=pRK010w⁺} / *CyOGFP(w⁻)*;

RJK258*, w^{1118} ; *{w⁺mC=pTL538[chop2-D156H(XXM)]}attP^{VK00018}/CyO*;

RJK300*, w^{1118} ; *{w⁺mC=pTL537[chop2D156H(XXM)::tdtomato]}attP^{VK00018}*
/CyOGFP(w⁻);

LAT112, w^{1118} ; *+/CyOGFPw⁻; P{UAS-iav-Gal4}[attP2]/TM6B, Tb*

Stocks of *Drosophila* flies were raised in transparent plastic tubes 10.5 cm (height) x 4.6 cm (diameter) filled with common laying medium and additionally some dry baker's yeast (Big vial in Fig. 2.B). Normally a paper filter was placed into the laying medium to extend the dry surface whereon 3rd instar larvae can pupate.

Fly crossings for experimental use were set up with initially around 21 virgins and 7 males in transparent fly tubes 6.4 cm (height) x 2.6 cm (diameter) which were covered with (small vial in Fig. 2.B) red plastic foil or aluminium foil, depending on the expressed ChR variant. The laying medium was covered with a small paper filter to prevent adult flies from sticking to the food.

Drosophila flies expressing Channelrhodopsin2-XXM, Channelrhodopsin2 wild-type or GtACR^{YE} received a supplementation of *all-trans-Retinal* (ATR) for a

more sufficient expression and reduced degradation of these constructs. ATR was added to the common laying medium and blended smoothly. This way, the larvae can ingest the ATR into their system where it is built into the opsin protein. Larvae were raised to 3rd instar level at 25 °C and on food containing 100 µM ATR. Moreover, if Channelrhodopsin2 was used, a “shortened” Channelrhodopsin2, called Channelrhodopsin2 wild-type, was employed, only containing the necessary 315 amino acids to reach full functionality (Nagel et al., 2003 and 2005). This “shortened” Channelrhodopsin2 is also the fundamental structure for all Channelrhodopsin2 mutants/variants described in this thesis.

2.2 Electrophysiology

2.2.1 The two-electrode voltage clamp (TEVC) technique

The main task of two-electrode voltage clamp (TEVC) is to hold the membrane potential (V_m) of the cell at its original state while recording indirect flowing currents to draw conclusions about the cell membrane conductance (TheAxonGuide, 2012). But what does that mean in detail and how is that even possible?

TEVC allows indirect measurement of cell membrane conductance. Conductance (G), inverse of resistance (R), is defined as the ratio of current (I) through and the voltage (V) across a certain membrane:

$$G = \frac{I}{V} = \frac{1}{R}$$

If the membrane potential deviates from this given potential, called command potential (V_{cmd}), due to current flow across the membrane, an equal current of inverted polarity is applied by the clamp circuitry to the cell. Indeed, the investigator measures this applied compensatory current. Thus, measuring the compensatory current and keeping the voltage 'clamped' (with a very small error) it is possible to determine the initial changes in conductance and therewith the activity of ion channels (TheAxonGuide, 2012).

The main parts of the TEVC setup are the two microelectrodes that are inserted directly into the cell (Fig. 7 B). The microelectrode wires are made of Ag (silver) and coated with a composite of Ag/AgCl (silver/silver-chloride). Electrodes are placed in glass pipettes filled up with 3M KCl (potassium chloride) solution. The salt solution provides a fluid connection from the cell to the electrode and, furthermore, the high electrolyte concentration reduces the electrode resistance (TheAxonGuide, 2012). The consequence is minimized rectifying current flow, a wider recording bandwidth and a lower voltage error. Furthermore, the high

electrolyte concentration dominates the junction potential formed between the pipette solution and the cell cytoplasm that leads to resulting junction potential that depends primarily on the mobility of cations and anions in the salt solution. This is important because anions are mainly slow large loaded proteins in the cell and cations are normally small and fast and this difference could lead to an artificially depolarised membrane resting potential. But, there is a risk that the high concentrated electrolyte solution could enter the cell and induce hyperosmotic swelling of the cell. It is possible to minimize this 'leak' by using very small tip diameters of the electrode but this also results in problems as e.g. higher noise, limited recording bandwidth and, of course, diminished current passing ability (TheAxonGuide, 2012).

The two microelectrodes themselves differ in their dedicated function, the voltage sensing microelectrode (ME1) and current-passing microelectrode (ME2). Consequently, ME2 is connected to a high gain differential amplifier that logs the differences between V_m and V_{cmd} via ME1 and the voltage of the output of this voltage source leads to current flow through ME2 into the cell and compensates the upcoming deviations (cf. Fig. 7.B). The speed of this compensation mechanism (called gain [μ], in units V/V) can be adjusted by determining how many volts the output changes for each dV between V_m and V_{cmd} . Because the time (τ) needed to charge the cell capacitance (C_m) is proportional to the resistance of ME2 (R_{p2}) and gain (μ), this gain can be used to some extent to compensate C_m and R_{p2} to improve clamp response on a voltage step (cf. Fig. A). The given formula is:

$$\tau = \frac{R_{p2} * C_m}{\mu}$$

Furthermore, another very important issue in electrophysiology is how the error of the voltage clamp occurs. This can be described in equations that take the membrane resistance (R_m) and the resistance of ME2 (R_{p2}) into account and as well show how the gain (μ) can be used to minimise the resulting error. Fortunately, it can be shown that an applied step change in the V_{cmd} causes a

change in the membrane potential identical to the current response caused by a step change in membrane conductance (TheAxonGuide, 2012). This is important to know to detect currents across the cell membrane. Therefore V_m is determined as:

$$V_m = V_{cmd} \frac{\mu K}{\mu K + 1}$$

whereas μ is the gain of the clamp amplifier and K is the attenuation of the amplifier due to R_m and the resistance of R_{p2}

$$K = \frac{R_m}{R_m + R_{p2}}$$

Hence it follows that the larger the product of μK becomes the smaller the resulting difference between V_m and V_{cmd} gets. Therefore the ideal case could be reached if μ would become infinite or R_{p2} zero. Since there is a limit how much gain can be used to obtain a useful signal, because if μ is very large oscillations occur that will cover the signal, so that assets and drawbacks have to be balanced carefully. Moreover, if K is maximised (which means that R_{p2} is minimised) it has to be evaluated how small R_{p2} can realistically become, due to the fact that very low resistance of ME2 results in a blunter micropipette that is more likely to destroy the cell membrane. As a result, balancing these different factors is fundamental for conclusive electrophysiological recordings (TheAxonGuide, 2012).

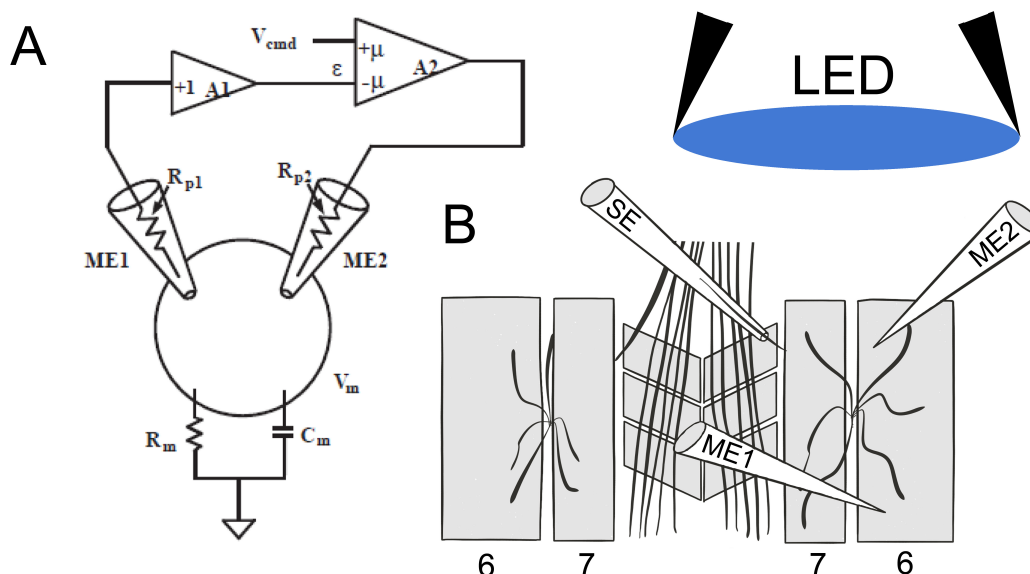


Figure 7 | Two-electrode voltage clamp circuitry

(A) Circuitry diagram of TEVC (TheAxonGuide, 2012). Via ME1 the voltage of V_m is transmitted and then recorded by a unity-gain buffer amplifier (A1). Afterwards, V_m is compared to V_{cmd} and current proportional to the difference (ϵ) is forced via ME2 into the cell. This is realised by a high-gain differential amplifier (A2; gain = μ) with a polarity of μ that the current in ME2 reduces ϵ . (B) Sketch of TEVC and light application. The suction electrode (SE) was used to trigger eEPSCs, if no Channelrhodopsin was employed. LED was used to apply light of different wavelengths (440nm / 490nm) and different light intensities directly at the *Drosophila* NMJ via an upright microscope.

There are some more limitations or difficulties known for the TEVC technique, like thermal and excess noise of the input micropipette (ME1) or capacitive coupling between the ME's. However, the two-electrode voltage clamp is a very suitable procedure for clamping large cells (like larval VLM6). Even to record large currents (in the mA spectrum) with a high resolution in time and comparatively low voltage errors. For these reasons, TEVC has become a commonly used investigation technique, especially for the late 3rd instar larval *Drosophila* NMJ (Harris and Littleton, 2015). Experiments performed in this thesis also employed a (Cool) light emitting diode (LED) to stimulate the *Drosophila* motoneuron directly via expressed Channelrhodopsins (Fig. 7.B).

2.2.2 TEVC setup for recordings in general

TEVC recordings were obtained at 22°C from the VLM 6 in anterior abdominal segments A2 or A3, of late male 3rd instar larvae. To operate on these larvae, they were dissected in ice cold Ca²⁺-free haemolymph-like solution 3 [HL-3; (Stewart et al., 1994)], described as follows: larvae were pinned down with the dorsal side facing up at head and tail. Then an initial transversal cut was made right before the tail, only severing the dorsal part of the larvae. A longitudinal cut along the dorsal midline of the larva was made and the larva was gently stretched, forming a rectangle, with four insect pins. Internal organs were removed carefully in total and then the segmental nerves were cut near the ventral nerve chord and kept long enough to facilitate effective stimulation via suction electrode.

HL-3	pH was adjusted to 7.2 by 1 M NaOH
70 mM NaCl	1.06404, Merck
5 mM KCl	1.04933, Merck
20 mM MgCl ₂	1.05833, Merck
10 mM NaHCO ₃	S6297, Sigma Aldrich
5 mM D-(+)-Trehalose	T5251, Sigma Aldrich
115 mM Sucrose	S9378, Sigma Aldrich
5 mM HEPES	54457, Sigma Aldrich
1 mM CaCl ₂	21097, Fluka Analytics

For TEVC, the ice-cold Ca^{2+} -free HL-3 solution was discarded and HL-3 at room temperature (RT; 22°C), containing 1mM CaCl_2 , was used for electrophysiological recordings.

To record evoked excitatory postsynaptic currents (eEPSCs) or extinction of eEPSCs in TEVC mode, sharp micropipettes filled with 3 mM KCl and resistances of 10-20 M Ω (Kittel et al., 2006; Wagh et al., 2006) were employed. All cells chosen for analysis had resting potentials from -50 mV down to -80mV, and input resistance of ≥ 4 M Ω . For recording the cells were clamped at -60 mV. Data were acquired with an Axoclamp 900A amplifier (Molecular Devices), signals were sampled at 10 kHz, low-pass filtered at 1 kHz and analysed with Clampfit 10.2 (cf. Scholz et al., 2017).

Furthermore, if eEPSCs were obtained under light irradiation, a LED was utilised at different wavelengths (440nm, 490nm) and light intensities (1 $\mu\text{W}/\text{mm}^2$ up to 40 $\mu\text{W}/\text{mm}^2$). The light was applied via the upright microscope (Olympus BX51WI, 40x water-immersion lens), covering the viewable area the investigator adjusted previously (cf. Scholz et al., 2017).

2.3 Confocal microscopy

2.3.1 Basics of confocal microscopy

Microscopy is one of the most important techniques of today's biomedical science. The use of conventional microscopy (or rather light microscopy) is limited due to focusing problems in biology specimens leading to blurred images. The solution of this problem is called confocal microscopy where an additional pinhole diaphragm is placed in the optical path to eliminate light coming from beyond the intended focus level (Fig 8.A) (LSM5Manual, 2005). Therefore, an image recorded with a confocal microscope consists of many slices (z-planes) of a certain extent and each recorded slice has an improved contrast and a minimized blur compared to whole image recording by conventional microscopy. As a result the final images appear very clear and can also be used for quantification of changes in protein levels, for example at the *Drosophila* NMJ (Kittel et al., 2006; Ehmann et al., 2014).

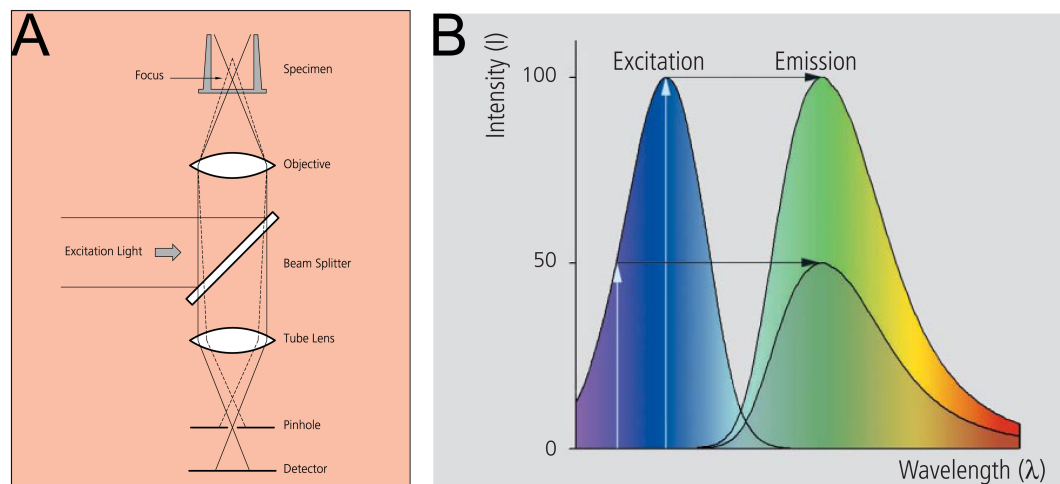


Figure 8 | Confocal microscopy

(A) Schematic simplified illustration; depicts principle of laser scanning confocal microscopy. (LSM5Manual, 2005) (B) Example graph of difference between excitation wavelength and resulting emission that is recorded during confocal imaging (Modified from LSM5Brochure 2005).

To distinguish one protein from others a distinctive staining is necessary. Therefore, compounds of fluorescent proteins bound to antibodies, which in turn

bind to certain biological structures, are employed. Subsequently, the fluorescent protein is stimulated with a distinct wavelength and the detector of the microscope records the resulting emission that has a longer wavelength with less energy (cf. Fig 8.B). Staining with more than one fluorescent compound is possible and usually applied, but in this case it is very important to ensure that the excitation/emission wavelengths have a minimum overlap among the different fluorescent compounds, especially the peak-emissions. Otherwise, excitation of one compound also leads to excitation of the other compound and an overlapping incoming signal in the detector that as a result leads to a diminished distinguishability of the different structures. If fluorescent proteins are employed, as described above, the imaging technique is called epifluorescence microscopy.

Out of this reason it is very important to choose the right fluorescent compounds to reach a high resolution.

2.3.2 Immunohistochemistry of the ChO

Immunohistochemistry was performed as described in Scholz et al. 2017. For imaging of the chordotonal organ the following protocol was applied: 3rd instar larvae were dissected in Ca²⁺-free HL-3 (Stewart et al., 1994) fixed in 4% paraformaldehyde (PFA) for 10 min (at RT) and blocked overnight at 4°C in 1% PBT [phosphate buffer saline [PBS] with 1% Triton X-100 (T8787, Sigma-Aldrich)] supplemented with 5% normal goat serum [NGS; (005-000-001, Jackson ImmunoResearch)]. Primary antibodies were diluted in 1% PBT (5% NGS) incubated at 4°C overnight. Subsequently, the samples were rinsed twice and washed three times for 20 min using 1% PBT. The secondary antibodies were added to 1% PBT (with 5% NGS) and incubated overnight at 4°C. Then the filets were washed, two times short and three times for 20 min, with 1% PBT and finally mounted in Vectashield (H1000, Vector Laboratories). Afterwards, they were stored for at least over night at 4°C. The following primary antibodies were employed: rabbit- α -RFP (red-fluorescent protein; 1:500), mouse- α -

Cadherin-2 (N-Cadherin; 1:50). Secondary antibodies: anti horse radish peroxidase (α -HRP) conjugated with Alexa Fluor-488 goat- α -mouse (1:250; Jan & Jan 1982), Cy3-conjugated goat- α -rabbit (1:250; Dianova), Alexa Fluor-488 conjugated goat- α -mouse (1:250, Invitrogen). Confocal images were acquired with an LSM 5 Pascal (Zeiss).

2.3.3 Immunohistochemistry of the NMJ

Immunohistochemistry of the NMJ was performed as described previously (Schmid and Sigrist, 2008; Ehmann et al., 2014). The protocol reads as follows: full-grown 3rd instar *Drosophila* larvae were dissected in ice-cold HL-3 and filets were fixed for about 10 min (at RT) using 4% paraformaldehyde (PFA) and blocked for 30 min in PBT [PBS with 0.05% Triton X-100 (T8787, Sigma-Aldrich)] containing 5% normal goat serum [NGS; (005-000-001, Jackson ImmunoResearch)]. Afterwards, preparations were incubated with primary antibodies at 4°C over night. On the next day filets were washed, two times short and three times for 20 min with PBT, secondary antibodies (in PBT) and 5% NGS were added and incubated for 2 h (at RT). Subsequently, the filets were washed three times with PBT and then mounted in Vectashield (H1000, Vector Laboratories). A α -HRP conjugated with Alexa Fluor 488 goat- α -mouse (A11029, Invitrogen) was used as a secondary antibody at a dilution of 1:250. Localisation of ChR2^{XXM}::tdtomato was imaged as an endogenous signal.

10x PBS

74g NaCl	1.06404, Merck
----------	----------------

12.46g Na ₂ HPO ₄ * 2H ₂ O	1.06580, Merck
---	----------------

4.14g NaH ₂ PO ₄ * 2H ₂ O	1.06345, Merck
--	----------------

Fill up to 1 l with H₂O. The pH was adjusted to 7.4 using 1 M NaOH or 1 M HCl.

4% PFA in 1x PBS

8g PFA	Merck 1.04005
--------	---------------

150ml H ₂ O	Dissolve PFA in H ₂ O, heat up to 55°C
------------------------	---

2 N NaOH	Merck 1.09136; add some drops until solution becomes clear
----------	--

20 ml 10x PBS	
---------------	--

Fill up to 200 ml using H₂O; pH was adjusted to 7.4 using 1 Mol NaOH or 1 Mol HCl

2.3.4 Immunohistochemistry of the ventral nerve cord (VNC)

Immunohistochemistry of the larval ventral nerve cord (whole mounts) was performed according to Scholz et al. (2015). For the isolation of larval brain basically the same procedure as for muscle filets was executed. Additionally, motoneurons and surrounding tissue were carefully removed using spring scissors and forceps. Then the prepared brain was transferred to a 24-well plate inset. Larval brains were fixed for 10 min in 4 % PFA. Afterwards the larval

brains were blocked for 5 hours (5% NGS and 0.05% PBT; RT). Subsequently, the samples underwent over night incubation (4 °C) of primary antibody diluted in blocking solution [0.05% PBT +5% NGS and rabbit- α -RFP (1:500)]. The next day the samples were washed four times for 30 min and incubated with secondary antibody over night (0.05% PBT +5% NGS and α -HRP conjugated with Alexa Fluor-488 (1:250), Cy3-conjugated goat- α -rabbit [(1:250), 4 °C]. The day after, the probes were washed and subjected to Vectashield incubation (4 °C, over night) before mounting in Vectashield on cover slips prepared with reinforcement washers.

2.3.5 Data acquisition

All described images were acquired with a Zeiss LSM5 Pascal confocal system (objectives: 63x/1.25, plan-neofluar, oil immersions; 10/0.3, plan-neofluar,air) and laser power was adjusted individually for each NMJ, VNC or Chordotonal organ. Compounds stained with Alex-488 were excited at 488 nm by an Argon-laser and compounds stained with Cy3 were excited at 543 nm by a He-Ne laser.

2.4 Optogenetic tools

2.4.1 Channelrhodopsin2-XXM at the NMJ

Behavioural experiments were performed as described below. For investigating larval locomotion light from a mercury lamp passed through a GFP excitation band-pass filter was used to photostimulate crawling larvae expressing tagged or untagged ChR2^{XXM} (or other ChR2 descendants for comparison) in their motoneurons (*ok6-Gal4* driver)(Sanyal, 2009). Measurements determined the time between light-induced immobilisation and resumed movement (defined as anterior displacement of posterior end) during on-going irradiation.

To analyse behaviour of adult flies a different experimental setup was created. Here 10 flies were anaesthetised and put for 5 to 10 minutes in a covered Petri dish (10cm diameter) to recover fully. Recovery was tested by turning the petri dish carefully and screening for non-recovered flies (they would normally fall down and not stay attached to the Petri dish). If all 10 flies were fully recovered the Petri dish was vertically positioned in front of five blue LED's (440 nm) of steady intensity. To alter the resulting irradiation the distance of the Petri dish to the LED's was changed. Per data point 60 adult flies (1-15 days after eclosion) were irradiated and sets of 10 flies were used up to four times (after 5-10 min of recovery time) at different light intensities, but every set of 10 flies was only irradiated once at individual light intensities. While adult flies received irradiation the Petri dish was tapped after 5 s by the investigator and the immobilised flies were counted for 5 s. After 10 s in total, the recovery time was measured. Subsequently, 'recovery time' was denoted as the time until 50% of all flies initially immobilised were remobilised. Remobilisation was defined for each fly, if the following behaviour occurred: moving 'two steps' forward.

Electrophysiological recordings with ChR2^{XXM} expressed at the larval NMJ were obtained as described in chapter 2.2.2.

2.4.2 GtACR at the larval NMJ and muscle tissue

Behavioural experiments were carried out by Sven Dannhäuser and performed as described in his MSc-Thesis. In short, larvae were put under a blue light source (1 mW/mm^2) and the time until immobilisation or remobilisation was measured.

Electrophysiological data was acquired with little alternation to ChR2^{XXM} measurements. In order to examine direct inhibitory effects of GtACR in larval motoneurons a 10 Hz or 30 Hz stimulation protocol was employed for 7 s whereby an additional light irradiation ($1 \text{ }\mu\text{W/mm}^2$, 490nm) was applied after 3 s for a duration of 2 s directly at the NMJ via the optical path of the microscope.

Examination of the observed 'baseline shift' was investigated as follows, using previously described settings of TEVC. *Drosophila* larvae were prepared as for TEVC. GtACR1::YE expressed in motoneurons (*ok6-Gal4*), GtACR1::YE expressed in muscle tissue (*G7-Gal4*) and 'undriven' GtACR1::YE were compared to which extent a 'baseline shift' or rather a direct depolarisation occurs in TEVC. Therefore a stimulation protocol of 6 s was employed whereby light irradiation lasted for 2 s in between 2 s rest before and after. Stimulation started at $1 \text{ }\mu\text{W/mm}^2$ and proceeded up to $40\mu\text{W/mm}^2$ in several steps of intensity for each NMJ within the described protocol. To reach statistical significance 9-10 NMJs of 3-4 individual larvae were investigated for each genotype.

2.4.3 Channelrhodopsin2-XXM in the ChO

Electrophysiological measurements were carried out essentially as previously described (Scholz et al., 2015) and were performed by Chonglin Guan. In brief, activity of lch5 neurons was recorded from the axon bundle using a suction electrode coupled to an EPC 10 USB amplifier (HEKA Instruments) and analysed in Clampfit 10.2 (Molecular Devices). Mechanical stimulation was applied through a piezo-actuated, fire-sealed glass electrode placed on the

muscle covering the cap cells. Spontaneously active neurons were stimulated optogenetically or at the indicated sine wave frequencies (three cycles of 1 s stimulation preceded by 1 s rest for each frequency). Data were sampled at 10 kHz and a notch filter was used to remove the specific stimulation frequency from the current trace.

Light from a mercury lamp (Nikon Intensilight C-HGFI) passed a GFP filter (460-500 nm band-pass) for photostimulation of lch5 neurons via ChR2^{XXM}::tdtomato (*iav-Gal4>UAS-chop2XXM::tdtomato*; 100 μ M retinal food supplementation). Increasing light intensities (approx. 0.04, 0.08, 0.17, 0.34, 0.68, 1.35, 2.71, 5.42 mW/mm²) were applied with intermittent 10 s breaks. Genotypes were blinded for electrophysiological recordings of ChOs.

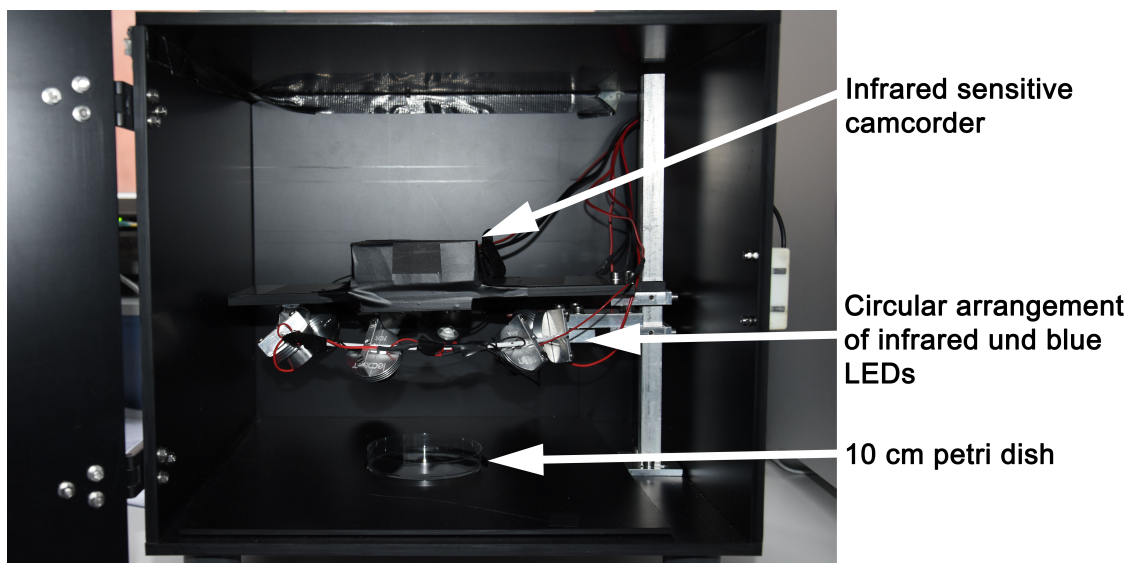


Figure 9 | Light application setup for behavioural experiments

Image of the setup used for behavioural experiments. Arrows indicate characteristic features of this setup.

Behavioural experiments of *Drosophila* larvae expressing ChR2^{XXM} in their chordotonal organs, without supplement of ATR, were performed as follows. Larvae were put in a petri dish of 10 cm diameter filled up to half with 1% agar gel. Afterwards, this petri dish was placed in a light proofed box (cf. Fig. 9). Above the petri dish an infrared sensitive USB-Camcorder was placed and around this recorder, fixed on a ring, one set of three infrared LED's and one

set of three blue LED's was mounted (cf. Fig. 9). Per run, seven larvae were put in the middle of the petri dish and allowed to crawl in darkness for 130 s. Subsequently, the same set of larvae were re-arranged in the middle of the petri dish and the light protocol, as illustrated in Fig. 17.B., was applied. Analysis of the 'head-swing'-duration was evaluated by analysing the recorded video file.

2.5 Data analysis

Data were analysed in Prism 7.0 (GraphPad). Group means were compared by two-tailed Student's t-test. The assumption of normality of the sample distribution was violated as indicated by the D'Agostino & Pearsons omnibus normality test, whereas group means were compared by two-tailed Mann-Whitney U test. Where indicated in figures asterisks denote the level of significance: * $p \leq 0.05$, ** $p \leq 0.01$, *** $p \leq 0.001$. Bar charts indicate mean \pm SEM if not stated otherwise.

3 Results

3.1 Characterization of Channelrhodopsin2-XXM at the *Drosophila*

NMJ

Channelrhodopsin2 wild-type (ChR2-wt) can lead to an effective depolarisation of neuronal cells and even to a full body contraction of *Drosophila* larvae if expressed in motoneurons (Nagel et al., 2003; Ljaschenko et al., 2013; Dawydow et al., 2014). However, ChR2-wt is not sufficient to lead to a detectable behavioural effect in adult flies, due to the opaqueness of the adults compared to the almost translucent *Drosophila* larvae (Dawydow et al., 2014). Here, functionality and characteristics of a modified Channelrhodopsin2, Channelrhodopsin2-XXM (ChR2^{XXM}), expressed at the NMJ of larval and adult *Drosophila melanogaster* are described. Recently, a different ChR2 variant was characterised and named Channelrhodopsin2-XXL (ChR2^{XXL}) that was found to work very sufficiently even in adult flies (Dawydow et al., 2014). This channel possesses a single amino acid substitution at position 156, aspartic acid with cysteine (D156C), which leads to a massive change in channel function (Dawydow et al., 2014). This becomes obvious in increased photostimulation efficiency deriving from high cellular expression and a dramatically extended open state lifetime of around 1 minute. Hence this variant was termed ChR2^{XXL}, which stands for extra high expression and long open state. To stay in this terminology, ChR2^{XXM} was named due to extra high expression and medium open state. Here, a similar amino acid replacement was performed where aspartic acid at position 156 was replaced by histidine (D156H). This leads to a shorter open state lifetime compared to ChR2^{XXL} (but longer compared to ChR2-wt) and thus more precise timing but still a high expression of the protein.

3.1.1 Expression of ChR2^{XXM}::tdtomato at the larval NMJ

Due to its very efficient expression ChR2^{XXM} is detectable at the *Drosophila* NMJ as an endogenous signal if tagged to a red fluorescent protein (RFP). Here, a very small and efficient RFP called tdtomato was used and it was found

that ChR2^{XXM}::tdtomato aligns perfectly with the α -HRP (anti horse radish peroxidase) counterstaining that marks neuronal membranes in *Drosophila melanogaster*. Moreover, well detectable expression of ChR2^{XXM} in the larval ventral nerve cord (VNC) was found due to expression in the cell bodies of the motoneurons (Fig. 10).

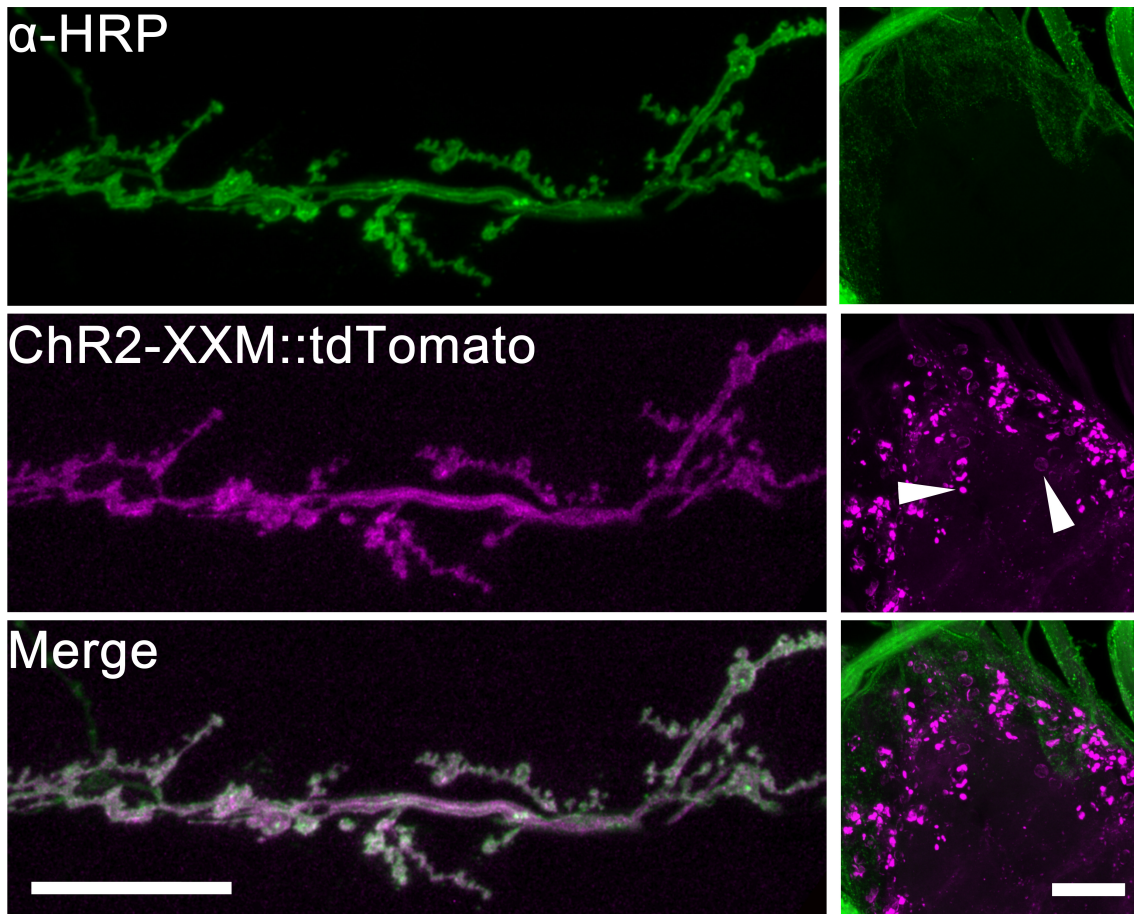


Figure 10 | Expression of ChR2-XXM::tdtomato at larval the NMJ and VNC

3rd instar larvae expressing ChR2^{XXM}::tdtomato in their motoneurons (*ok6-Gal4*); were dissected and stained with α -HRP (Horse radish peroxidase). Confocal images on the left side were recorded from segment A2 of muscle segment 6/7. The second image shows ChR2^{XXM}::tdtomato expression at the NMJ. Scale bar = 25 μ m. Right sided images were recorded from the VNC, indicating that ChR2^{XXM}::tdtomato is also expressed in the motoneuron axons inside the ventral nerve cord of *Drosophila* larvae. Scale bar = 25 μ m. Arrowheads indicate cell bodies. Images are maximum projections.

3.1.2 Electrophysiological recordings at the larval NMJ

Since an even distribution of ChR2^{XXM}::tdtomato at the larval NMJ was observed, electrophysiological measurements at the *Drosophila* NMJ were performed to verify, if this good distribution leads to a functional impact.

Results of electrophysiological recordings were in line with the stainings. The measurements demonstrate efficient recruitment of ChR2^{XXM}::tdtomato to evoke one single eEPSC at light intensities as low as 1 $\mu\text{W}/\text{mm}^2$ with a pulse duration of 50 ms (Fig. 11.B). Higher light intensity (7 $\mu\text{W}/\text{mm}^2$) led to fusillades of eEPSCs for approximately one second (Fig. 11.A).

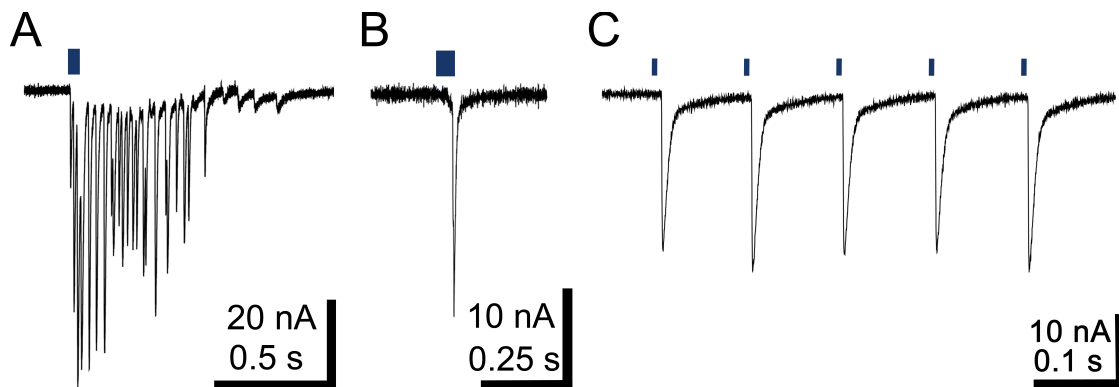


Figure 11 | Electrophysiological recording at the *Drosophila* NMJ (TEVC)

3rd instar larvae raised on ATR supplemented food and expressing ChR2^{XXM}::tdtomato in their motoneurons were prepared for TEVC recording and muscles were clamped to -60 mV. Light irradiation was mainly applied on NMJ area. (A) A light intensity of $\sim 7 \mu\text{W}/\text{mm}^2$ with a duration of 50 ms was used to trigger fusillades of eEPSCs. (B) Light intensity was reduced to 1 $\mu\text{W}/\text{mm}^2$ to trigger one single eEPSC, with unaltered pulse duration. (C) 1 ms light pulses with an intensity of around 40 $\mu\text{W}/\text{mm}^2$ were used to trigger multiple single eEPSCs in a row.

Altering the light intensity and pulse duration, recruitment of ChR2-XXM channels/units can be controlled precisely. To reach high resolution in time, the light intensity was raised to 40 $\mu\text{W}/\text{mm}^2$ and pulse duration was reduced to 1 ms (Fig. 11.C). Thus a single light evoked EPSC could be triggered. However, 40 $\mu\text{W}/\text{mm}^2$ is still a very low intensity for efficiently evoking neuronal activity. Therefore, ChR2^{XXM} is a perfect tool if high precision in time is needed and low light intensities are required to reduce possible heat irritations and cell damage.

3.1.3 Larval behaviour

ChR2-wt is known to lead to an effective full body contraction of *Caenorhabditis elegans* and in *Drosophila* larvae if expressed in motoneurons, although this contraction lasts only for a few seconds and very high light intensities are needed in *Drosophila melanogaster* (Dawydow et al., 2014). Thus, comparing periods of total body contraction in larvae of different Channelrhodopsin variants provides a proper way to investigate photostimulation efficiency *in vivo*.

Therefore, three different variants of Channelrhodopsin driven in larval motoneurons with or without supplementation of ATR under continuous light irradiation were tested. Supplementation is needed because most *Drosophila* cells, in contrast to vertebrate cells (e.g. cortical cells of mice) contain considerably less ATR. However, new Channelrhodopsin variants show a much higher affinity to bind ATR, which leads to an increased expression pattern and is accompanied by increased photostimulation efficiency, even in non-supplemented food (Dawydow et al., 2014; Scholz et al., 2017).

ChR2^{XXL}, which is shown here for comparison, has been characterised very well before and was found to lead to an effective immobilisation of larvae for over 60 min at light intensities as low as 40 nW/mm² (blue light spectrum 440nm) if ATR was supplemented (Dawydow et al., 2014); Fig. 12). In this work ChR2^{XXL}::tdtomato, without ATR supplementation, and ChR2-wt (with ATR supplementation) were compared to the newly developed ChR2^{XXM}::tdtomato (with or without ATR supplementation). No relevant differences between tagged and non-tagged ChR2^{XXL} were found. ChR2^{XXL} leads to an effective full body contraction in larvae at light intensities of 0.5 μW/mm² or 0.1 μW/mm² (Fig. 12.A). In contrast, larvae expressing ChR2-wt, fed with ATR supplemented food needed higher light intensities (between 0.03 mW/mm² and 0.2 mW/mm²) to show effective immobilisation compared to the other ChR2 mutants (Fig. 12.A). Both (new) tested variants, ChR2^{XXM} and ChR2^{XXM}::tdtomato, are situated between these two extremes. Interestingly, ChR2^{XXM} and ChR2^{XXM}::tdtomato showed indistinguishable light sensitivity if fly food was supplemented with ATR.

Light intensities of $2 \mu\text{W}/\text{mm}^2$ already resulted in an effective body muscle contraction of the larvae lasting longer than 100 seconds. However, if fly food was non-supplemented with ATR and ChR2^{XXM} was employed light intensities of $40 \mu\text{W}/\text{mm}^2$ were necessary to reach effective contraction (Fig. 12.A).

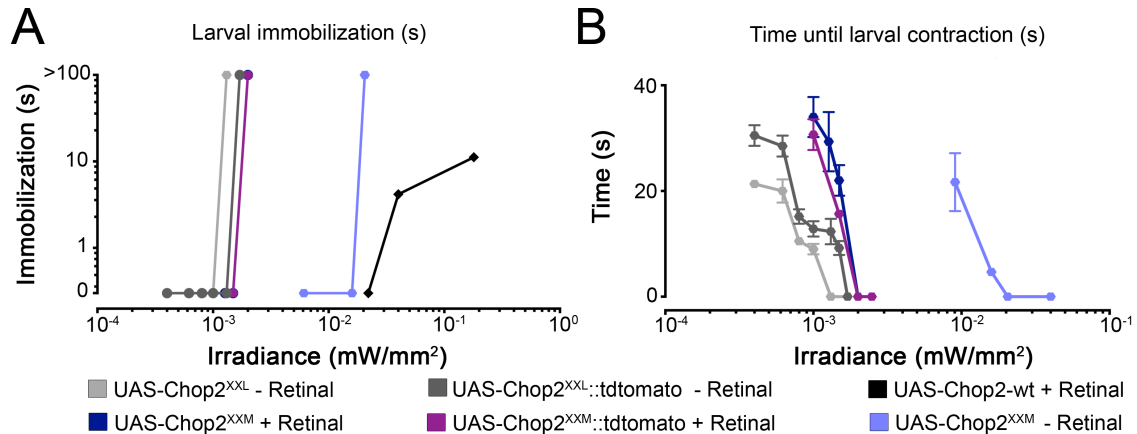


Figure 12 | Immobilisation of *Drosophila* larvae expressing different ChR variants

(A) Different Channelrhodopsin variants are expressed in the larval motoneuron (presynaptic) leading to full body contraction at specific intensities of light. Time was measured when the larvae performed immediate full muscle contraction at given light irradiation. Note that no difference between $\text{ChR2}^{\text{XXM}::\text{tdtomato}}$ and ChR2^{XXM} could be measured, thus this two genotypes lie on top of each other in this graph. (B) At lower light intensities larvae displayed a dosage-dependent response to light. Also, larvae showed full body contraction but only over a certain period of time. The time plotted was needed until full body contraction under given light intensity occurred. Here, ChR2-wt is missing, because no such effect was observable at the given light intensities.

If light intensities were too low to result in an instant full body contraction of larvae, a dosage-dependent behaviour was observable (Figure 12.B).

3.1.4 Adult behaviour

To test for efficacy of ChR2^{XXM} to evoke light induced muscular contraction in adult flies, a second behavioural setup was established. Thereby, two different characteristics of Channelrhodopsin in a two-parted experiment were evaluated. At first, adult flies were used to investigate light sensitivity of different Channelrhodopsin variants *in vivo* (Fig. 13.A) and in another setup, recovery time after light irradiation was monitored to draw conclusions on the effect of channel closing kinetics in the living organism (Fig. 13.C).

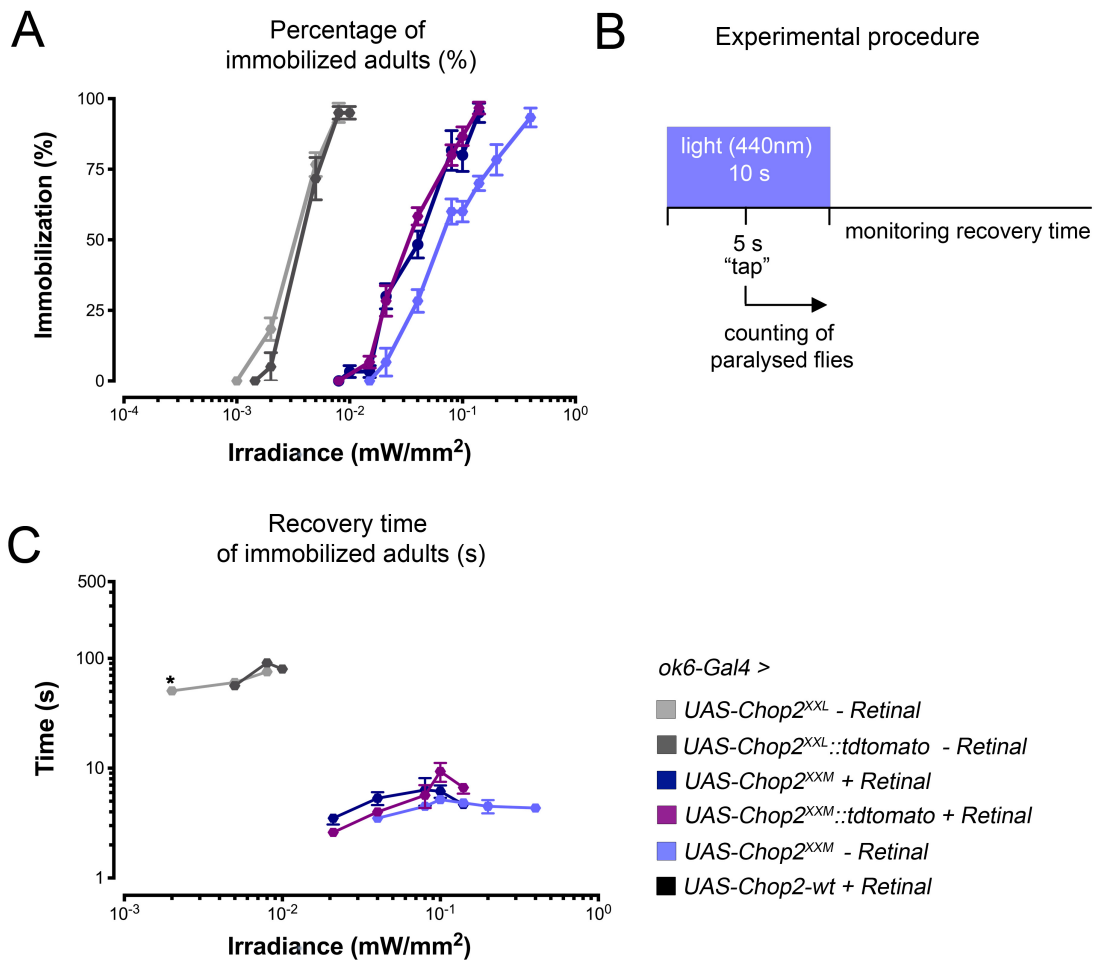


Figure 13 | Light sensitivity of adult *Drosophila* expressing different ChR variants

(A) *Drosophila* flies expressing different ChR variants in their motoneurons were raised to adult stage. Per data point 6 petri dishes of ten flies (ten flies $\hat{=}$ n = 1) each were taken for statistical analysis. Light irradiation was done for 10 seconds and percentage of all paralysed flies was counted. (B) Time scale for analysis of light irradiation on adult flies. (C) Recovery time. After 10 seconds of light irradiation, time was measured until 50% of all initially paralysed flies were recovered. This was done to estimate the channel closing time. (C*) n = 3 instead of n = 6.

Therefore, the experimental protocol was performed as described in Fig 13.B. Flies were placed in a vertical fixed petri dish and irradiated at different light intensities for 10 seconds. After 5 seconds the petri dish was tapped twice to make sure all immobilised flies lay on the bottom for counting. Then recovery time was benchmarked when 50% of all initially immobilized flies were moving again.

Here ChR2^{XXM}::tdtomato was found to be congruent with ChR2^{XXM} in relation to light intensity needed for immobilization and recovery time, if flies were raised on ATR supplemented food. Comparing ChR2^{XXM} (w/o ATR) a right shift in light sensitivity occurred, which can also be seen in larvae (Fig. 13.A). As expected, the recovery time (time until 50% of all initially paralysed flies were recovered; Fig. 13.C) remained the same since no effect of retinal supplementation on channel closing kinetics is known for Channelrhodopsin (Nagel et al., 2003 and 2005).

ChR2^{XXL}::tdtomato displayed higher light sensitivity in adult flies (~100% immobilised at 8 μ W/mm²) compared to ChR2^{XXM}::tdtomato [~100% immobilised at 140 μ W/mm² (with ATR) 400 μ W/mm² (without ATR)]. Compared to ChR2^{XXM}::tdtomato, the recovery time of ChR2^{XXL}::tdtomato variants was found to be ten times longer (~ 3 - 9s vs. ~ 60 - 90s; cf. Fig. 13.C). This is in line with previous studies that reported an open-state life-time of about 76 s for ChR2^{XXL} (Dawydow et al., 2014).

3.2 Analysis of the chordotonal organ using Channelrhodopsin2-

XXM

Chordotonal organs, as described before (cf. chapter 1.3.3.), are mainly responsible for mechanosensation in *Drosophila melanogaster*. Experiments performed here focused on the pentascolopodial chordotonal organ (lch5), which consists of five chordotonal neurons combined to one unit (there is also an lch1, consisting only of one chordotonal neuron). At each hemisegment there is one lch5 together with three lch1 neurons (Langenhan et al., 2016). Since, this mechanosensory system is very important and by far not fully understood, it was investigated here, how simultaneous, *in vivo*, activation of the chordotonal organ and mutations of *dCIRL* lead to an altered behavioural pattern or changes in ChO physiology. It is already known that absence of *dCIRL* (*dCIRL^{KO}*) results in stereotypic behavioural patterns of 3rd instar larvae where an increased pausing in larval movement and profuse head swing behaviour can be observed (Scholz et al., 2015).

In the following sets of experiments *ChR2^{XXM}::tdtomato* was expressed in the chordotonal organ (*iav-Gal4*) to investigate how direct changes of cation concentration may affect mechanosensory responses in *Drosophila* larvae with functional *dCIRL*. Furthermore, employing electrophysiology could scrutinize that *ChR2^{XXM}* expressed in chordotonal organs is efficient to bypass mechanoreceptive deficits triggered by the absence of *dCIRL*.

3.2.1 Expression in the chordotonal organ

Since *ChR2^{XXM}::tdtomato* is known to distribute very evenly at the larval NMJ if driven by *ok6-Gal4* (cf. Fig. 10), the expression pattern of *ChR2^{XXM}::tdtomato* within the lch5 organ was scrutinized, by employing *iav-Gal4* (inactive-Gal4).

First stainings of lch5 against Cadherin-2 (binds to the area around the scolopale space) merged with the endogenous *tdtomato* signal revealed that *ChR2^{XXM}* is mainly located in the chordotonal neuron even in parts of the

dendrite and the cilium (Fig. 14.C,D), but signal quality was very low at these structures. Thus, a second staining using an RFP-antibody (α -RFP) was performed to enhance endogenous tdtomato intensity in order to have a closer look on the actual distribution of ChR2^{XXM}::tdtomato, especially in the areas where staining was weak before, like the cilia and the dendrites (cf. Fig. 14.A,B). Thereby, ChR2^{XXM}::tdtomato was found to spread quite evenly in dendrites and cilia covering both structures in whole length.

This could be verified by an anti-HRP counterstaining that displays the end of the dendrite and beginning of the cilium. It covers roughly the area of the middle of the cilium and from the dendritic cap into the cap cell. As a result, one can distinguish the proximal and distal part of the cilium precisely and find ChR2^{XXM}::tdtomato expressed very distinctively here.

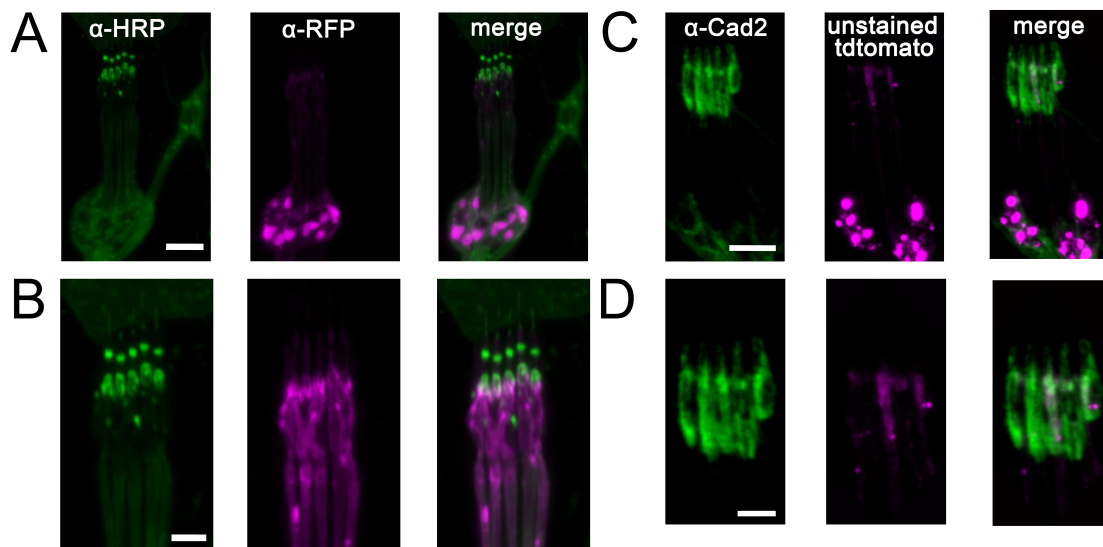


Figure 14 | Expression of ChR2-XXM::tdtomato in the chordotonal organ

Images of ICh5 in 3rd instar *Drosophila* larvae. **(A)** ICh5 stained with anti-HRP (green) and anti-RFP (magenta), which binds to tdtomato and acts as a booster. **(B)** Inset of the ciliary area shown in **(A)**. **(C)** ICh5 stained with anti-Cadherin2 antibody (green), which binds to parts of the scolopale space (cf. Fig. 5.A, anatomy of the chordotonal organ) that surrounds the cilium. The second row shows endogeneous tdtomato expression. As expected, the intrinsic signal of ChR2^{XXM}::tdtomato is weaker than the actual expression **(A,B)**, signal boosted. **(D)** Inset of **(C)**. **(A,C)** Scale bar = 10 μ m **(B,D)** Scale bar 5 μ m.

There was also an interest if ChR2^{XXM}::tdtomato is only expressed at the beginning of the mechanosensory pathway – the lch5 organ – or even at the end of it – the projection neuron in the VNC. Therefore, immunostainings against HRP and RFP were performed to stain VNCs of *Drosophila* larvae. Here, a clearly identifiable expression of ChR2^{XXM}::tdtomato inside the VNC was found as shown in Fig. 15.

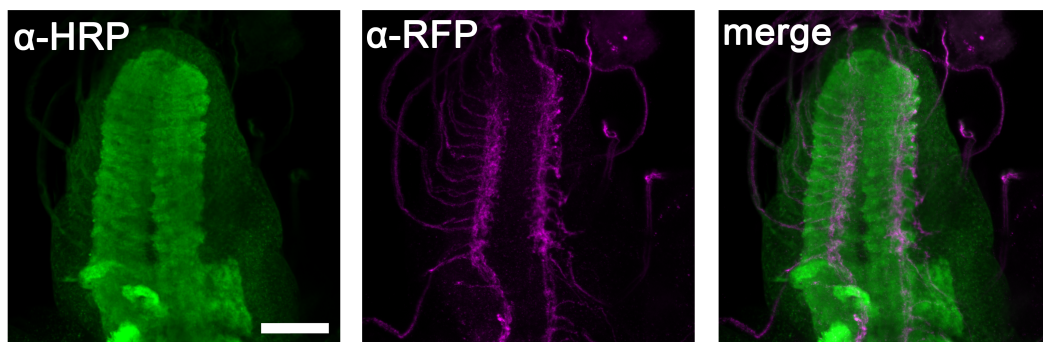


Figure 15 | Expression of ChR2-XXM::tdtomato in the larval VNC

Staining of ChR2^{XXM}::tdtomato with anti-RFP (magenta) to show evenly spread expression in the VNC if driven by iav-Gal4. Scale bar = 50µm.

This demonstrates that ChR2^{XXM} is well expressed along the whole mechanosensory pathway, as determined by iav-Gal4. The distinct localisation of the projecting sensory axon terminals, inside the VNC, was investigated and described very recently by Tsubouchi et al. (2017), even though they only analysed adult *Drosophila melanogaster* in their study.

3.2.2 Electrophysiological recordings

Based on previous behavioural observations the hypothesis that *dCIRL* does not promote membrane excitability per se to help initiate and propagate action potentials in the sensory neuron was tested (Scholz et al., 2017). Therefore, electrophysiological techniques combined with an optogenetic approach were employed to perform measurements at the lch5 and to bypass the receptor potential effectively.

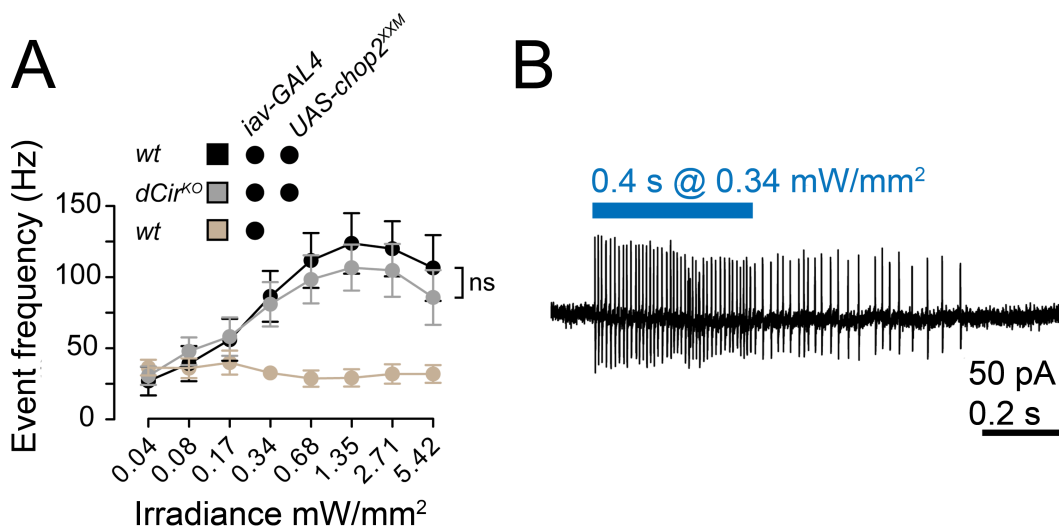


Figure 16 | Activation of lch5 by ChR2-XXM

Data shown in this figure have been acquired by C. Guan; adapted and modified from Scholz et al. 2017. **(A)** Changes in event frequency triggered in the lch5 organ by ChR^{XXM} are not significantly different in wild-type compared to *dCIRL^{KO}* larvae expressing ChR2^{XXM} if different intensities of 440 nm light were applied to the organ. **(B)** Example trace of a recording at the lch5 organ to illustrate how light irradiation triggers elevated event frequencies.

In this experimental setup it could be shown that blue light (440 nm), by bypassing the receptor potential, at certain light intensities did not lead to significant differences between larvae expressing ChR2^{XXM} in the lch5 with intact latrophilin or in *dCIRL^{KO}* larvae (Fig. 16.A). As a control, wild type larvae crossed to *iav-Gal4* were used. These larvae did not respond with changes in basal activation of lch5 if blue light was applied (Figure 16.A). To sum up, the hypothesis stated (at the beginning of 3.2.2.) has proved to be true.

3.2.3 Light-induced head-swing behaviour

As previously mentioned, *dCIRL^{KO}* larvae had impressive alterations in their behaviour patterns or more precisely in their ability to elicit goal-directed movement (Scholz et al., 2015). These larvae show persistent extensive 'head-swing behaviour' or 'startle-response'. Based on earlier publications, this was assumed to be a result of a diminished mechanosensational resolution along with a lower basic activity of the lch5 in the absence of latrophilin (Scholz et al., 2015).

In our experimental setup the hypothesis if the opposite – accelerated activation levels of the *lch5* – has any behavioural effects in *Drosophila* larvae was tested. Interestingly, expression of $\text{ChR2}^{\text{XXM}}::\text{tdtomato}$ in the *lch5* is sufficient to provoke a similar head-swing behaviour in larvae as previously described for $d\text{CIRL}^{\text{KO}}$ larvae (Fig. 17.A, B). This ‘startle-response’ did not last for the whole time of light application most likely due to adaption mechanisms of the mechanosensory system. Larvae expressing $\text{ChR2}^{\text{XXM}}::\text{tdtomato}$ in their *lch5* showed a significantly longer head-swing behaviour compared to larvae that carry an undriven $\text{UAS-ChR2}^{\text{XXM}}::\text{tdtomato}$ construct (Fig. 17.A). These larvae were chosen as controls to check for possible leak expression of the $\text{ChR2}^{\text{XXM}}::\text{tdtomato}$ construct. Impressively, this observation was made under a light irradiation as low as $3 \mu\text{W}/\text{mm}^2$. This light intensity was chosen because it was found to be sufficient to lead to a full body contraction of larvae with ChR2^{XXM} expressed at their NMJs.

To quantify this light-induced head-swing or ‘startle-response’ of the larvae, a protocol with spaced light application interrupted by a resting period as displayed in Fig. 17.B was designed. Preceding this light stimulation protocol each test group of larvae (seven each) was allowed to crawl for the whole duration of the protocol in complete darkness. The reason for this procedure was, to examine if spontaneous head-swing behaviour appears significantly different at given time points in test and control groups. Here, all larvae tested showed no detectable difference. Subsequently, the light stimulation protocol was performed and revealed that larvae with $\text{ChR2}^{\text{XXM}}::\text{tdtomato}$ in their *ChO* respond to light with a significantly longer head-swing behaviour compared to controls (Fig. 17.A).

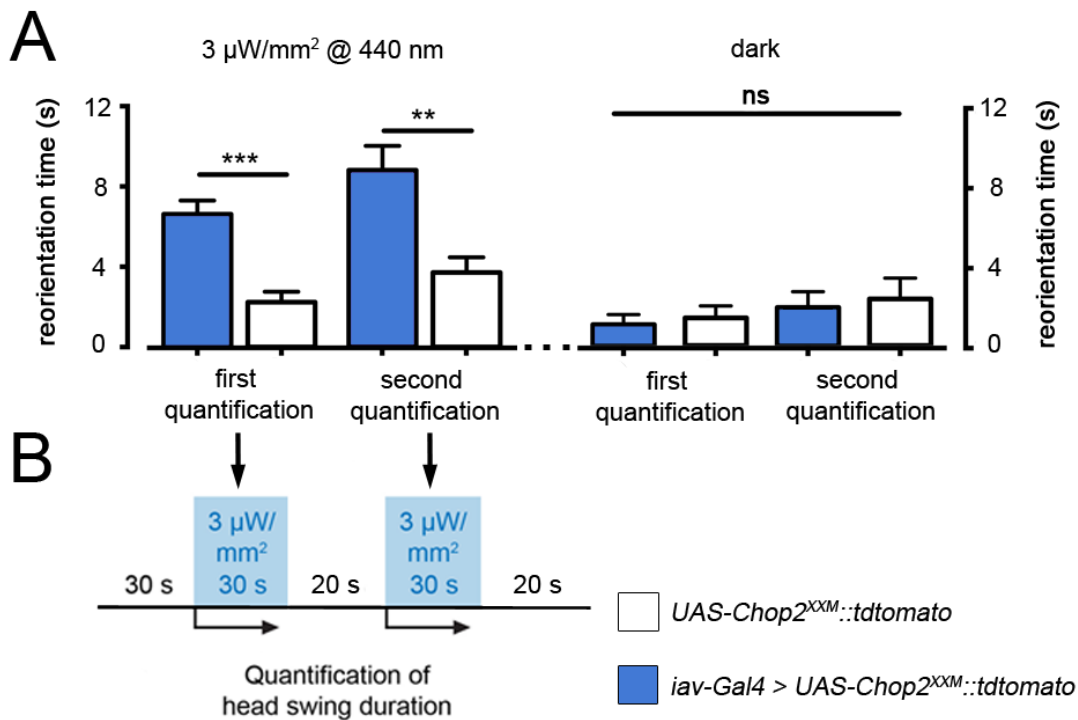


Figure 17 | Quantification of head swing duration

(A) 3rd instar larvae raised on ATR supplemented food and expressing *ChR2^{XXM}::tdtomato* in their chordotonal organ were exposed to light and head swing duration was measured. As a control group 3rd instar larvae carrying only the *UAS-*Chop2^{XXM}::tdtomato** were used. To exclude that larvae carrying *iav-Gal4* show increased head swing behaviour, independent of light irradiation, a dark control setup was employed. Therefore, same time points were used to measure head swing duration and check if head swing occurs more often in *iav-Gal4* flies ($n = 21$). (B) Description of the protocol used to visualise head swing behaviour. Modified from Scholz et al. 2017.

Even specific types of leak expression, e.g. unintentional expression of *ChR2^{XXM}::tdtomato* in the ChO organ of the control flies, can not be completely excluded, it could be found that targeted expression of *ChR2^{XXM}::tdtomato* in the *lch5* is sufficient to influence stereotype behavioural patterns of *Drosophila* larvae.

3.3 Application of *Guillardia theta* Anion Channelrhodopsin at the *Drosophila* NMJ

Guillardia theta Anion Channelrhodopsin (GtACR) (Fig. 18.A) is the first described naturally occurring light-sensitive Cl⁻-conducting channel (Fig. 18.B,C; Govorunova et al. 2015). Two different GtACRs have been extracted from the genome of *Guillardia theta* and are described in the original publication (Govorunova et al., 2015). GtACR1, which shows its sensitivity peak at 515 nm and GtACR2 that has its maximum of sensitivity at 470 nm. Furthermore, both Anion Channelrhodopsins (ACR) have been described as very sensitive even to low light intensities and are therefore a useful tool for light controlled inhibition.

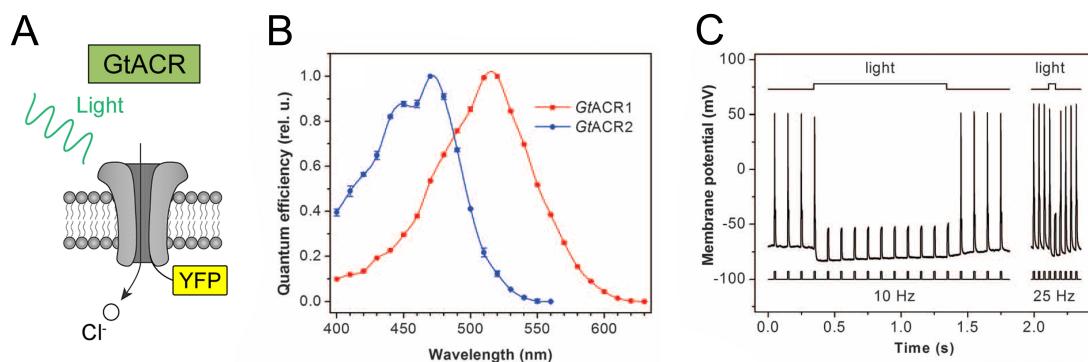


Figure 18 | Function of GtACR

(A) Schematic depiction of GtACR1::YFP function (B) Action spectra of photocurrents of GtACR1 and GtACR2 (C) Photoinhibition of spiking induced by pulsed current injection in a typical neuron expressing GtACR2 at 26 $\mu\text{W}/\text{mm}^2$. (A) Kindly provided by R.J. Kittel (B,C) Adapted and modified from Govorunova et al. (2016).

Moreover, the discovery of these ACR's is very interesting for future clinical research, because inhibition of neurons can be useful in various ways to understand neurological diseases. For instance, defects of chloride channels in human muscles lead to muscle dystrophies, which are characterised by shortcomings in relaxation but also hypertrophic deregulations of muscle tissue (e.g. Myotonia congenita type Thomsen, Myotonia congenita type Becker) (Hahn and Salajegheh, 2016; Pedersen et al., 2016; Walters, 2017). However, a more obvious approach to employ GtACRs is the implementation of these ACRs in neuronal populations to investigate the consequences of inhibiting certain cellular populations.

Therefore, the effect of GtACR1 on the motoneuron (presynaptic) and the larval muscle tissue (postsynaptic) was investigated.

3.3.1 Expression at the larval NMJ

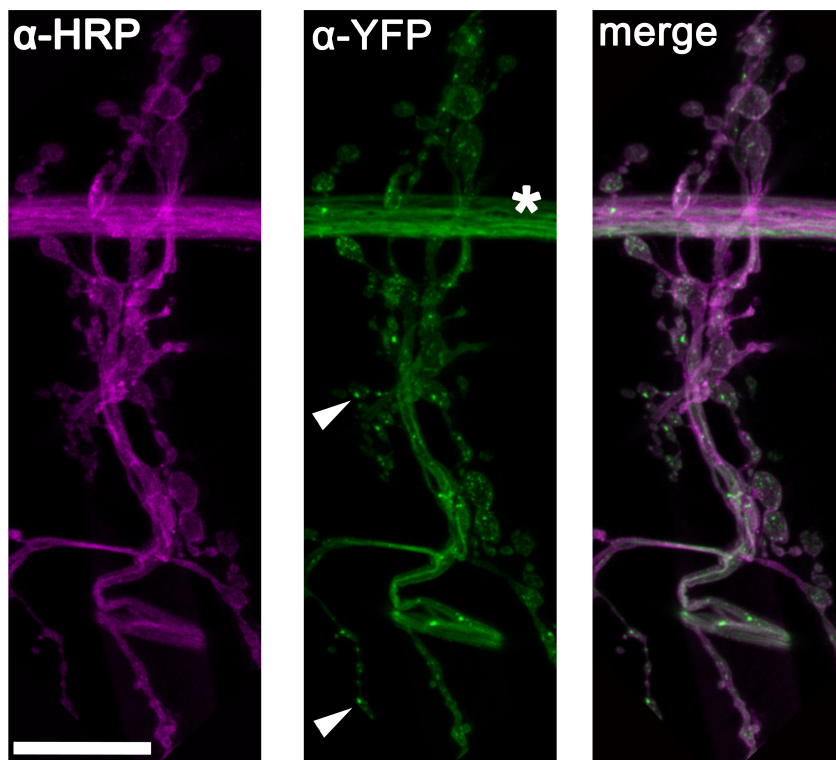


Figure 19 | Expression of GtACR1::YE at the larval NMJ

GtACR1::YE was stained with an anti-YFP (green) antibody and merged with an anti-HRP counterstaining (magenta) to evaluate its presynaptic distribution. Arrowheads show examples of 'proteincluster'. Asterisk denotes traversing part of a motoneuron. Scale bar = 25 μ m.

As described for the characterisation of ChR2^{XXM} previously, the distribution of GtACR1::YE at the larval NMJ, especially at the boutons, was checked. In contrast to ChR2^{XXM}::tdtomato, GtACR1::YE shows a less even distribution at the NMJ with some parts appearing as clustered photoprotein (arrowheads in Fig. 19) on the presynaptic side.

3.3.2 Electrophysiological recordings at the larval NMJ

Here in particular, the inhibiting effect of GtACR1::YE expressed in the larval motoneuron was demonstrated. In accordance to earlier publications on GtACR1 it was found that GtACR1::YE behaves very sensitive to light (490 nm, cyan). Indeed, a light intensity as low as $1 \mu\text{W}/\text{mm}^2$ of cyan light (490 nm) led, independent from given frequencies (10 Hz, 30 Hz), to complete extinction of all eEPSCs, in this setup (Fig.20.A,B).

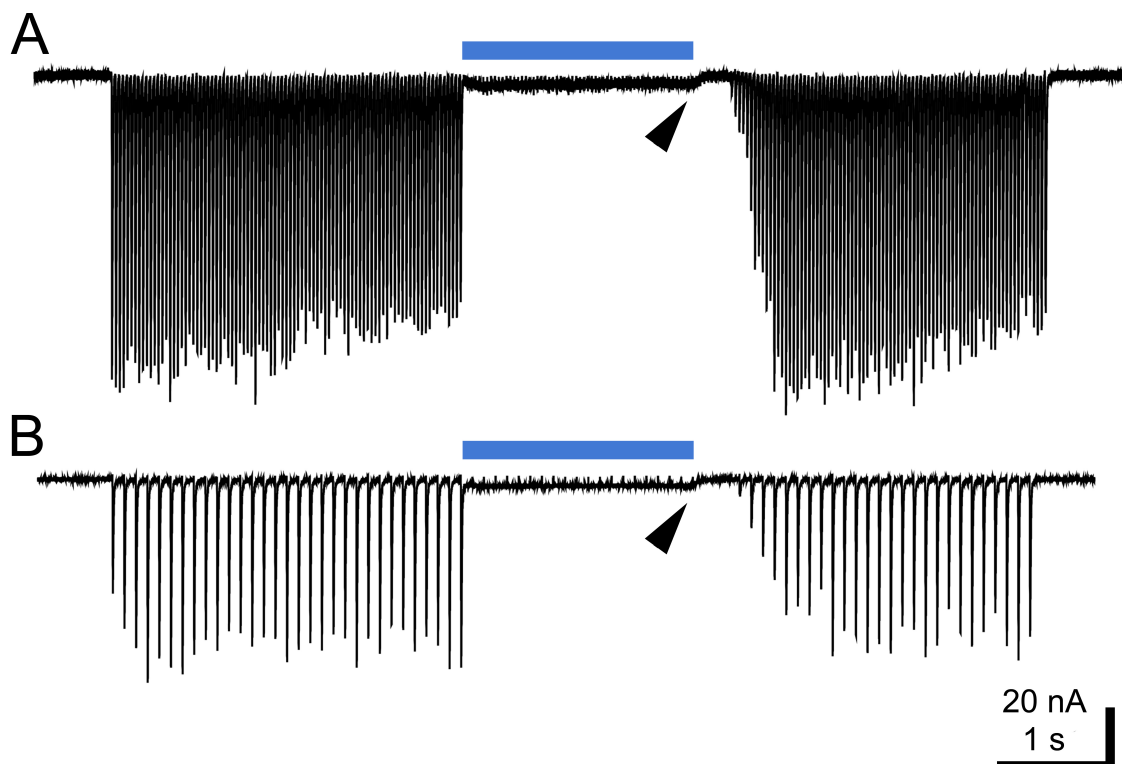


Figure 20 | Extinguishment of eEPSCs by GtACR1::YE

3rd instar larvae were prepared for electrophysiology and the corresponding nerve of the clamped muscle was stimulated via a suction electrode. While the nerve was stimulated at different frequencies the nerve was also irradiated by cyan light (490nm, **A, B**) at the lowest possible intensity ($0.5 \mu\text{W}/\text{mm}^2$). Stimulation artefacts were removed for clarity. (**A,B**) Cyan light silenced eEPSCs completely and instantly when applied on experimental larvae. Therefore, stimulation of GtACR1::YE in motoneurons leads to inhibition of electrical transmission. Arrowheads indicate observed shift of Baseline (cf. MSc-Thesis of S. Dannhäuser 2016).

Furthermore, if mixed/white light was employed, varying the intensity of applied light could control the level of inhibition in the larval motoneuron very effectively (Fig. 21). In this 'white light' setup only high and low light intensity was defined.

To reach a higher resolution in time a 30 Hz stimulation frequency was used and a reduction of the resulting eEPSC amplitude depending on the light intensity was found. This demonstrates that at a given light intensity GtACRs may interfere very precisely within cellular communication beyond switching a cell/neuron simply 'off'.

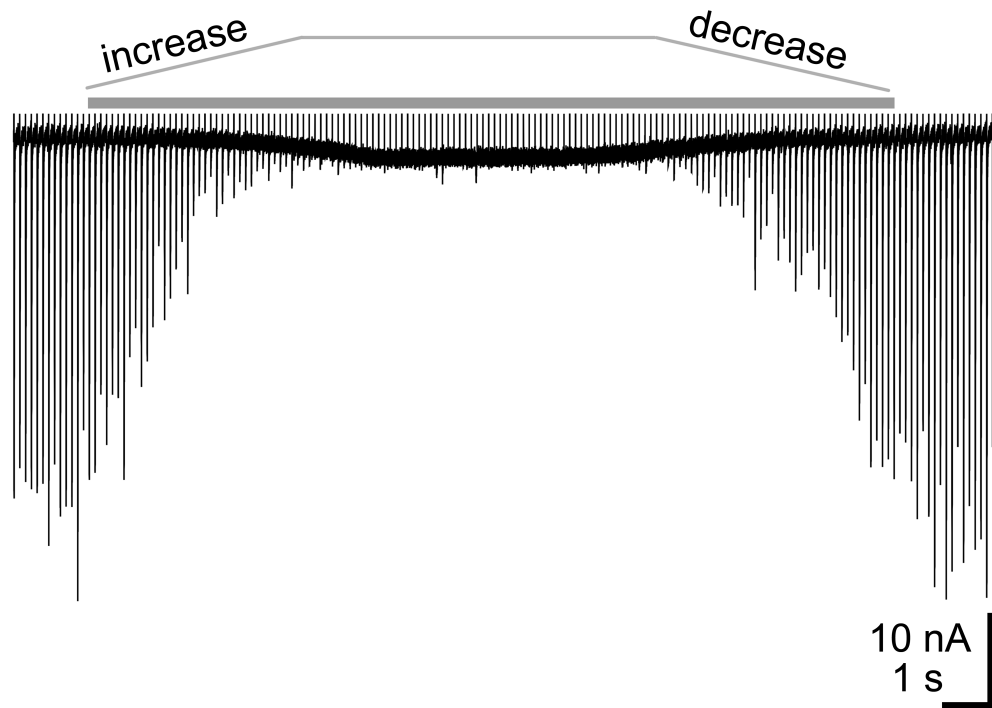


Figure 21 | Extinguishment of eEPSCs using white light and GtACR1::YE

Preparation as described earlier for cyan light setup. Stimulation artefacts were removed for clarity. Graph indicates that reduction of eEPSC amplitude is directly proportional to activation of GtACR1. In contrast to pure cyan light stimulation white light irradiation shows an increment of inhibition. Therefore the intensity of the white light was increased while EPSCs were triggered until a plateau of complete eEPSC inhibition was reached, then light intensity was reduced until eEPSCs could be evoked as before light stimulation (cf. Dannhäuser 2016).

As emphasised in Fig. 20, a conspicuous baseline-shift during stimulation of GtACR1::YE in the larval motoneuron was observed. Surprisingly, this baseline-shift deviates in the same direction as excitatory currents, something that was not expected though GtACR1 is described as a Cl^- -conducting channel. Therefore, GtACR1::YE driven directly in the muscle to the original genotype was compared to exclude possible disruptive factors of synaptic transmission. Additionally an 'undriven' GtACR1::YE was employed as a control.

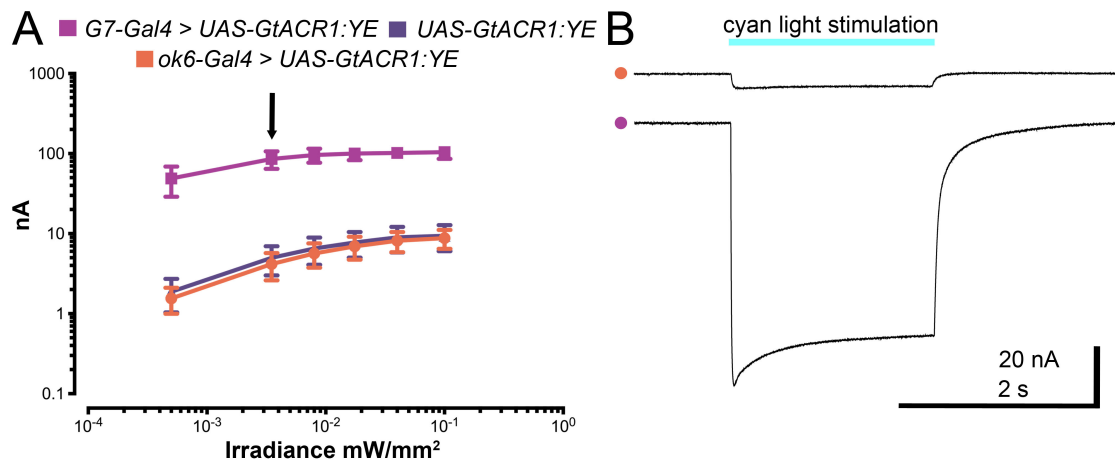


Figure 22 | Depolarisation of larval muscles carrying GtACR1::YE

A) Peak depolarisation in muscle tissue of larvae expressing GtACR1::YE on the presynaptic side (*ok6-Gal4*), postsynaptic side (*G7-Gal4*) or larvae carrying only the *UAS-GtACR1::YE* complex without targeted expression in any larval tissue. Data shown as mean \pm SD. **(B)** Sample traces of depolarisation plateau measured in *ok6-Gal4 > UAS-GtACR1::YE* and *G7-Gal4 > UAS-GtACR1::YE* *Drosophila* larvae. Arrow in **(A)** indicates irradiance of sample traces ($3.5 \mu\text{W}/\text{mm}^2$).

The same ‘extent of baseline-shift’ or rather depolarisation in muscle cells in the ‘undriven’ GtACR1 larvae as in the larvae expressing GtACR1::YE in motoneurons could be found. Furthermore, ten times higher shifts in the baseline potential were observable if GtACR1::YE was expressed directly in the muscle cell and activated by cyan light as compared to the other experimental groups.

This observation might lead to two conclusions. First, some GtACR1::YE is even expressed functionally without the use of a common driver line. An effect which was also described lately by Mohammad et al. (2017). Secondly, the activation of GtACR1::YE - a selective chloride-conducting channel - leads to excitatory changes of the membrane potential in the muscle, whereas it inhibits in the motoneuron. Therefore, depending on the cell population and different intracellular chloride concentrations, the resulting effect of GtACR activation spans from distinct inhibition to depolarisation. As a consequence, chloride concentrations of the used cell population should be analysed, if not known, before employing GtACR.

3.3.3 Larval behaviour

In addition to electrophysiological experiments and stainings, simple behaviour patterns of larvae expressing different tagged GtACR1s in motoneurons were also analysed. Therefore, in addition to GtACR1::YE, a GtACR1 fused to a Flag tag was employed and expressed in larval motoneurons.

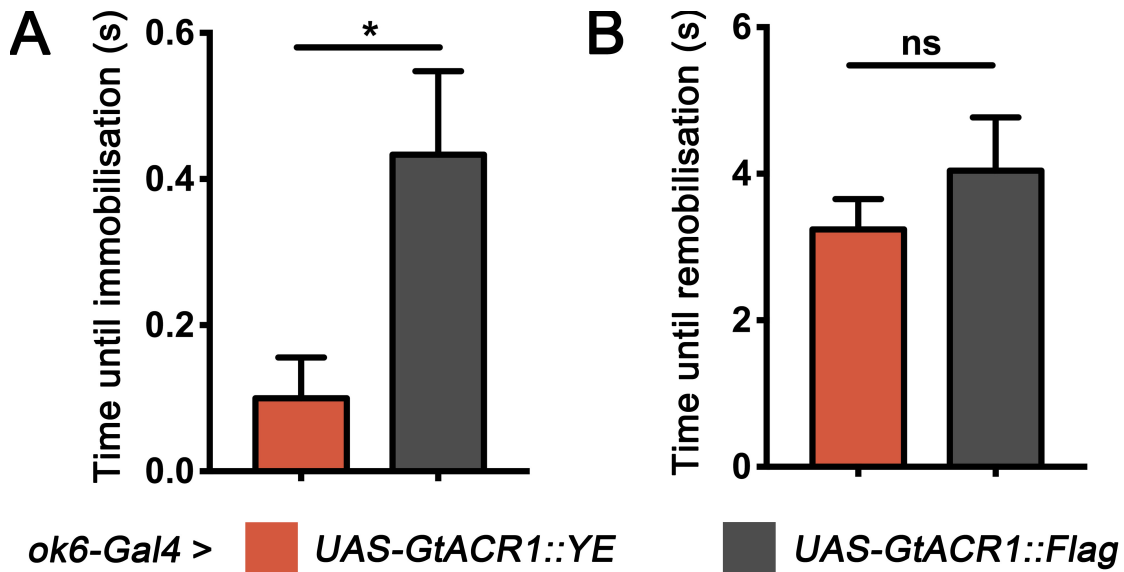


Figure 23 | Larval immobilisation by GtACR1::YE or GtACR1::Flag

(A) Bar chart indicates a slightly significant delay ($p = 0.0202$, $n = 30$) until effective immobilisation occurs of larvae expressing GtACR1::YE as compared to GtACR1::Flag (*ok6-Gal4* was used to drive expression in motoneurons). Light intensity of 1 mW/mm^2 at 470 nm wavelength. (B) No significant differences were found between both groups when the light was switched off until larval remobilisation occurred ($p > 0.05$, $n \geq 24$). Data acquired by S. Dannhäuser (Dannhäuser, 2016).

Immobilisation and relaxation (increased body length) due to light exposition could be observed. Furthermore, illumination (1 mW/mm^2 ; 470 nm) of larvae expressing GtACR1::YE or GtACR1::Flag showed slightly significant differences until effective immobilisation occurred (Fig. 23.A), even though all tested larvae immobilised within 1 sec. The difference observed in the immobilisation time has been discussed previously (Dannhäuser, 2016). It was referred to the additional endoplasmatic reticulum export signal (expressed along with the YFP signal), which may lead to better expression at the axonal terminals (Dannhäuser, 2016). However, no significant differences of the remobilisation of the larvae after the light source was switched off could be observed (Fig. 23.B).

4 Discussion

4.1 Channelrhodopsin2-XXM

4.1.1 Channelrhodopsin2-XXM – a new optogenetic tool

In this thesis it could be shown that Channelrhodopsin2-XXM is a useful tool with high accuracy in time. ChR2^{XXM} helped to investigate reasons for malfunctioning of the *Drosophila* chordotonal organ and clarify intracellular signalling by dCIRL, in *dCIRL*^{KO} mutants, which will be discussed later on.

Operating in a determined part of an *in vivo* (neuronal) system with very high temporal precision and minimized irritation of surrounding tissue are the main development goals for optogenetic tools. For example, the *Drosophila* chordotonal organ is not only sensitive to proprioception but also to heat (Sokabe and Tominaga, 2009) which could appear as a problem if common ChR2-wt was employed. As reported previously, this channel is activated at high light intensities. Thus, care has to be taken to identify possible heat-induced side effects. Hence, an optogenetic tool that works efficiently at low light intensity levels but without restrictions in temporal precision was needed. As a result, Channelrhodopsin2-XXM was chosen as an attractive tool for this particular purpose (even though it offers slightly reduced temporal precision compared to ChR2-wt).

Three main characteristics of ChR2^{XXM} could be figured out. First, it is very sensitive to low light intensities *in vivo* (from 3 $\mu\text{W}/\text{mm}^2$ if ATR is supplemented). Second, it possesses a high temporal precision and third, it works sufficiently even over longer periods of irradiation. To give an example on high precision and sensitivity: it could be demonstrated that a 1 $\mu\text{W}/\text{mm}^2$ and 50 ms light pulse is sufficient to trigger one single eEPSC at the *Drosophila* NMJ (Fig. 11.B). Furthermore, if the pulse duration was reduced to 1 ms and the light intensity was increased to 40 $\mu\text{W}/\text{mm}^2$ a sufficient 10 Hz stimulation could be carried out (Fig. 11.C).

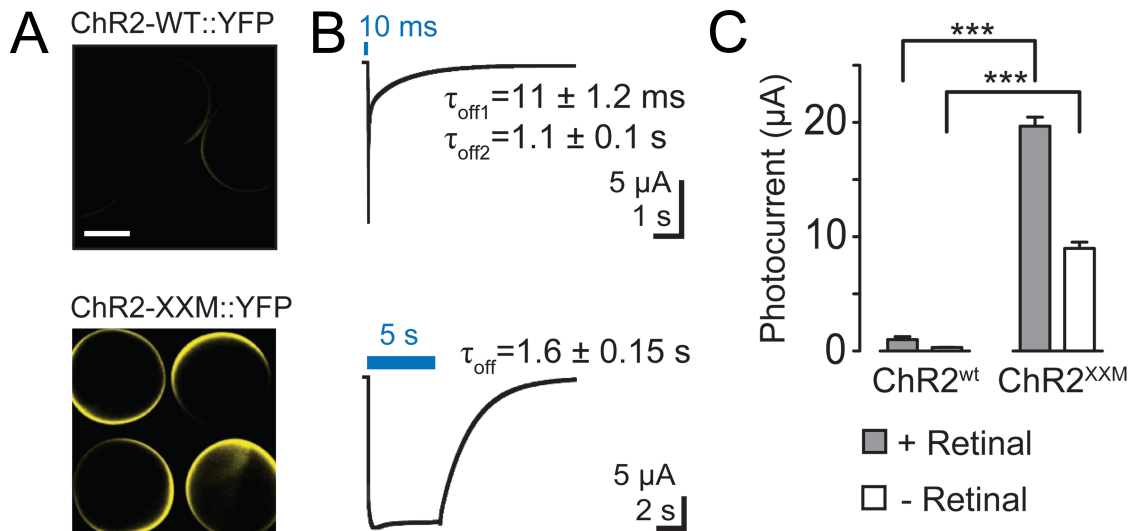


Figure 24 | Expression and kinetics of ChR2-XXM in *Xenopus* Oocytes

Data acquisition by G. Nagel and staff. **(A)** Expression of ChR2-WT::YFP and ChR2-XXM::YFP in *Xenopus* oocytes (without ATR supplementation) imaged by confocal microscopy. **(B)** Representative photocurrents of ChR2-XXM::YFP in oocytes (473 nm, ~ 12.4 mW/mm²). Short light pulses are followed by a rapid biphasic photocurrent decay (t_{off1} : 80%, t_{off2} : 20%), whereas the longer time constant (t_{off}) dominates upon prolonged photostimulation. Data shown as mean \pm SD, $n = 4$ recordings from individual oocytes incubated with 1 mM all-trans-retinal. **(C)** Quantification of photocurrent amplitudes in oocytes with and without retinal supplementation. Data presented as mean \pm SEM. All data and description shown are recently published in (Scholz et al., 2017).

The characteristics of ChR2^{XXM} are due to an extraordinary high protein expression and membrane binding ability as compared to ChR2-wt (cf. Fig. 24.A) in addition to a prolonged open-state lifetime. Alterations of the ChR2^{XXM} photocycle result from a genetic change in the amino acid sequence that leads to an altered structure of the hydrogen bond in Channelrhodopsin-2. The hydrogen bond forms between C128 in Helix 3 and D156 in Helix 4 (Berndt et al., 2009; Bamann et al., 2010; Schneider et al., 2015). Bamann et al. could show that alterations of C128 or D156 lead to increased open states and therefore a drastically changed photocycle, whereby alternating of D156 leads to increased photostimulation efficiency. Therefore this key amino acid region is very interesting to screen for other ChR2 mutations with alternations in light sensitivity and stimulation efficiency.

Obviously, there are Channelrhodopsin variants that show some of the mentioned characteristics but lack others if used in an *in vivo* system. Earlier

described variants, for instance, the original ChR2 lacks light sensitivity (e.g., it has no detectable effect on adult *Drosophila* if expressed in motoneurons) and sufficiency over longer periods of stimulation. Another example is the recently described ChR2^{XXL} (replacement of aspartic acid with cysteine at position 156 – D156C), which is extremely sensitive to light and displays very good expression of the protein but lacks the temporal precision (Dawydow et al., 2014). In fact, short weak light pulses of blue light (5 $\mu\text{W}/\text{mm}^2$) lead to detectable eEPSCs for approximately 70 s. Nonetheless, ChR2^{XXL} is an attractive tool for long-lasting stimulations at extremely low light intensities.

In this study, aspartic acid at position 156 was replaced by a histidine (D156H). This mutation leads a medium open-state lifetime and an increased expression of the protein compared to ChR2-wt even without the supplement of all-trans-retinal chromophore (Fig. 24.A). The chromophore ATR is linked to lysine 257 in helix 7 and has to be available in the cell during the protein expression of Chop2-wt otherwise Chop2-wt degrades and can not form ChR2-wt. Because of this degradation process, which is seen in *Drosophila* due to insufficient levels of intracellular ATR, ChR2-wt can only be effectively employed if high amounts of ATR are supplemented. However, the expression of ChR2-wt at the larval NMJ remains still low compared to ChR2^{XXM} or ChR2^{XXL} (Schroll et al., 2006; Pulver et al., 2009; Ljaschenko et al., 2013).

It was also shown that some mutants are somewhat resistant to degradation and are able to bind ATR as a chromophore if added later (Ullrich et al., 2013). This leads to better initially protein expression of the mutated channels at the cell membrane and improved functionality (Dawydow et al., 2014). For ChR2^{XXM} this also seems to be true. Interestingly, if ChR2^{XXM} was tagged with a photoprotein, supplement of ATR was needed to reach the same functionality as the untagged ChR2^{XXM}. Possibly this is due to interferences between phototagged Chop2^{XXM} and the chromophore.

The Initially performed characterisation of ChR2^{XXM} in *Xenopus laevis* oocytes displayed pinpoint accuracy of channel kinetics (10 ms: $\tau_{\text{off1}} = 11 \pm 1.2$ ms SD, $\tau_{\text{off2}} = 1.1 \pm 0.1$ s SD, Fig.24.B) and, most important, a ten-fold increase of the photocurrent amplitude compared to ChR2-wt. ChR2^{XXM} as a new powerful variant of ChR2 can be classified nearby ReaChR (red-activatable ChR; Lin et al. 2013) if earlier performed comparisons are taken into account (Dawydow et al., 2014). Nevertheless, a full body contraction of larvae longer than 100 s needs approximately 20-fold more light irradiance if ReaChR is expressed in larval motoneurons (2 $\mu\text{W}/\text{mm}^2$ at 460nm vs. ~ 40 $\mu\text{W}/\text{mm}^2$ at 623nm).

To sum up, ChR2^{XXM} extends the variety of Channelrhodopsins by one ChR with pinpoint accuracy at low light intensities and a wide field of possible applications.

4.1.2 Mechanosensation by light – ChR2-XXM in the lch5

Since Channelrhodopsins are easy applicable tools for direct well-controlled cell depolarisation, ChR2^{XXM}, as a new and effective optogenetic tool that enables convenient accessibility to the ChO, could be employed. Imaging of the larvae expressing ChR2^{XXM}::tdtomato in their lch5 (*iav-Gal4*) revealed strong expression of the protein along the dendrites of the lch5. Moreover, expression of ChR2^{XXM}::tdtomato till the projection neuron in the VNC of the larvae was found, which allows reliable conclusions on an even distribution of the protein along the whole pathway.

Since it could be shown that defects of *dCIRL* lead to an altered mechanosensation the chordotonal organ (Scholz et al., 2015), ChR2^{XXM} was employed to differentiate to what extent signal transduction or transmission (or both) is affected in *dCIRL*^{KO} larvae. In detail, ChR2^{XXM} was used to 'by-pass' signal transduction of the ChO (it causes directly changes of the membrane potential). The definite effect of *dCIRL* on signal perception and the chordotonal organ itself will be discussed in chapter 4.3.

4.2 GtACR

4.2.1 Use of GtACR as an optogenetic inhibitor tool

In this thesis the inhibitory power of GtACR1, a Cl⁻-conducting Channelrhodopsin, was evaluated precisely. As described in recent publications our data supports the observation that GtACR1 is a very effective hyperpolarizing/silencing tool at low to very low light intensities (Sineshchekov et al., 2015). GtACR1 is very efficient in extinguishing electrically triggered eEPSCs in the motoneurons of *Drosophila* larvae. The used GtACR1::YE was sufficient in suppressing eEPSCs completely at all time and at all intensities tested (lowest intensity 0.5 $\mu\text{W}/\text{mm}^2$ at 490 nm). Furthermore, control of the 'inhibition level' was possible very smoothly by an employed white light source (Fig. 21). Here a decrease in eEPSCs amplitudes as a function of higher light intensity was detected. Differences that could be observed in behavioural experiments (cf. Fig. 23.A,B) between GtACR::YE and GtACR::Flag may arise from the fact that the YE is a YFP, combined with an endoplasmatic reticulum (ER) export signal to lead to a better cellular expression (cf. Klapoetke et al. 2014). In fact, beside the significant difference in behaviour (Fig. 23.A) an increased localisation at the larval NMJ could be observed by confocal imaging (Dannhäuser, 2016). In sum, GtACR1 is an attractive tool if very precise control of single neurons in a complex network is needed, e.g. to simulate realistic communication in a neuronal network even with precise control of amplitudes.

4.2.2 'Baseline-shift' as a mentionable side effect of GtACR

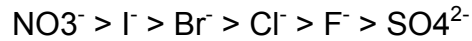
Interestingly, it could be noticed that stimulation of GtACR leads to a detectable positive shift of the baseline. This observation could not be brought into accordance with chloride conduction along the motoneuron terminal boutons. Therefore, it was hypothesised that either the used motoneuron driver line (*ok6-Gal4*) has some off-target expression in the larval muscle tissue or the used UAS-construct (*UAS-GtACR1*) has some leak-expression in other relevant larval tissues. Initially, the conspicuous 'baseline-shift' was assumed to be most

likely to leak-expression of the UAS-construct, because the motoneuron driver line (*ok6-Gal4*) is broadly used and well characterised. Actually, the same plateau depolarisation if stimulated 'undriven' *UAS-GtACR1* and even significantly stronger if expressed *GtACR1* directly in larval muscle tissue (*G7-Gal4*) was found. This leads to the conclusion that the observed depolarisation is an effect of direct *GtACR* stimulation in larval muscle tissue and accompanying an effect of leak-expression if *GtACR* is not expressed in the muscle tissue. Subsequently, it was tried to detect the photoprotein (YFP) by immunofluorescence microscopy, but no signal of *GtACR1::YE* could be detected without staining.

To sum up, observations lead to two main questions or even obstacles. First, how could activation of a high selective Cl^- -conduction channel result in immense depolarisation of the larval muscle tissue? Second, if the used *UAS-GtACR1* construct leads to relevant leak expression in larval (muscle) tissue could it also lead to even more delicate side effects? For example, if *UAS-GtACR1* has also relevant expression in the VNC or just parts of it, behavioural settings using this construct (and genomic injection side) have to be reconsidered. However, due to the exceptional expression of *UAS-GtACR1* 'side-effects' arise as a consequence, because a possible leak-expression is boosted, too.

Even though no leak expression of *GtACR1::YE* using confocal microscopy was detectable and therefore possible 'areas of leak-expression' could not be identified, a reconstruction (e.g. change of the genomic injection side) of the *UAS-GtACR1* carrying fly line is strongly recommended, because sensitivity of confocal microscopy is much lower compared to electrophysiology. Anyhow, the previously described 'baseline-shift' can be assumed as direct channel kinetics, therefore it had to be admitted that a gradient for chloride from the inside to the outside of the cell was the reason for depolarisation via *GtACR1*. Side effects of other metal cations or even protons could be excluded with reasonable certainty, because *GtACR1* is known to be highly chloride selective

(Govorunova et al., 2015; Sineshchekov et al., 2015). However, GtACR1 is permeable for the following anions in descending order:



Whereby GtACR1 is shown to be impermeable for SO_4^{2-} . Therefore, it could not be confirmed fully that the strong depolarisation was just due to potential chloride efflux, even though high concentrations of NO_3^- , I^- or Br^- in *Drosophila* larval muscle cell were not expected.

Anyhow, specific studies on muscle tissue of mammals could show that smooth muscles contain more chloride than expected if chloride would distribute accordingly to the Donnan equilibrium (Chipperfield and Harper, 2000). Moreover, paradox effects of optogenetic inhibition tools in hippocampal neuronal tissue have been described very recently (Mahn et al., 2016; Wiegert and Oertner, 2016) showing that GtACR1 expression leads to depolarisation at bouton level due to higher chloride concentrations inside the boutons compared to the soma (where GtACR1 triggers an inhibiting effect). To clarify this, experiments with high/low external chloride concentrations and a setup concerning intracellular electrolyte analysis would be desirable.

These experiments indicate that inhibitory tools that interfere mainly with chloride ions may generate delicate effects, even the contrary effect as initially intended. Therefore, to reduce possible side effects, an optogenetic tool is needed, that interferes with neurons/cells mainly via changes of potassium concentration, because in most cases potassium works as a physiological counterpart of sodium (or calcium) induced excitation.

4.3 Chordotonal organ and *dCIRL*

In this thesis ChR2^{XXM} was employed to investigate the distinctive function of a recently intensively studied adhesion GPCR – *dCIRL*/atrophilin - in the chordotonal organ of *Drosophila melanogaster* in more detail. As mentioned before, ChR2^{XXM} paved the way to direct non-invasive stimulation of the chordotonal organ of *Drosophila melanogaster* larvae. Experiments carried out in this thesis demonstrate that a direct activation of the ICh5 by light induced depolarisation is sufficient to lead to a prolonged ‘startle-response’ in *Drosophila* larvae (Fig. 17.A). Since the ‘startle-response’ physiologically arises from an adequate (mechanical) stimulus of the chordotonal organ (Zhou et al., 2012; Scholz et al., 2015) this behaviour pattern can be used as an indicator of sufficient *in vivo* activation of the Cho. Furthermore, ChR2^{XXM} and ChR2^{XXM}::tdtomato work sufficiently at low light intensities (3 $\mu\text{W}/\text{mm}^2$ were used for *in vivo* experiments), therefore heat effects as described in earlier studies, could be justifiably neglected (Liu et al., 2003; Kwon et al., 2010; Barbagallo and Garrity, 2015).

Interestingly, the effect of direct ChO activation from optical irritation behaviour could not be distinguished initially. No significant differences between larvae expressing ChR2^{XXM}::tdtomato in their ChO compared to control larvae (*UAS-ChR2^{XXM}::tdtomato* crossed to wt) at higher light intensities (data not shown) were found. Subsequently, blue light irradiation to the minimal possible level where ChR2^{XXM} still works effectively (2-3 $\mu\text{W}/\text{mm}^2$) was reduced. Thus, it was possible to detect strong significant differences between the two experimental groups and it could be concluded that direct depolarisation of the ChO by ChR2^{XXM} leads to larval behaviour similar to mechanical activation of the ICh5. Moreover, earlier publications could demonstrate that knockout of *dCIRL* (*dCIRL^{KO}*) results in extensive ‘head-swing behaviour’ or ‘startle response’ leading to complete deregulation of larval locomotion due to a profoundly reduced mechanosensation (Scholz et al., 2015).

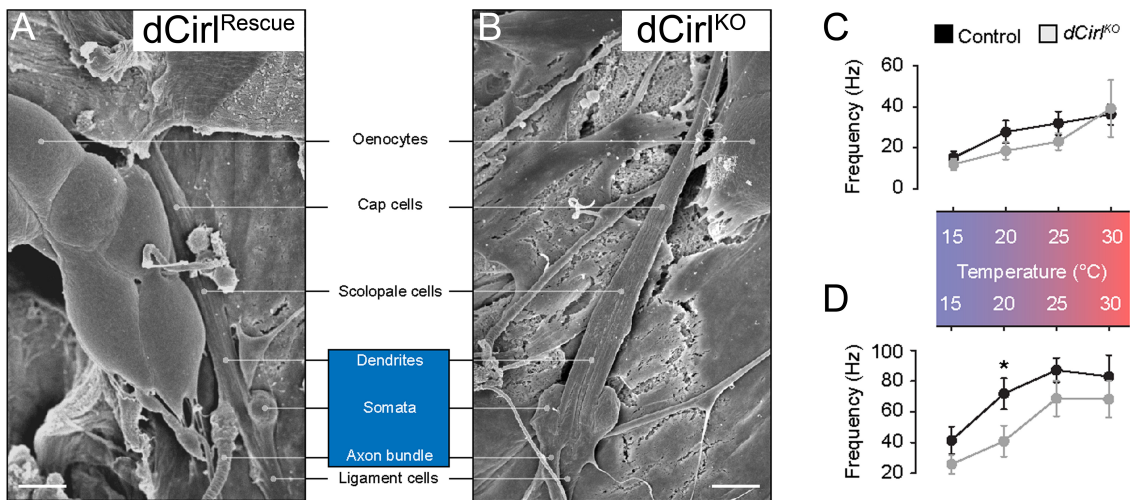


Figure 25 | Electron microscopy and temperature sensation of the ChO

(A) Electron micrograph of *lch5* in *dCIRL^{Rescue}* and *dCIRL^{KO}* animals **(B)** show no detectable morphological differences. The organ consists of a chain of support cell types that suspend the mechanosensory neurons (blue) between body wall and musculature. Scale bars 10 μ m. **(C,D)** Quantification of action current frequencies without **(C)** and with mechanical stimulation **(D)** in control (black) and *dCIRL^{KO}* larvae (gray). Asterisk denotes $p \leq 0.05$ comparing event frequency at 20 °C with a Student's t- test. Data are presented as mean \pm SEM, $n = 8$ per genotype. EM-recordings, graphs and graph description (partly) taken from Scholz et al. 2017 (Scholz et al., 2017).

Since it remained unclear if the *dCIRL^{KO}* mutation as well has an effect on the chordotonal organ itself or if only the peripheral signal perception mediated by latrophilin is impaired, the employment of *ChR2^{XXM}* could elucidate these questions. Electrophysiological recordings from the *lch5* revealed no significant differences in event frequency at certain light intensities in *dCIRL^{KO}* larvae or controls expressing *ChR2^{XXM}::tdtomato* in their chordotonal organs. Correspondingly, signal transmission in and after the *lch5* remains unaffected in these larvae. Further observations that *dCIRL^{KO}* showed no altered thermosensation between 15 °C – 30 °C support the conclusion that *dCIRL* has a mechano-specific role in the chordotonal organ (Fig. 25.C,D; Scholz et al. 2017). Moreover, electron micrographs could not show any morphological defects of the chordotonal organ in *dCIRL^{KO}* *Drosophila* larvae (Fig. 25.A,B). These observations along with the findings that elongation of the N-terminal fragment of *dCirl* results in reduced action current frequencies may lead to the deduction that the 'operating range' of *dCIRL* is most likely to be constrained

between cutis and the chordotonal organ itself. Moreover, subsequent performed experiments in the corresponding paper to this thesis could clearly show that high cAMP levels 'muted' the functional response of the chordotonal organ similar to *dCIRL*^{KO} mutants (Scholz et al., 2017). Additionally, mechanic stimulation of wildtype neurons triggered a cAMP decrease that was missing in *dCIRL*^{KO} larvae, indicating that *dCIRL* shapes mechanosensation by activity dependent suppression of cAMP (Scholz et al., 2017).

4.4 Clinical relevance of this thesis and Outlook

4.4.1 Application of optogenetic tools for therapeutic purposes

Optogenetic tools nowadays have a wide spectrum of functionality and thus a versatile field of application. For example, they can be used for long-lasting stimulation (Dawydow et al., 2014) or in setups where pin-point accuracy in time is required (Kleinlogel et al. 2011; Scholz et al. 2017). Additionally, there are optogenetic effectors that may interfere with second messenger pathways with high precision (Stierl et al., 2011; Gao et al., 2015). Thus, optogenetics deliver an easy accessible method to interfere with a well-defined cell population in many different ways.

However, clinical usage of optogenetic tools to treat movement disorders (e.g. Parkinson's disease, dystonia or choreatic movements) or neuropsychiatric disorders (e.g. depression, schizophrenia or dementia) is still not established. This is probably due to ethical concerns and technical problems to integrate Channelrhodopsins vector based in a particular area of the human brain, though ChR2 has been already proven to integrate successfully in human brain tissue (Andersson et al., 2016). Moreover, optogenetic tools are on their way to be used in a therapeutic manner. For example, it is already possible to integrate ChR2 in retina ganglion cells of photoreceptor deficient animals (Bi et al., 2006). It is even possible to restore hearing impairment by the use of ChR2 (Shimano et al., 2013). These few examples already demonstrate the clinical relevance of this technique. But compared to the human brain, these structures are relatively easy to access and modify, although there are already minimal invasive methods to intervene with human brain tissue.

A well-known example is deep brain stimulation (DBS) where an electrical field is generated to interfere with specific structures in the brain (basal ganglia) to mainly treat movement disorders. This technique is broadly accepted as a well-established therapeutic procedure (Perlmutter and Mink, 2006) with very good benefit for patients, e.g. with Parkinson's disease (Volkman et al. 2001 and

2007). It would be very interesting to examine if this approach could be improved further in precision and thus in the resulting therapeutic effect by integration of optogenetic proteins in specific areas of the human brain tissue. But therefore network studies of the relevant neuronal circuits in mammals are inevitable to define exact pathways where 'light-inducible channel proteins' could be integrated to evoke a determined clinical effect and to reduce unwanted side effects.

Moreover, optogenetic approaches are a very effective way to define exact pathways in model organisms but they are not suitable for clinical usage in the central nervous system at the current stage. One main reason for this is that optogenetic tools have not been shown to be 'safe' for application in the human central nervous system. However, there are already methods that deliver the light to the exact anatomical structure (Dufour and De Koninck, 2015; Segev et al., 2016) even wirelessly (Wentz et al., 2011; Montgomery et al., 2015; Park et al., 2015) and genetic applications like the recombinant adeno-associated virus (rAAV) that allow the integration of ChR in specific anatomical structures. But yet, further genetic and technological research is needed to achieve an even better accuracy in utilisation of the given optogenetic tools. Even though, (red-) sensitive optogenetic tools already exist which can be activated through an intact skull of an awake mouse (Lin et al., 2013), they still need extremely high light intensities. Therefore, further improvement of Channelrhodopsins that offer a high spatiotemporal resolution, like chETA [E123T, up to 200Hz; (Gunaydin et al., 2010)] or the double mutant E123T/T159C [up to 60 Hz;(Berndt et al., 2011)] but work, in contrast to chETA or the double mutant, sufficiently at very low light intensities (to reduce heat side-effects) is desirable. An example of a ChR that may fulfil these criteria is ChR2^{XXM} even though the spatiotemporal resolution has not been tested to this extent (Scholz et al., 2017).

However, utilisation of optogenetic tools is not limited to the central or peripheral nervous system. There are existing applications of light sensitive channel proteins to heart muscle cells or skeletal muscle cells to either regulate

malfunction or control movements very accurate (Bruegmann et al., 2010, 2015, 2016; Pianca et al., 2017).

Nevertheless, optogenetics are just one way to obtain control of a distinct neuronal (or other) cell population. Research in further easy accessible and controllable 'channel proteins' should have high priority. For example, gaining control of neuronal populations by ultra sound or, as already possible, magnetothermally (Chen et al., 2015) could also be very useful. Since, initially no "application device" like fibre optics or electrodes is needed, even to the price of possible local heat development and as consequence thereof cell damage.

With respect to the very fast development and improvement of optogenetics in the last decade, there will be definitely further path breaking innovations in fundamental and clinical research.

4.4.2 Latrophilin

Recent investigation of Latrophilin (*dCIRL*) demonstrates that Latrophilin works as a crucial regulation protein for incoming stimuli. Since, aGPCRs are the 2nd largest class of the seven trans-membrane receptor family and expressed ubiquitously in mammals and invertebrates, it is only a matter of time until aGPCRs will be used in greater extent as pharmacological targets (Langenhan et al., 2016). In this context, one can think of poorly understood clinical syndromes probably caused by defects or malfunctioning in *CIRL* or other aGPCRs.

Therefore, further research could reveal new highly potent pharmacological targets and also a better understanding of undertreated diseases or to be more precise in diseases associated with mechanosensory deficits. Thereby diseases characterised by a malfunctioning nociceptive system should be of major interest since nociceptive perception is an important part of the

mechanosensory system. Furthermore defects in nociception constitute a broad spectrum of undertreated and not sufficiently understood clinical syndromes that are very sorrowful to affected patients (Sommer, 2016).

5 Summary

Since Channelrhodopsins has been described first and introduced successfully in freely moving animals (Nagel et al., 2003 and 2005), tremendous impact has been made in this interesting field of neuroscience. Subsequently, many different optogenetic tools have been described and used to address long-lasting scientific issues. Furthermore, beside the 'classical' Channelrhodopsin-2 (ChR2), basically a cation-selective ion channel, also altered ChR2 descendants, anion selective channels and light-sensitive metabotropic proteins have expanded the optogenetic toolbox. However, in spite of this variety of different tools most researches still pick Channelrhodopsin-2 for their optogenetic approaches due to its well-known kinetics.

In this thesis, an improved Channelrhodopsin, Channelrhodopsin2-XXM (ChR2^{XXM}), is described, which might become a useful tool to provide ambitious neuroscientific approaches by dint of its characteristics. Here, ChR2^{XXM} was chosen to investigate the functional consequences of *Drosophila* larvae lacking latrophilin in their chordotonal organs. Finally, the functionality of GtACR, was checked at the *Drosophila* NMJ. For a in-depth characterisation, electrophysiology along with behavioural setups was employed.

In detail, ChR2^{XXM} was found to have a better cellular expression pattern, high spatiotemporal precision, substantial increased light sensitivity and improved affinity to its chromophore retinal, as compared to ChR2. Employing ChR2^{XXM}, effects of latrophilin (*dCIRL*) on signal transmission in the chordotonal organ could be clarified with a minimum of side effects, e.g. possible heat response of the chordotonal organ, due to high light sensitivity. Moreover, optogenetic activation of the chordotonal organ, *in vivo*, led to behavioural changes. Additionally, GtACR1 was found to be effective to inhibit motoneuronal excitation but is accompanied by unexpected side effects. These results demonstrate that further improvement and research of optogenetic tools is highly valuable and required to enable researchers to choose the best fitting optogenetic tool to address their scientific questions.

6 References

Abbott, L. F. and Nelson, S. B. (2000) 'Synaptic plasticity: Taming the beast', *Nature Neuroscience*, 3(11s), pp. 1178–1183. doi: 10.1038/81453.

Adams, M. D. et al. (2000) 'The genome sequence of *Drosophila melanogaster*', *Science*, 287(March), pp. 2185–2195. doi: 10.1126/science.287.5461.2185.

Adrian, E. D. (1926) 'The impulses produced by sensory nerve-endings: Part I.', *The Journal of physiology*, 61(1), pp. 49–72. doi: 16993776.

Adrian, E. D., Cattell, M. and Hoagland, H. (1931) 'Sensory discharges in single cutaneous nerve fibres', *J. Physiol.*, 72(4), pp. 377–391. doi: 10.1113/jphysiol.1931.sp002781.

Anderson, M. S., Halpern, M. E. and Keshishian, H. (1988) 'Identification of the neuropeptide transmitter proctolin in *Drosophila* larvae: characterization of muscle fiber-specific neuromuscular endings.', *Journal of Neuroscience*, 8(1), pp. 242–55

Andersson, M., Avaliani, N., Svensson, A., Wickham, J., Pinborg, L. H., Jespersen, B., Christiansen, S. H., Bengzon, J., Woldbye, D. P. D. and Kokaia, M. (2016) 'Optogenetic control of human neurons in organotypic brain cultures', *Scientific Reports*. Nature Publishing Group, 6(April), pp. 1–5. doi: 10.1038/srep24818.

Araç, D., Boucard, A. A., Bolliger, M. F., Nguyen, J., Soltis, S. M., Südhof, T. C. and Brunger, A. T. (2012) 'A novel evolutionarily conserved domain of cell-adhesion GPCRs mediates autoproteolysis', *EMBO Journal*, 31(6), pp. 1364–1378. doi: 10.1038/emboj.2012.26.

Arenkiel, B. R., Peca, J., Davison, I. G., Feliciano, C., Deisseroth, K., Augustine, G. J. J., Ehlers, M. D. and Feng, G. (2007) 'In Vivo Light-Induced Activation of Neural Circuitry in Transgenic Mice Expressing Channelrhodopsin-2', *Neuron*, 54(2), pp. 205–218. doi: 10.1016/j.neuron.2007.03.005.

Atwood, H. L., Govind, C. K. and Wu, C.-F. (1993) 'Differential ultrastructure of synaptic terminals on ventral longitudinal abdominal muscles in *Drosophila* larvae', *Journal of Neurobiology*, 24(8), pp. 1008–1024. doi: 10.1002/neu.480240803.

Bamann, C., Gueta, R., Kleinlogel, S., Nagel, G. and Bamberg, E. (2010) 'Structural guidance of the photocycle of channelrhodopsin-2 by an interhelical hydrogen bond', *Biochemistry*, 49(2), pp. 267–278. doi: 10.1021/bi901634p.

- Barbagallo, B. and Garrity, P. A.** (2015) 'Temperature sensation in *Drosophila*', *Current Opinion in Neurobiology*, 34, pp. 8–13. doi: 10.1016/j.conb.2015.01.002.
- Bellen, H. J., Tong, C. and Tsuda, H.** (2010) 'a History Lesson for the Future', *Neuroscience*, 11(july), pp. 514–522. doi: 10.1038/nrn2839.
- Bennett, M. R.** (1999) 'The early history of the synapse: From plato to sherrington', *Brain Research Bulletin*, 50(2), pp. 95–118. doi: 10.1016/S0361-9230(99)00094-5.
- Bennett, M. V. L. and Zukin, R. S.** (2004) 'Electrical Coupling and Neuronal Synchronization in the Mammalian Brain', *Neuron*, 41(4), pp. 495–511. doi: 10.1016/S0896-6273(04)00043-1.
- Berndt, A., Yizhar, O., Gunaydin, L. A., Hegemann, P. and Deisseroth, K.** (2009) 'Bi-stable neural state switches.', *Nature neuroscience*, 12(2), pp. 229–34. doi: 10.1038/nn.2247.
- Berndt, A., Schoenenberger, P., Mattis, J., Tye, K. M., Deisseroth, K., Hegemann, P. and Oertner, T. G.** (2011) 'High-efficiency channelrhodopsins for fast neuronal stimulation at low light levels', *Proceedings of the National Academy of Sciences*, 108(18), pp. 7595–7600. doi: 10.1073/pnas.1017210108.
- Berndt, A., Lee, S. Y., Ramakrishnan, C. and Deisseroth, K.** (2014) 'Structure-Guided Transformation of Channelrhodopsin into a Light-Activated Chloride Channel', *Science*, 344(6182), pp. 420–424. doi: 10.1126/science.1252367.
- Berthold, P., Tsunoda, S. P., Ernst, O. P., Mages, W., Gradmann, D. and Hegemann, P.** (2008) 'Channelrhodopsin-1 Initiates Phototaxis and Photophobic Responses in *Chlamydomonas* by Immediate Light-Induced Depolarization', *the Plant Cell Online*, 20(6), pp. 1665–1677. doi: 10.1105/tpc.108.057919.
- Bi, A., Cui, J., Ma, Y. P., Olshevskaya, E., Pu, M., Dizhoor, A. M. and Pan, Z. H.** (2006) 'Ectopic Expression of a Microbial-Type Rhodopsin Restores Visual Responses in Mice with Photoreceptor Degeneration', *Neuron*, 50(1), pp. 23–33. doi: 10.1016/j.neuron.2006.02.026.
- Bliss, T. V and Collingridge, G. L.** (1993) 'A synaptic model of memory: long-term potentiation in the hippocampus.', *Nature*, 361(6407), pp. 31–39. doi: 10.1038/361031a0.
- Bliss, T. V and Lømo, T.** (1973) 'Long-lasting potentiation of synaptic transmission in the dentate area of the anaesthetized rabbit following stimulation of the perforant path', *J. Physiol.*, 232, pp. 331–356

Boyden, E. S., Zhang, F., Bamberg, E., Nagel, G. and Deisseroth, K. (2005) 'Millisecond-timescale, genetically targeted optical control of neural activity', *Nature Neuroscience*, 8(9), pp. 1263–1268. doi: 10.1038/nn1525.

Brand, A. H. and Perrimon, N. (1993) 'Targeted gene expression as a means of altering cell fates and generating dominant phenotypes.', *Development (Cambridge, England)*, 118(2), pp. 401–15. doi: 10.1101/lm.1331809.

Broadie, K. S. and Bate, M. (1993) 'Development of the embryonic neuromuscular synapse of *Drosophila melanogaster*', *The Journal of neuroscience*, 13(January), pp. 144–166. Available at: <http://www.ncbi.nlm.nih.gov/pubmed/8093713>.

Bruegmann, T., Malan, D., Hesse, M., Beiert, T., Fuegemann, C. J., Fleischmann, B. K. and Sasse, P. (2010) 'Optogenetic control of heart muscle in vitro and in vivo', *Nature Methods*, 7(11), pp. 897–900. doi: 10.1038/nmeth.1512.

Bruegmann, T., Van Bremen, T., Vogt, C. C., Send, T., Fleischmann, B. K. and Sasse, P. (2015) 'Optogenetic control of contractile function in skeletal muscle', *Nature Communications*. Nature Publishing Group, 6, pp. 1–8. doi: 10.1038/ncomms8153.

Bruegmann, T., Boyle, P. M., Vogt, C. C., Karathanos, T. V., Arevalo, H. J., Fleischmann, B. K., Trayanova, N. A. and Sasse, P. (2016) 'Optogenetic defibrillation terminates ventricular arrhythmia in mouse hearts and human simulations', *Journal of Clinical Investigation*, 126(10), pp. 3894–3904. doi: 10.1172/JCI88950.in.

Chen, R., Romero, G., Christiansen, M. G., Mohr, A. and Anikeeva, P. (2015) 'Wireless magnetothermal deep brain stimulation', *Science*, 347(6229), pp. 1477–1480. doi: 10.1126/science.1261821.

Chipperfield, A. R. and Harper, A. A. (2000) 'Chloride in smooth muscle', *Progress in Biophysics and Molecular Biology*, 74(3–5), pp. 175–221. doi: 10.1016/S0079-6107(00)00024-9.

Choquet, D. and Triller, A. (2013) 'The dynamic synapse', *Neuron*. Elsevier Inc., 80(3), pp. 691–703. doi: 10.1016/j.neuron.2013.10.013.

Clapham, D. E., Runnels, L. W. and Strübing, C. (2001) 'The TRP ion channel family', *Nature Reviews Neuroscience*, 2(6), pp. 387–396. doi: 10.1038/35077544.

Cox, J. J. et al. (2006) 'An SCN9A channelopathy causes congenital inability to experience pain.', *Nature*, 444(7121), pp. 894–898. doi: 10.1038/nature05413.

Crick, F. (1999) 'The impact of molecular biology on neuroscience', *Philosophical transactions of the Royal Society of London. Series B, Biological sciences*, 354(1392), pp. 2021–2025. doi: 10.1098/rstb.1999.0541.

Curti, S., Hoge, G., Nagy, J. I. and Pereda, A. E. (2012) 'Synergy between Electrical Coupling and Membrane Properties Promotes Strong Synchronization of Neurons of the Mesencephalic Trigeminal Nucleus', *Journal of Neuroscience*, 32(13), pp. 4341–4359. doi: 10.1523/JNEUROSCI.6216-11.2012.

Curti, S. and Pereda, A. E. (2004) 'Voltage-Dependent Enhancement of Electrical Coupling by a Subthreshold Sodium Current', *Journal of Neuroscience*, 24(16), pp. 3999–4010. doi: 10.1523/JNEUROSCI.0077-04.2004.

Dannhäuser, S. (2016) *Molecular organisation of circadian pacemaker neuron active zones in Drosophila melanogaster*. Wuerzburg

Dawydow, A., Gueta, R., Ljaschenko, D., Ullrich, S., Hermann, M., Ehmann, N., Gao, S., Fiala, A., Langenhan, T., Nagel, G. and Kittel, R. J. (2014) 'Channelrhodopsin-2-XXL, a powerful optogenetic tool for low-light applications.', *Proceedings of the National Academy of Sciences of the United States of America*, 111(38), pp. 13972–7. doi: 10.1073/pnas.1408269111.

Deisseroth, K., Feng, G., Majewska, A. K., Miesenbock, G., Ting, A. and Schnitzer, M. J. (2006) 'Next-Generation Optical Technologies for Illuminating Genetically Targeted Brain Circuits', *Journal of Neuroscience*, 26(41), pp. 10380–10386. doi: 10.1523/JNEUROSCI.3863-06.2006.

Deisseroth, K. (2011) 'Optogenetics', *Nature Methods*, 8(1), pp. 26–29. doi: 10.1038/nmeth.f.324.

Deisseroth, K. and Hegemann, P. (2017) 'The form and function of channelrhodopsin', *Science*, 357(6356), p. eaan5544. doi: 10.1126/science.aan5544.

DeVries, S. H., Qi, X., Smith, R., Makous, W. and Sterling, P. (2002) 'Electrical coupling between mammalian cones', *Current Biology*, 12(22), pp. 1900–1907. doi: 10.1016/S0960-9822(02)01261-7.

DiAntonio, A., Petersen, S. A., Heckmann, M. and Goodman, C. S. (1999) 'Glutamate receptor expression regulates quantal size and quantal content at the Drosophila neuromuscular junction.', *The Journal of neuroscience : the official journal of the Society for Neuroscience*, 19(8), pp. 3023–32. doi: 1999/04/07 00:01.

Domanico, D., Fragiotta, S., Cutini, A., Grenga, P. L. and Vingolo, E. M. (2015) 'Psychosis, Mood and Behavioral Disorders in Usher Syndrome: Review of the Literature.', *Medical hypothesis, discovery and innovation in ophthalmology*, 4(2), pp. 50–5. doi: 10.1097/WCO.0b013e32834ef8b2.

Duffy, J. B. (2002) 'GAL4 system in Drosophila: a fly geneticist's Swiss army knife.', *Genesis (New York, N.Y. : 2000)*, 34(1–2), pp. 1–15. doi: 10.1002/gene.10150.

Dufour, S. and De Koninck, Y. (2015) 'Optrodes for combined optogenetics and electrophysiology in live animals', *Neurophotonics*, 2(3), pp. 031205-14. doi: 10.1117/1.NPh.2.3.

Ehmann, N., van de Linde, S., Alon, A., Ljaschenko, D., Keung, X. Z., Holm, T., Rings, A., DiAntonio, A., Hallermann, S., Ashery, U., Heckmann, M., Sauer, M. and Kittel, R. J. (2014) 'Quantitative super-resolution imaging of Bruchpilot distinguishes active zone states.', *Nature communications*. Nature Publishing Group, 5, p. 4650. doi: 10.1038/ncomms5650.

Ehmann, N., Sauer, M. and Kittel, R. J. (2015) 'Super-resolution microscopy of the synaptic active zone.', *Frontiers in cellular neuroscience*, 9(January), p. 7. doi: 10.3389/fncel.2015.00007.

Elias, G. M. and Nicoll, R. A. (2007) 'Synaptic trafficking of glutamate receptors by MAGUK scaffolding proteins', *Trends in Cell Biology*, pp. 343–352. doi: 10.1016/j.tcb.2007.07.005.

Elliot, T. R. (1905) 'The action of adrenalin', *The Journal of Physiology*, 32, pp. 401–467. doi: 10.1210/endo-3-3-321.

Faminzin, A. S. (1866) 'Die Wirkung des Lichtes auf die Bewegung der Chlamidomonas pulvisculus Ehr., Euglena viridis Ehr. und Oscillatoria insignis Tw.', *In Melanges Biologiques tires du Bulletin de l'Academie Imperial des Sciences De St.-Petersbourg*, pp. 73–93

Fatt, P. (1954) 'Biophysics of junctional transmission', *Physiological Reviews*, 34, pp. 674–710

Featherstone, D. E., Rushton, E., Rohrbough, J., Liebl, F. and Karr, J. (2005) 'An Essential Drosophila Glutamate Receptor Subunit That Functions in Both Central Neuropil and Neuromuscular Junction', *Journal of Neuroscience*, 25(12), pp. 3199–3208. doi: 10.1523/JNEUROSCI.4201-04.2005.

Feldman, D. E. (2012) 'The Spike-Timing Dependence of Plasticity', *Neuron*, pp. 556–571. doi: 10.1016/j.neuron.2012.08.001.

Foster, K. W., Saranak, J., Patel, N., Zarilli, G., Okabe, M., Kline, T. and Nakanishi, K. (1984) 'A rhodopsin is the functional photoreceptor for phototaxis in the unicellular eukaryote *Chlamydomonas*', *Nature*, 311(5988), pp. 756–759. doi: 10.1038/311756a0.

Fouquet, W., Oswald, D., Wichmann, C., Mertel, S., Depner, H., Dyba, M., Hallermann, S., Kittel, R. J., Eimer, S. and Sigrist, S. J. (2009) 'Maturation of active zone assembly by *Drosophila* Bruchpilot', *Journal of Cell Biology*, 186(1), pp. 129–145. doi: 10.1083/jcb.200812150.

Galarreta, M. and Hestrin, S. (2001) 'Spike transmission and synchrony detection in networks of GABAergic interneurons', *Science*, 292(5525), pp. 2295–2299. doi: 10.1126/science.1061395.

Gao, S., Nagpal, J., Schneider, M. W., Kozjak-Pavlovic, V., Nagel, G. and Gottschalk, A. (2015) 'Optogenetic manipulation of cGMP in cells and animals by the tightly light-regulated guanylyl-cyclase opsin CyclOp', *Nature Communications*. Nature Publishing Group, a division of Macmillan Publishers Limited. All Rights Reserved., 6. doi: 10.1038/ncomms9046.

Getting, P. A. (1974) 'Modification of Neuron Properties by Electrotonic Synapses. I. Input Resistance, Time Constant, and Integration', *Journal of neurophysiology*, 37, pp. 846–857

Getting, P. and Willows, A. O. D. (1974) 'Modification Synapses. II. of Neuron Properties by Electrotonic Burst Formation by Electrotonic Synapses', *Journal of neurophysiology*, 37, pp. 858–868

Glanzman, D. L. (2010) 'Common Mechanisms of Synaptic Plasticity in Vertebrates and Invertebrates', *Current Biology*. Elsevier Ltd, 20(1), pp. R31–R36. doi: 10.1016/j.cub.2009.10.023.

Gong, Z., Son, W., Chung, Y. D., Kim, J., Shin, W. D., McClung, C. A., Lee, Y., Lee, H. W., Chang, D.-J., Kaang, B.-K., Cho, H., Oh, U., Hirsh, J., Kernan, M. J. and Kim, C. (2004) 'Two Interdependent TRPV Channel Subunits, Inactive and Nanchung, Mediate Hearing in *Drosophila*', *Journal of Neuroscience*, 24(41), pp. 9059–9066. doi: 10.1523/JNEUROSCI.1645-04.2004.

Gorczyca, D., Ashley, J., Speese, S., Gherbesi, N., Thomas, U., Gundelfinger, E., Gramates, L. S. and Budnik, V. (2007) 'Postsynaptic Membrane Addition Depends on the Discs-Large-Interacting t-SNARE Gtaxin', *Journal of Neuroscience*, 27(5), pp. 1033–1044. doi: 10.1523/JNEUROSCI.3160-06.2007.

Gorczyca, M., Augart, C. and Budnik, V. (1993) 'Insulin-like receptor and insulin-like peptide are localized at neuromuscular junctions in *Drosophila*.', *The Journal of neuroscience : the official journal of the Society for Neuroscience*, 13(9), pp. 3692–704. doi: 10.1016/S2215-0366(16)30284-X.Epidemiology.

Gorczyca, M. and Budnik, V. (2006) 'Appendix: Anatomy of the Larval Body Wall Muscles and NMJs in the third instar larval stage', *International Review of Neurobiology*, 75(06), pp. 367–373. doi: 10.1016/S0074-7742(06)75016-4.

Govorunova, E. G., Sineshchekov, O. A., Janz, R., Liu, X. and Spudich, J. L. (2015) 'Natural light-gated anion channels: A family of microbial rhodopsins for advanced optogenetics', *Science*, 349(6248), pp. 647–650. doi: 10.1126/science.aaa7484.

Govorunova, E. G., Sineshchekov, O. A. and Spudich, J. L. (2016) 'Proteomonas sulcata ACR1: A Fast Anion Channelrhodopsin', *Photochemistry and Photobiology*, 92(2), pp. 257–263. doi: 10.1111/php.12558.

Gunaydin, L. A., Yizhar, O., Berndt, A., Sohal, V. S., Deisseroth, K. and Hegemann, P. (2010) 'Ultrafast optogenetic control', *Nature Neuroscience*. Nature Publishing Group, 13(3), pp. 387–392. doi: 10.1038/nn.2495.

Hahn, C. and Salajegheh, M. K. (2016) 'Myotonic disorders: A review article', *Iranian Journal of Neurology*, 15(1), pp. 46–53. doi: 10.1017/CBO9781107415324.004.

Hamann, J. et al. (2015) 'International Union of Basic and Clinical Pharmacology. XCIV. Adhesion G Protein–Coupled Receptors', *Pharmacological Reviews*, 67(2), pp. 338–367. doi: 10.1124/pr.114.009647.

Harris, K. P. and Littleton, J. T. (2015) 'Transmission, development, and plasticity of synapses', *Genetics*, 201(2), pp. 345–375. doi: 10.1534/genetics.115.176529.

Harz, H. and Hegemann, P. (1991) 'Rhodopsin-regulated calcium currents in *Chlamydomonas*', *Nature*, pp. 489–491. doi: 10.1038/351489a0.

Hebb, D. O. (1949) *The Organization of Behavior, The Organization of Behavior*. John Wiley. doi: 10.2307/1418888.

Hegemann, P., Oesterbelt, D. and Steiner, M. (1985) 'The photocycle of the chloride pump halorhodopsin. I: Azide-catalyzed deprotonation of the chromophore is a side reaction of photocycle intermediates inactivating the pump.', *The EMBO journal*, 4(9), pp. 2347–50. Available at: <http://www.pubmedcentral.nih.gov/articlerender.fcgi?artid=554508&tool=pmcentrez&rendertype=abstract>.

- Herberholz, J., Antonsen, B. L. and Edwards, D. H.** (2002) 'A lateral excitatory network in the escape circuit of crayfish.', *The Journal of Neuroscience*, 22(20), pp. 9078–85. doi: 22/20/9078 [pii].
- Hoang, B. and Chiba, A.** (2001) 'Single-Cell Analysis of Drosophila Larval Neuromuscular Synapses', *Developmental Biology*, 229(1), pp. 55–70. doi: 10.1006/dbio.2000.9983.
- Ibanez, C.** (2017) 'The 2017 Nobel Prize in Physiology or Medicine - Press Release. Scientific Background Discoveries of Molecular Mechanisms Controlling the Circadian Rhythm', *The Nobel Assembly*, pp. 1–7. Available at: https://www.nobelprize.org/nobel_prizes/medicine/laureates/2017/advanced-medicineprize2017.pdf.
- Jan, L. Y. and Jan, Y. N.** (1976) 'L-Glutamate as an excitatory transmitter at the Drosophila larval neuromuscular junction', *J. Physiol.*, 262, pp. 215–236
- Jan, L. Y. and Jan, Y. N.** (1976) 'Properties of the larval neuromuscular junction in Drosophila melanogaster.', *The Journal of physiology*, 262(1), pp. 189–214. doi: 10.1113/jphysiol.1976.sp011592.
- Jan, L. Y. and Jan, Y. N.** (1982) 'Antibodies to horseradish peroxidase as specific neuronal markers in Drosophila and in grasshopper embryos.', *Proceedings of the National Academy of Sciences*, 79(8), pp. 2700–2704. doi: 10.1073/pnas.79.8.2700.
- Jiao, W., Masich, S., Franzén, O. and Shupliakov, O.** (2010) 'Two pools of vesicles associated with the presynaptic cytosolic projection in Drosophila neuromuscular junctions', *Journal of Structural Biology*. Elsevier Inc., 172(3), pp. 389–394. doi: 10.1016/j.jsb.2010.07.007.
- Johansen, J., Halpern, M. E., Johansen, K. M. and Keshishian, H.** (1989) 'Stereotypic morphology of glutamatergic synapses on identified muscle cells of Drosophila larvae.', *The Journal of neuroscience : the official journal of the Society for Neuroscience*, pp. 710–725
- Kandel, E. R.** (1976) *Cellular Basis of Behaviour: An introduction to Behavioural Neurobiology*. San Francisco: W.H. Freeman
- Kandel, E. R.** (2001) 'The molecular biology of memory storage: A dialogue between gene and synapses', *Science*, 294(5544), pp. 1030–1038. doi: 10.1126/science.1067020.
- Kandel, E. R.** (2009) 'The Biology of Memory: A Forty-Year Perspective', *Journal of Neuroscience*, 29(41), pp. 12748–12756. doi: 10.1523/JNEUROSCI.3958-09.2009.

- Kandel, E. R., Schwartz, J. H., Jessell, T. M., Siegelbaum, S. A. and Hudspeth, A. J.** (2012) *Principles of Neural Science*. doi: 10.1036/0838577016.
- Kato, H. E., Zhang, F., Yizhar, O., Ramakrishnan, C., Nishizawa, T., Hirata, K., Ito, J., Aita, Y., Tsukazaki, T., Hayashi, S., Hegemann, P., Maturana, A. D., Ishitani, R., Deisseroth, K. and Nureki, O.** (2012) 'Crystal structure of the channelrhodopsin light-gated cation channel', *Nature*, 482(7385), pp. 369–374. doi: 10.1038/nature10870.
- Kaufmann, N., DeProto, J., Ranjan, R., Wan, H. and Van Vactor, D.** (2002) 'Drosophila liprin- α and the receptor phosphatase Dlar control synapse morphogenesis', *Neuron*, 34(1), pp. 27–38. doi: 10.1016/S0896-6273(02)00643-8.
- Kazama, H.** (2015) 'Systems neuroscience in Drosophila: Conceptual and technical advantages', *Neuroscience*. IBRO, 296, pp. 3–14. doi: 10.1016/j.neuroscience.2014.06.035.
- Keshishian, H., Chiba, a, Chang, T. N., Halfon, M. S., Harkins, E. W., Jarecki, J., Wang, L., Anderson, M., Cash, S. and Halpern, M. E.** (1993) 'Cellular mechanisms governing synaptic development in Drosophila melanogaster.', *Journal of neurobiology*, 24(6), pp. 757–787. doi: 10.1002/neu.480240606.
- Kittel, R. J., Wichmann, C., Rasse, T. M., Fouquet, W., Schmidt, M., Schmid, A., Wagh, D. A., Pawlu, C., Kellner, R. R., Willig, K. I., Hell, S. W., Buchner, E., Heckmann, M. and Sigrist, S. J.** (2006) 'Bruchpilot promotes active zone assembly, Ca²⁺ channel clustering, and vesicle release', *Science*, 312(May), pp. 1051–1054. Available at: 10.1126/science.1126308.
- Klapoetke, N. C. et al.** (2014) 'Independent optical excitation of distinct neural populations.', *Nature methods*, 11(3), pp. 338–46. doi: 10.1038/nmeth.2836.
- Klapoetke, N. C. et al.** (2014) 'Independent optical excitation of distinct neural populations', *Nat Methods*, 11(3), pp. 338–346. doi: 10.1038/nmeth.2836.
- Kleinlogel, S., Feldbauer, K., Dempski, R. E., Fotis, H., Wood, P. G., Bamann, C. and Bamberg, E.** (2011) 'Ultra light-sensitive and fast neuronal activation with the Ca²⁺-permeable channelrhodopsin CatCh.', *Nature neuroscience*. Nature Publishing Group, 14(4), pp. 513–518. doi: 10.1038/nn.2776.
- Koh, K., Joiner, W. J., Wu, M. N., Yue, Z., Smith, C. J. and Sehgal, A.** (2008) 'Identification of SLEEPLESS, a novel sleep-promoting factor', 321(5887), pp. 372–376. doi: 10.1126/science.1155942. Identification.

Konopka, R. J. and Benzer, S. (1971) 'Clock mutants of *Drosophila melanogaster*.' *Proceedings of the National Academy of Sciences of the United States of America*, 68(9), pp. 2112–6. doi: 10.1073/pnas.68.9.2112.

Krasnoperov, V. G. et al. (1997) 'alpha-Latrotoxin stimulates exocytosis by the interaction with a neuronal G-protein-coupled receptor.' *Neuron*, 18(6), pp. 925–37. doi: 10.1016/s0896-6273(00)80332-3.

Krause, B. S., Grimm, C., Kaufmann, J. C. D., Schneider, F., Sakmar, T. P., Bartl, F. J. and Hegemann, P. (2017) 'Complex Photochemistry within the Green-Absorbing Channelrhodopsin ReaChR', *Biophysical Journal*. Biophysical Society, 112(6), pp. 1166–1175. doi: 10.1016/j.bpj.2017.02.001.

Kwon, Y., Shen, W. L., Shim, H.-S. and Montell, C. (2010) 'Fine Thermotactic Discrimination between the Optimal and Slightly Cooler Temperatures via a TRPV Channel in Chordotonal Neurons', *Journal of Neuroscience*, 30(31), pp. 10465–10471. doi: 10.1523/JNEUROSCI.1631-10.2010.

Lai, S. L. and Lee, T. (2006) 'Genetic mosaic with dual binary transcriptional systems in *Drosophila*', *Nature Neuroscience*, 9(5), pp. 703–709. doi: 10.1038/nn1681.

Langenhan, T., Piao, X. and Monk, K. R. (2016) 'Adhesion G protein-coupled receptors in nervous system development and disease', *Nature Reviews Neuroscience*. Nature Publishing Group, 17(9), pp. 550–561. doi: 10.1038/nrn.2016.86.

Lee, J., Moon, S., Cha, Y. and Chung, Y. D. (2010) '*Drosophila* TRPN(=NOMPC) channel localizes to the distal end of mechanosensory cilia', *PLoS ONE*, 5(6). doi: 10.1371/journal.pone.0011012.

Lima, S. Q. and Miesenböck, G. (2005) 'Remote control of behavior through genetically targeted photostimulation of neurons', *Cell*, 121(1), pp. 141–152. doi: 10.1016/j.cell.2005.02.004.

Lin, J. Y., Knutsen, P. M., Muller, A., Kleinfeld, D. and Tsien, R. Y. (2013) 'ReaChR: a red-shifted variant of channelrhodopsin enables deep transcranial optogenetic excitation', *Nature neuroscience*, 16(10), pp. 1499–1508. doi: 10.1038/nn.3502.

Liu, K. S. Y., Siebert, M., Mertel, S., Knoche, E., Wegener, S., Wichmann, C., Matkovic, T., Muhammad, K., Depner, H., Mettke, C., Bückers, J., Hell, S. W., Müller, M., Davis, G. W., Schmitz, D. and Sigrist, S. J. (2011) 'RIM-binding protein, a central part of the active zone, is essential for neurotransmitter release', *Science*, 334(6062), pp. 1565–1569. doi: 10.1126/science.1212991.

Liu, L., Yermolaieva, O., Johnson, W. A., Abboud, F. M. and Welsh, M. J. (2003) 'Identification and function of thermosensory neurons in *Drosophila* larvae', *Nature Neuroscience*, 6(3), pp. 267–273. doi: 10.1038/nn1009.

Liu, L., Li, Y., Wang, R., Yin, C., Dong, Q., Hing, H., Kim, C. and Welsh, M. J. (2007) '*Drosophila* hygrosensation requires the TRP channels water witch and nanchung', *Nature*, 450(7167), pp. 294–298. doi: 10.1038/nature06223.

Ljaschenko, D., Ehmann, N. and Kittel, R. J. (2013) 'Hebbian Plasticity Guides Maturation of Glutamate Receptor Fields InVivo', *Cell Reports*. The Authors, 3(5), pp. 1407–1413. doi: 10.1016/j.celrep.2013.04.003.

Loewenstein, W. R. (1959) 'the Generation of Electric Activity in a Nerve Ending', *Annals of the New York Academy of Sciences*, 81(2), pp. 367–387. doi: 10.1111/j.1749-6632.1959.tb49320.x.

Loewi, O. (1921) 'Über humorale Übertragbarkeit der Herznervenwirkung.', *Mitteilung Pflügers Arch Ges Physiol*, 189, pp. 239–242

LSM5Brochure (2005) 'LSM 5 Pascal Laser Scanning Microscope Brochure'

LSM5Manual (2005) *LSM 5 Pascal Laser Scanning Microscope Manual*, Zeiss

Mahn, M., Prigge, M., Ron, S., Levy, R. and Yizhar, O. (2016) 'Biophysical constraints of optogenetic inhibition at presynaptic terminals.', *Nature neuroscience*, 19(4), pp. 554–6. doi: 10.1038/nn.4266.

Marrus, S. B., Portman, S. L., Allen, M. J., Moffat, K. G. and DiAntonio, A. (2004) 'Differential Localization of Glutamate Receptor Subunits at the *Drosophila* Neuromuscular Junction', *The Journal of Neuroscience*, 24(6), pp. 1406–1415. doi: 10.1523/JNEUROSCI.1575-03.2004.

Menon, K. P., Carrillo, R. A. and Zinn, K. (2013) 'Development and plasticity of the *Drosophila* larval neuromuscular junction', *Wiley Interdisciplinary Reviews: Developmental Biology*, 2(5), pp. 647–670. doi: 10.1002/wdev.108.

Minke, B. and Cook, B. (2002) 'TRP Channel Proteins and Signal Transduction', *Physiological Reviews*, 82(2), pp. 429–472. doi: 10.1152/physrev.00001.2002.

Mohammad, F., Stewart, J. C., Ott, S., Chlebikova, K., Chua, J. Y., Koh, T.-W., Ho, J. and Claridge-Chang, A. (2017) 'Optogenetic inhibition of behavior with anion channelrhodopsins', *Nature Methods*, 14(3), pp. 271–274. doi: 10.1038/nmeth.4148.

Monastiriotti, M., Gorczyca, M., Rapus, J., Eckert, M., White, K. and Budnik, V. (1995) 'Octopamine immunoreactivity in the fruit fly *Drosophila melanogaster*.' *The Journal of comparative neurology*, 356(2), pp. 275–287. doi: 10.1002/cne.903560210.

Montgomery, K. L., Yeh, A. J., Ho, J. S., Tsao, V., Iyer, S. M., Grosenick, L., Ferenczi, E. A., Tanabe, Y., Deisseroth, K., Delp, S. L. and Poon, A. S. Y. (2015) 'Wirelessly powered, fully internal optogenetics for brain, spinal and peripheral circuits in mice', *Nature Methods*, 12(10), pp. 969–974. doi: 10.1038/nmeth.3536.

Nagel, G., Ollig, D., Fuhrmann, M., Kateriya, S., Musti, A. M., Bamberg, E. and Hegemann, P. (2002) 'Channelrhodopsin-1: a light-gated proton channel in green algae.', *Science (New York, N.Y.)*, 296(5577), pp. 2395–8. doi: 10.1126/science.1072068.

Nagel, G., Szellas, T., Huhn, W., Kateriya, S., Adeishvili, N., Berthold, P., Ollig, D., Hegemann, P. and Bamberg, E. (2003) 'Channelrhodopsin-2, a directly light-gated cation-selective membrane channel', *Proceedings of the National Academy of Sciences*, 100(24), pp. 13940–13945. doi: 10.1073/pnas.1936192100.

Nagel, G., Brauner, M., Liewald, J. F., Adeishvili, N., Bamberg, E. and Gottschalk, A. (2005) 'Light activation of Channelrhodopsin-2 in excitable cells of *Caenorhabditis elegans* triggers rapid behavioral responses', *Current Biology*, 15(24), pp. 2279–2284. doi: 10.1016/j.cub.2005.11.032.

Oesterhelt, D. and Stoerkenius, W. (1971) 'Rhodopsin-like protein from the purple membrane of *Halobacterium halobium*', *Nature New Biology*, 233(39), pp. 149–152. doi: 10.1038/newbio233149a0.

Ohtsuka, T., Takao-Rikitsu, E., Inoue, E., Inoue, M., Takeuchi, M., Matsubara, K., Deguchi-Tawarada, M., Satoh, K., Morimoto, K., Nakanishi, H. and Takai, Y. (2002) 'CAST: A novel protein of the cytomatrix at the active zone of synapses that forms a ternary complex with RIM1 and Munc13-1', *Journal of Cell Biology*, 158(3), pp. 577–590. doi: 10.1083/jcb.200202083.

Owald, D., Fouquet, W., Schmidt, M., Wichmann, C., Mertel, S., Depner, H., Christiansen, F., Zube, C., Quentin, C., K?rner, J., Urlaub, H., Mechtler, K. and Sigrist, S. J. (2010) 'A Syd-1 homologue regulates pre- and postsynaptic maturation in *Drosophila*', *Journal of Cell Biology*, 188(4), pp. 565–579. doi: 10.1083/jcb.200908055.

Owald, D., Khorramshahi, O., Gupta, V. K., Banovic, D., Depner, H., Fouquet, W., Wichmann, C., Mertel, S., Eimer, S., Reynolds, E., Holt, M., Aberle, H. and Sigrist, S. J. (2012) 'Cooperation of Syd-1 with Neurexin synchronizes pre-with postsynaptic assembly', *Nature Neuroscience*. Nature Publishing Group, 15(9), pp. 1219–1226. doi: 10.1038/nn.3183.

Pape, H.-C., Brenner, B., Silbernagl, S., Klinke, R. and Kurtz, A. (2010) *Physiologie*. 6th edn. Stuttgart: Stuttgart ; New York, NY : Thieme

Park, S. II et al. (2015) 'Soft, stretchable, fully implantable miniaturized optoelectronic systems for wireless optogenetics', *Nature Biotechnology*. Nature Publishing Group, 33(12), pp. 1280–1286. doi: 10.1038/nbt.3415.

Pedersen, T. H., Riisager, A., de Paoli, F. V., Chen, T.-Y. and Nielsen, O. B. (2016) 'Role of physiological ClC-1 Cl⁻ ion channel regulation for the excitability and function of working skeletal muscle', *The Journal of General Physiology*, 147(4), pp. 291–308. doi: 10.1085/jgp.201611582.

Pereda, A. E. (2014) 'Electrical synapses and their functional interactions with chemical synapses', *Nature Reviews Neuroscience*. Nature Publishing Group, 15(4), pp. 250–263. doi: 10.1038/nrn3708.

Pereda, A. E., Bell, T. D. and Faber, D. S. (1995) 'Retrograde synaptic communication via gap junctions coupling auditory afferents to the Mauthner cell.', *The Journal of Neuroscience*, 15(9), pp. 5943–55. Available at: <http://www.ncbi.nlm.nih.gov/pubmed/7666179>.

Perlmutter, J. S. and Mink, J. W. (2006) 'Deep Brain Stimulation', *Annual Review of Neuroscience*, 29(1), pp. 229–257. doi: 10.1146/annurev.neuro.29.051605.112824.

Petersen, S. A., Fetter, R. D., Noordermeer, J. N., Goodman, C. S. and DiAntonio, A. (1997) 'Genetic analysis of glutamate receptors in drosophila reveals a retrograde signal regulating presynaptic transmitter release', *Neuron*, 19(6), pp. 1237–1248. doi: 10.1016/S0896-6273(00)80415-8.

Phelan, P., Nakagawa, M., Wilkin, M. B., Moffat, K. G., O'Kane, C. J., Davies, J. a and Bacon, J. P. (1996) 'Mutations in shaking-B prevent electrical synapse formation in the Drosophila giant fiber system.', *The Journal of neuroscience*, 16(3), pp. 1101–1113

Pianca, N., Zaglia, T. and Mongillo, M. (2017) 'Will cardiac optogenetics find the way through the obscure angles of heart physiology?', *Biochemical and Biophysical Research Communications*. Elsevier Ltd, 482(4), pp. 515–523. doi: 10.1016/j.bbrc.2016.11.104.

Potter, C. J., Tasic, B., Russler, E. V., Liang, L. and Luo, L. (2010) 'The Q system: A repressible binary system for transgene expression, lineage tracing, and mosaic analysis', *Cell*, 141(3), pp. 536–548. doi: 10.1016/j.cell.2010.02.025.

Prahlad, A., Spalthoff, C., Kong, D., Großhans, J., Göpfert, M. C. and Schmidt, C. F. (2017) 'Mechanical Properties of a *Drosophila* Larval Chordotonal Organ', *Biophysical Journal*. Elsevier, 113(12), pp. 2796–2804. doi: 10.1016/j.bpj.2017.08.061.

Prokop, A. (1999) 'Integrating bits and pieces: Synapse structure and formation in *Drosophila* embryos', *Cell and Tissue Research*, pp. 169–186. doi: 10.1007/s004410051345.

Pulver, S. R., Pashkovski, S. L., Hornstein, N. J., Garrity, P. a and Griffith, L. C. (2009) 'Temporal dynamics of neuronal activation by Channelrhodopsin-2 and TRPA1 determine behavioral output in *Drosophila* larvae.', *Journal of neurophysiology*, 101(6), pp. 3075–88. doi: 10.1152/jn.00071.2009.

Qin, G., Schwarz, T., Kittel, R. J., Schmid, A. and Rasse, T. M. (2005) 'Four Different Subunits Are Essential for Expressing the Synaptic Glutamate Receptor at Neuromuscular Junctions of *Drosophila*', *Journal of Neuroscience*, 25(12), pp. 3209–3218. doi: 10.1523/JNEUROSCI.4194-04.2005.

Quinn, W. G., Harris, W. A. and Benzer, S. (1974) 'Conditioned behavior in *Drosophila melanogaster*.', *Proceedings of the National Academy of Sciences of the United States of America*, 71(3), pp. 708–12. doi: VL - 71.

Ramon y Cajal, S. (1894) 'The Croonian Lecture: La Fine Structure des Centres Nerveux', *Proceedings of the Royal Society of London*, 44(January), pp. 444–468. doi: 10.2307/115494.

Ratnaparkhi, A., Lawless, G. M., Schweizer, F. E., Golshani, P. and Jackson, G. R. (2008) 'A *Drosophila* model of ALS: Human ALS-associated mutation in VAP33A suggests a dominant negative mechanism', *PLoS ONE*, 3(6). doi: 10.1371/journal.pone.0002334.

Saitoe, M., Tanaka, S., Takata, K. and Kidokoro, Y. (1997) 'Neural activity affects distribution of glutamate receptors during neuromuscular junction formation in *Drosophila* embryos', *Developmental Biology*, 184(1), pp. 48–60. doi: 10.1006/dbio.1996.8480.

Sanyal, S. (2009) 'Genomic mapping and expression patterns of C380, OK6 and D42 enhancer trap lines in the larval nervous system of *Drosophila*', *Gene Expression Patterns*. Elsevier B.V., 9(5), pp. 371–380. doi: 10.1016/j.gep.2009.01.002.

Schmid, A., Qin, G., Wichmann, C., Kittel, R. J., Mertel, S., Fouquet, W., Schmidt, M., Heckmann, M. and Sigrist, S. J. (2006) 'Non-NMDA-Type Glutamate Receptors Are Essential for Maturation But Not for Initial Assembly of Synapses at *Drosophila* Neuromuscular Junctions', *Journal of Neuroscience*, 26(44), pp. 11267–11277. doi: 10.1523/JNEUROSCI.2722-06.2006.

Schmid, A., Hallermann, S., Kittel, R. J., Khorramshahi, O., Frölich, A. M. J., Quentin, C., Rasse, T. M., Mertel, S., Heckmann, M. and Sigrist, S. J. (2008) 'Activity-dependent site-specific changes of glutamate receptor composition in vivo', *Nature Neuroscience*, 11(6), pp. 659–666. doi: 10.1038/nn.2122.

Schmid, A. and Sigrist, S. J. (2008) 'Analysis of Neuromuscular Junctions', in *Drosophila - Methods and Protocols*, pp. 239–251. Available at: http://link.springer.com/protocol/10.1007/978-1-59745-583-1_14%5Cnhttp://link.springer.com/content/pdf/10.1007/978-1-59745-583-1_14.

Schneider, F., Grimm, C. and Hegemann, P. (2015) 'Biophysics of Channelrhodopsin', *Annual Review of Biophysics*, 44(1), pp. 167–186. doi: 10.1146/annurev-biophys-060414-034014.

Scholz, N., Gehring, J., Guan, C., Ljaschenko, D., Fischer, R., Lakshmanan, V., Kittel, R. J. and Langenhan, T. (2015) 'The Adhesion GPCR Latrophilin/CIRL Shapes Mechanosensation', *Cell Reports*. The Authors, 11(6), pp. 866–874. doi: 10.1016/j.celrep.2015.04.008.

Scholz, N., Guan, C., Nieberler, M., Grotemeyer, A., Maiellaro, I., Gao, S., Beck, S., Pawlak, M., Sauer, M., Asan, E., Rothmund, S., Winkler, J., Prömel, S., Nagel, G., Langenhan, T. and Kittel, R. J. (2017) 'Mechano-dependent signaling by Latrophilin/CIRL quenches cAMP in proprioceptive neurons', *eLife*, 6. doi: 10.7554/eLife.28360.

Schroll, C., Riemensperger, T., Bucher, D., Ehmer, J., Völler, T., Erbguth, K., Gerber, B., Hendel, T., Nagel, G., Buchner, E. and Fiala, A. (2006) 'Light-Induced Activation of Distinct Modulatory Neurons Triggers Appetitive or Aversive Learning in Drosophila Larvae', *Current Biology*, 16(17), pp. 1741–1747. doi: 10.1016/j.cub.2006.07.023.

Schuster, C. M., Ultsch, A., Schloss, P., Cox, J. A., Schmitt, B. and Betz, H. (1991) 'Molecular cloning of an invertebrate glutamate receptor subunit expressed in Drosophila muscle.', *Science*, 254(5028), pp. 112–114. doi: 10.1126/science.1681587.

Schuster, C. M., Davis, G. W., Fetter, R. D. and Goodman, C. S. (1996) 'Genetic dissection of structural and functional components of synaptic plasticity. I. Fasciclin II controls synaptic stabilization and growth', *Neuron*, 17(4), pp. 641–654. doi: 10.1016/S0896-6273(00)80197-X.

Segev, E., Reimer, J., Moreaux, L. C., Fowler, T. M., Chi, D., Sacher, W. D., Lo, M., Deisseroth, K., Tolias, A. S., Faraon, A. and Roukes, M. L. (2016) 'Patterned photostimulation via visible-wavelength photonic probes for deep brain optogenetics', *Neurophotonics*, 4(1), p. 011002. doi: 10.1117/1.NPh.4.1.011002.

- Sherrington, C. S.** (1897) *The central nervous system., Text Book of Physiology, 7th edn, part III (Foster, M., ed.) Macmillan and Co., London*
- Shimano, T., Fyk-Kolodziej, B., Mirza, N., Asako, M., Tomoda, K., Bledsoe, S., Pan, Z. H., Molitor, S. and Holt, A. G.** (2013) 'Assessment of the AAV-mediated expression of channelrhodopsin-2 and halorhodopsin in brainstem neurons mediating auditory signaling', *Brain Research*. Elsevier, 1511, pp. 138–152. doi: 10.1016/j.brainres.2012.10.030.
- Sineshchekov, O. A., Govorunova, E. G., Li, H. and Spudich, J. L.** (2015) 'Gating mechanisms of a natural anion channelrhodopsin', *Proceedings of the National Academy of Sciences*, 112(46), p. 201513602. doi: 10.1073/pnas.1513602112.
- Sokabe, T. and Tominaga, M.** (2009) 'A temperature-sensitive TRP ion channel, Painless, functions as a noxious heat sensor in fruit flies', *Communicative and Integrative Biology*, 2(2), pp. 170–173. doi: 10.4161/cib.7708.
- Sommer, C.** (2016) 'Exploring pain pathophysiology in patients', *Science*, 354(6312), pp. 588–592. doi: 10.1126/science.aaf8935.
- Stewart, B. A., Atwood, H. L., Renger, J. J., Wang, J. and Wu, C. F.** (1994) 'Improved stability of Drosophila larval neuromuscular preparations in haemolymph-like physiological solution', *Journal of Comparative Physiology A*, 175, pp. 179–191
- Stierl, M., Stumpf, P., Udvari, D., Gueta, R., Hagedorn, R., Losi, A., Gärtner, W., Petereit, L., Efetova, M., Schwarzel, M., Oertner, T. G., Nagel, G. and Hegemann, P.** (2011) 'Light modulation of cellular cAMP by a small bacterial photoactivated adenylyl cyclase, bPAC, of the soil bacterium *Beggiatoa*', *Journal of Biological Chemistry*, 286(2), pp. 1181–1188. doi: 10.1074/jbc.M110.185496.
- Stocker, H. and Gallant, P.** (2008) 'Getting Started: An Overview on Raising and Handling Drosophila', in *Drosophila - Methods and Protocols*, pp. 27–44
- Südhof, T. C.** (2001) 'α-Latrotoxin and its receptors : Neurexins and CIRL / Latrophilins', *Annual Reviews Neuroscience*, 24(Simmons 1991), pp. 933–962. doi: 10.1146/annurev.immunol.20.091101.091806.
- Südhof, T. C.** (2012a) 'The presynaptic active zone', *Neuron*, 75(1), pp. 11–25. doi: 10.1016/j.neuron.2012.06.012.
- Südhof, T. C.** (2012b) 'The presynaptic active zone', *Neuron*, pp. 11–25. doi: 10.1016/j.neuron.2012.06.012.

TheAxonGuide (2012) *The Axon Guide for Electrophysiology & Biophysics Laboratory Techniques*. Edited by I. Foster City, CA: Axon Instruments. doi: 10.1136/bjo.2009.169052.

Thomas, U., Kim, E., Kuhlendahl, S., Koh, Y. H., Gundelfinger, E. D., Sheng, M., Garner, C. C. and Budnik, V. (2012) 'Synaptic Clustering of the Cell Adhesion Molecule Fasciclin II by Discs-Large and its Role in the Regulation of Presynaptic Structure', *Neuron*, 13(5), pp. 511–518. doi: 10.1038/ni.2247.Intrathymic.

Todd, K. L., Kristan, W. B. and French, K. A. (2010) 'Gap Junction Expression Is Required for Normal Chemical Synapse Formation', *Journal of Neuroscience*, 30(45), pp. 15277–15285. doi: 10.1523/JNEUROSCI.2331-10.2010.

Tovote, P., Esposito, M. S., Botta, P., Chaudun, F., Fadok, J. P., Markovic, M., Wolff, S. B. E., Ramakrishnan, C., Fenno, L., Deisseroth, K., Herry, C., Arber, S. and Lüthi, A. (2016) 'Midbrain circuits for defensive behaviour', *Nature*. Nature Publishing Group, 534(7606), pp. 206–212. doi: 10.1038/nature17996.

Tracey, W. D., Wilson, R. I., Laurent, G. and Benzer, S. (2003) 'painless, a Drosophila gene essential for nociception', *Cell*, 113(2), pp. 261–273. doi: 10.1016/S0092-8674(03)00272-1.

Tsubouchi, A., Yano, T., Yokoyama, T. K., Murtin, C., Otsuna, H. and Ito, K. (2017) 'Topological and modality - specific representation of somatosensory information in the fly brain', *Science*, 358(6363), pp. 615–623. Available at: <http://science.sciencemag.org/content/sci/358/6363/615.full.pdf>.

Ugur, B., Chen, K. and Bellen, H. J. (2016) 'Drosophila tools and assays for the study of human diseases.', *Disease models & mechanisms*, 9(3), pp. 235–44. doi: 10.1242/dmm.023762.

Ullrich, S., Gueta, R. and Nagel, G. (2013) 'Degradation of channelopsin-2 in the absence of retinal and degradation resistance in certain mutants', *Biological Chemistry*, 394(2), pp. 271–280. doi: 10.1515/hsz-2012-0256.

Van Vactor, D. and Sigrist, S. J. (2017) 'Presynaptic morphogenesis, active zone organization and structural plasticity in Drosophila', *Current Opinion in Neurobiology*. Elsevier Ltd, pp. 119–129. doi: 10.1016/j.conb.2017.03.003.

Veruki, M. L. and Hartveit, E. (2002) 'All (rod) amacrine cells form a network of electrically coupled interneurons in the mammalian retina', *Neuron*, 33(6), pp. 935–946. doi: 10.1016/S0896-6273(02)00609-8.

van der Voet, M., Harich, B., Franke, B. and Schenck, a (2015) 'ADHD-associated dopamine transporter, latrophilin and neurofibromin share a dopamine-related locomotor signature in *Drosophila*', *Molecular Psychiatry*. Nature Publishing Group, 10(May 2014), pp. 1–9. doi: 10.1038/mp.2015.55.

Volkman, J., Allert, N., Voges, J., Weiss, P. H., Freund, H. J. and Sturm, V. (2001) 'Safety and efficacy of pallidal or subthalamic nucleus stimulation in advanced PD.', *Neurology*, 56(4), pp. 548–551. doi: 10.1212/WNL.56.4.548.

Volkman, J. (2007) 'Deep brain stimulation for Parkinson ' s disease', *Parkinsonism & Related Disorders Parkinsonism*, 13, pp. 462–465

Wagh, D. A., Rasse, T. M., Asan, E., Hofbauer, A., Schwenkert, I., Dürrbeck, H., Buchner, S., Dabauvalle, M. C., Schmidt, M., Qin, G., Wichmann, C., Kittel, R., Sigrist, S. J. and Buchner, E. (2006) 'Bruchpilot, a protein with homology to ELKS/CAST, is required for structural integrity and function of synaptic active zones in *Drosophila*', *Neuron*, 49(6), pp. 833–844. doi: 10.1016/j.neuron.2006.02.008.

Walker, R. G. et al. (2000) 'A *Drosophila* mechanosensory transduction channel.', *Science (New York, N.Y.)*, 287(5461), pp. 2229–34. doi: 10.1126/science.287.5461.2229.

Walters, J. (2017) 'Muscle hypertrophy and pseudohypertrophy', *Practical Neurology*, pp. 369–379. doi: 10.1136/practneurol-2017-001695.

Wang, Y., Liu, X., Biederer, T. and Sudhof, T. C. (2002) 'A family of RIM-binding proteins regulated by alternative splicing: Implications for the genesis of synaptic active zones', *Proceedings of the National Academy of Sciences*, 99(22), pp. 14464–14469. doi: 10.1073/pnas.182532999.

Watson, J. and Crick, F. (1953) 'Molecular structure of nucleic acids', *Nature*, 171, pp. 737–738. doi: 10.1038/171737a0.

Weigmann, K., Klapper, R., Strasser, T., Rickert, C., Technau, G., Jäckle, H., Janning, W. and Klämbt, C. (2003) 'FlyMove - A new way to look at development of *Drosophila*', *Trends in Genetics*, 19(6), pp. 310–311. doi: 10.1016/S0168-9525(03)00050-7.

Wen, L., Wang, H., Tanimoto, S., Egawa, R., Matsuzaka, Y., Mushiake, H., Ishizuka, T. and Yawo, H. (2010) 'Opto-current-clamp actuation of cortical neurons using a strategically designed channelrhodopsin', *PLoS ONE*, 5(9). doi: 10.1371/journal.pone.0012893.

Wentz, C. T., Bernstein, J. G., Monahan, P., Guerra, A., Rodriguez, A. and Boyden, E. S. (2011) 'A Wirelessly Powered and Controlled Device for Optical Neural Control of Freely-Behaving Animals', *Journal of Neural Engineering*, 8(4), pp. 1–14. doi: 10.1088/1741-2560/8/4/046021.A.

- West, R. J. H., Furmston, R., Williams, C. A. C. and Elliott, C. J. H.** (2015) 'Neurophysiology of Drosophila Models of Parkinson ' s Disease', *Hindawi Publishing Corporation*, 2015, p. 11. Available at: <http://dx.doi.org/10.1155/2015/381281>.
- Wiegert, J. S. and Oertner, T. G.** (2016) 'How (not) to silence long-range projections with light', *Nature Neuroscience*, 19(4), pp. 527–528. doi: 10.1038/nn.4270.
- Wietek, J., Wiegert, J. S., Adeishvili, N., Schneider, F., Watanabe, H., Tsunoda, S. P., Vogt, A., Elstner, M., Oertner, T. G. and Hegemann, P.** (2014) 'Conversion of Channelrhodopsin into a Light-Gated Chloride Channel', *Science*, 344(6182), pp. 409–412. doi: 10.1126/science.1249375.
- Yack, J. E.** (2004) 'The structure and function of auditory chordotonal organs in insects', *Microscopy Research and Technique*, pp. 315–337. doi: 10.1002/jemt.20051.
- Yan, Z., Zhang, W., He, Y., Gorczyca, D., Xiang, Y., Cheng, L. E., Meltzer, S., Jan, L. Y. and Jan, Y. N.** (2013) 'Drosophila NOMPC is a mechanotransduction channel subunit for gentle-touch sensation', *Nature*, 493(7431), pp. 221–225. doi: 10.1038/nature11685.
- Yoshihara, M., Rheuben, M. B. and Kidokoro, Y.** (1997) 'Transition from growth cone to functional motor nerve terminal in Drosophila embryos.', *The Journal of neuroscience : the official journal of the Society for Neuroscience*, 17(21), pp. 8408–26. Available at: <http://www.ncbi.nlm.nih.gov/pubmed/9334414>.
- Zemelman, B. V, Lee, G. A., Ng, M. and Miesenböck, G.** (2002) 'Selective photostimulation of genetically chARGed neurons', *Neuron*, 33(1), pp. 15–22. doi: 10.1016/S0896-6273(01)00574-8.
- Zhang, F., Wang, L.-P., Boyden, E. S. and Deisseroth, K.** (2006) 'Channelrhodopsin-2 and optical control of excitable cells.', *Nature methods*, 3(10), pp. 785–92. doi: 10.1038/nmeth936.
- Zhang, F., Prigge, M., Beyrière, F., Tsunoda, S. P., Mattis, J., Yizhar, O., Hegemann, P. and Deisseroth, K.** (2008) 'Red-shifted optogenetic excitation: A tool for fast neural control derived from *Volvox carteri*', *Nature Neuroscience*, 11(6), pp. 631–633. doi: 10.1038/nn.2120.
- Zhang, W., Yan, Z., Jan, L. Y. and Jan, Y. N.** (2013) 'Sound response mediated by the TRP channels NOMPC, NANCHUNG, and INACTIVE in chordotonal organs of Drosophila larvae.', *Proceedings of the National Academy of Sciences of the United States of America*, 110(33), pp. 13612–7. doi: 10.1073/pnas.1312477110.

Zheng, C.-Y., Seabold, G. K., Horak, M. and Petralia, R. S. (2011) 'MAGUKs, Synaptic Development, and Synaptic Plasticity', *Neuroscientist*, 17(5), pp. 493–512. doi: 10.1177/1073858410386384.MAGUKs.

Zhong, Y. and Peña, L. A. (1995) 'A novel synaptic transmission mediated by a PACAP-like neuropeptide in drosophila', *Neuron*, 14(3), pp. 527–536. doi: 10.1016/0896-6273(95)90309-7.

Zhou, Y., Cameron, S., Chang, W.-T. and Rao, Y. (2012) 'Control of directional change after mechanical stimulation in *Drosophila*', *Molecular Brain*. *Molecular Brain*, 5(1), p. 39. doi: 10.1186/1756-6606-5-39.

Zito, K., Fetter, R. D., Goodman, C. S. and Isacoff, E. Y. (1997) 'Synaptic Clustering of Fasciclin II and Shaker: Essential Targeting Sequences and Role of Dlg', *Neuron*, 19(5), pp. 1007–1016. doi: 10.1016/S0896-6273(00)80393-1.

Zito, K., Parnas, D., Fetter, R. D., Isacoff, E. Y. and Goodman, C. S. (1999) 'Watching a synapse grow: Noninvasive confocal imaging of synaptic growth in *Drosophila*', *Neuron*, 22(4), pp. 719–729. doi: 10.1016/S0896-6273(00)80731-X.

7 Abbreviations

4-(2-hydroxyethyl)-1-piperazineethanesulfonic acid	HEPES
Active zone	AZ
Adhesion G-Protein coupled receptors	aGPCR
<i>All-trans-retinal</i>	ATR
arrestin-2, rhodopsin, alpha-subunit of the G protein	'chARGE'
attenuation of the amplifier	K
Bruchpilot	Brp
calcium	Ca ²⁺
calcium chloride	CaCl ₂
CAZ-associated structural protein	CAST
cell capacitance	C _m
Channelrhodopsin	ChR
Channelrhodopsin-2 wild type	ChR2-wt
Channelrhodopsin2-XXM	ChR2-XXM
chimera of ChR1 and ChR2	C1C2
Chordotonal organ	ChO
ChR2-E123T accelerated	ChETA
command potential	V _{cmd}
Cyclic adenosine monophosphate	cAMP
Cyclic guanosine monophosphate	cGMP
cytomatrix of the active zone	CAZ
deep brain stimulation	DBS
di-sodium hydrogen phosphate	Na ₂ HPO ₄
direct stochastic optical reconstruction microscopy	dSTORM
disc large	Dlg
<i>Drosophila</i> latrophilin	dCIRL
<i>Drosophila</i> latrophilin knock-out	dCIRL ^{KO}
electron microscopy	EM
endoplasmatic reticulum	ER
evoked excitatory postsynaptic current	eEPSC
extracellular domain	ECD

for example, <i>exempli gratia</i>	e.g.
Förster resonance energy transfer	FRET
G-Protein coupled receptors	GPCR
gain	μ
glutamate receptors	GluR
GPCR-Autoproteolysis-INDucing-domain	GAIN-domain
<i>Guillardia theta</i> anion-conducting Channelrhodopsin	GtACR
haemolymph-like solution 3	HL-3
Horse radish peroxidase	HRP
INACTIVE	iav
intersegmental nerve	ISN
kilo Dalton	kDa
light emitting diode	LED
magnesium chloride	MgCl ₂
mega Ohm	M Ω
membrane associated guanylat kinase	MAGUK
membrane potential	V _m
membrane resistance	R _m
microelectrode	ME1
micrometre	μm (10 ⁻⁶ meter)
microwatt	μW (10 ⁻⁶ Watt)
millimetre	mm
millimolar	mM
Millivolt	mV
molar	M
Neurexin	Nrx
neuromuscular junction	NMJ
no membrane potential C	NOMPC
normal goat serum	NGS
paraformaldehyde	PFA
pentascolopodial chordotonal organ	Ich5
phosphate buffered saline	PBS

postsynaptic density	PSD
potassium chloride	KCl
proportional resistance of ME2	R_{p2}
Rab3 interacting molecule	RIM
recombinant adeno-associated virus	rAAV
red-activatable Channelrhodopsin	ReaChR
Red-fluorescent protein	RFP
RIM-binding protein	RBP
room temperature	RT
segmental nerve	SN
silver	Ag
silver-chloride	AgCl
sodium bicarbonate	NaHCO ₃
sodium chloride	NaCl
sodium di-hydrogen phosphate	NaH ₂ PO ₄
sodium hydroxide	NaOH
standard deviation	SD
stimulated emission depletion	STED
subsynaptic reticulum	SSR
synaptic vesicles	SV
that is, id est	i.e.
time	τ
transient receptor potential	TRP
transverse nerve	TN
Two-electrode voltage clamp	TEVC
type I big boutons	Ib
type I small boutons	Is
ventral longitudinal body wall muscles	VLM
ventral nerve cord	VNC
voltage-gated calcium channel	VGCC
water	H ₂ O
wildtype	wt

8 Register of illustrations

Figure 1 Histological and functional parts of the active zone.....	3
Figure 2 Chemical synapse compared to electrical synapse.....	6
Figure 3 Life cycle of <i>Drosophila melanogaster</i>	11
Figure 4 Anatomy of <i>Drosophila</i> body wall and neuronal arrangement.....	13
Figure 5 Anatomy of the chordotonal organ	16
Figure 6 Channelrhodopsin, optogenetics and <i>Chlamydomonas</i>	20
Figure 7 Two-electrode voltage clamp circuitry	30
Figure 8 Confocal microscopy	33
Figure 9 Light application setup for behavioural experiments	40
Figure 10 Expression of Chr2-XXM::tdtomato at larval NMJ and VNC	44
Figure 11 Electrophysiological recording at <i>Drosophila</i> NMJ (TEVC)	45
Figure 12 Immobilisation of <i>Drosophila</i> larvae expressing different ChR variants	47
Figure 13 Light sensitivity of adult <i>Drosophila</i> expressing different ChR variants	48
Figure 14 Expression of ChR2-XXM::tdtomato in the chordotonal organ.....	51
Figure 15 Expression of ChR2-XXM::tdtomato in the larval VNC.....	52
Figure 16 Irrigation of Ich5 by ChR2-XXM.....	53
Figure 17 Quantification of head swing duration	55
Figure 18 Function of GtACR	56
Figure 19 Expression of GtACR::YE at the larval NMJ.....	57
Figure 20 Extinguishment of EPSCs by GtACR::YE	58
Figure 21 Extinguishment of EPSCs using white light and GtACR::YFP	59
Figure 22 Depolarisation of larval muscles carrying GtACR::YE.....	60
Figure 23 Larval immobilisation by GtACR::YE or GtACR::Flag	61
Figure 24 Expression and kinetics of ChR2-XXM in <i>Xenopus</i> Oocytes	63
Figure 25 Electron microscopy and temperature sensation of the ChO	70

9 Appendix

9.1 Acknowledgments

Zuerst möchte ich meinem Doktorvater Robert Kittel herzlich danken. Die hervorragende Betreuung und das sehr gute Vertrauensverhältnis schafften eine wesentliche Grundlage zur Anfertigung dieser Arbeit. Durch die sehr gute Zusammenarbeit und die zahlreichen konstruktiven Diskussionen konnte ich wertvolle Erfahrungen im wissenschaftlichen Arbeiten, Handeln und Denken sammeln, um so auch komplexen wissenschaftlichen Fragestellungen gezielt und effizient begegnen zu können. Mein nicht weniger großer Dank gilt Nadine Ehmann. Ihr danke ich besonders für zahlreiche Diskussionen und die umfassende Unterstützung, sowie für die grundlegende Einführung in einen Großteil der benötigten Methodik und die Fliegenarbeit. Herrn Georg Nagel danke ich für die Bereitstellung der notwendigen Konstrukte und die wertvollen Hinweise und Ratschläge während der Anfertigung dieser Arbeit. Manfred Heckmann danke ich für das Unterkommen in seinem Institut und seine Unterstützung.

Weiterhin danke ich Tobias Langenhan und Nicole Scholz, für interessante Diskussionen und die spannende und lehrreiche Zusammenarbeit an gemeinsamen Projekten. Auch danke ich Sven Dannhäuser für die kurzweilige und motivierte Zusammenarbeit bei der Charakterisierung des GtACR. Ich danke allen damaligen und jetzigen Mitarbeitern des Neurophysiologischen Instituts für die wunderbare und die produktive Arbeitsatmosphäre.

Danke auch an meine Eltern! Dafür, dass Sie mich vor und während meines Studiums immer unterstützt haben und ich mich auch sonst immer auf sie verlassen konnte. Zu guter Letzt danke ich meiner wunderbaren Frau Lisa, die mich immer unterstützt und viel Verständnis aufgebracht hat.

9.2 Curriculum vitae

Personal details

Surname	Grotemeyer
Forenames	Karl <u>Alexander</u>
Date of birth	25.03.1990
Place of birth	Münster, Nordrhein-Westfalen
Nationality	German
Marital status	married, one child

Scientific education

2009	Abitur, Wirtschaftswissenschaftliches Gymnasium, Saarbrücken
2009 - 2011	Undergraduate studies in biophysics, Universität des Saarlandes
2011 – 2013	Study of dentistry, Julius-Maximilians-Universität Würzburg
2013	Preliminary examination in dentistry
2013 - 2018	Medical studies, Julius-Maximilians-Universität Würzburg
2014	Preliminary examination in medical studies (M1)
2017	Written part of state exam in medical studies (M2)
2018	Oral part of state exam in medical studies (M3)

Clinical education

2012 (one week)	Oral and maxillofacial surgery, Klinikum Saarbrücken
2014 (one month)	Neurology, Universitätsklinikum Würzburg
2015 (one month)	Anaesthesiology, Universitätsklinikum Würzburg
2016 (one month)	Internal A+E unit, Juliusspital Würzburg
2016 (one month)	General practitioner, Dres. Vescovi/Schiel Würzburg
2017-2018	Practical year at Universitätsklinikum Würzburg
05/2017 – 09/2017	16 weeks at surgical department
09/2017 – 12/2017	16 weeks at neurological department
12/2017 – 04/2018	16 weeks at internal medicine department

Scientific assistance

2010 - 2011
10/2014
Leibniz Institut für Neue Materialien, Saarbrücken
Stroke-Unit, Universitätsklinikum Würzburg

Scientific work

2015 - 2018
MD (doctor medicinae) thesis: "Characterisation and application of new optogenetic tools in *Drosophila melanogaster*"
Julius-Maximilians-Universität Würzburg
Referee: Prof. Dr. Robert J. Kittel
Co-referee: Prof. Dr. Georg Nagel
Instructor: Prof. Dr. Robert J. Kittel

Scientific prizes

2009
BARMER-Preis: "Auszeichnung für hervorragende Leistungen im Fach Biologie"
2016
Poster prize (95th Annual Meeting of the Deutsche Physiologische Gesellschaft, Lübeck)
2017
Congress grant of the DGN (supported by Prof. Dr. N. Üçeyler)

Publication

Scholz, N.*, Guan, C.*, Nieberler, M.*, Grotemeyer, A* et al. (2017). Mechano-dependent signaling by Latrophilin/CIRL quenches cAMP in proprioceptive neurons, 1-21. eLife 2017;6:e28360. *equal contribution